

AFRL-PR-WP-TR-1998-2147

**ADVANCED COOLING FOR
HIGH POWER ELECTRIC
ACTUATORS**



**Michael G. Schneider
Daniel P. Domberg**

**Sundstrand Corp
PO Box 7002
Rockford IL 61125-7002**

OCTOBER 1998

FINAL REPORT FOR PERIOD JANUARY 1993 - OCTOBER 1998

APPROVED FOR PUBLIC RELEASE; DISTRIBUTION UNLIMITED

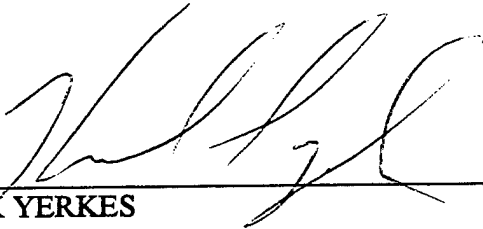
**PROPULSION DIRECTORATE
AIR FORCE RESEARCH LABORATORY
AIR FORCE MATERIEL COMMAND
WRIGHT-PATTERSON AIR FORCE BASE, OH 45433-7251**

1959030652

NOTICE

WHEN GOVERNMENT DRAWINGS, SPECIFICATIONS, OR OTHER DATA ARE USED FOR ANY PURPOSE OTHER THAN IN CONNECTION WITH A DEFINITELY GOVERNMENT RELATED PROCUREMENT, THE UNITED STATES GOVERNMENT INCURS NO RESPONSIBILITY OR ANY OBLIGATION WHATSOEVER. THE FACT THAT THE GOVERNMENT MAY HAVE FORMULATED OR IN ANY WAY SUPPLIED THE SAID DRAWINGS, SPECIFICATION, OR OTHER DATA, IS NOT TO BE REGARDED BY IMPLICATION, OR OTHERWISE IN ANY MANNER CONSTURED, AS LICENSING THE HOLDER, OR ANY OTHER PERSON OR CORPORATION; OR AS CONVEYING ANY RIGHTS OR PERMISSION TO MANUFACTURE, USE, OR SELL ANY PATENTED INVENTION THAT MAY IN ANY WAY BE RELATED THERETO.

THIS TECHNICAL REPORT HAS BEEN REVIEWED AND IS APPROVED FOR PUBLICATION.

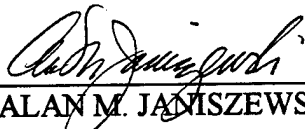


KIRK YERKES
Mechanical Engineer
Power Generation & Thermal Branch



PHILLIP G. COLEGROVE
Chief
Power Generation & Thermal Branch

FOR THE COMMANDER



ALAN M. JANISZEWSKI, Colonel, USAF
Chief
Power Division

IF YOUR ADDRESS HAS CHANGED, IF YOU WISH TO BE REMOVED FROM OUR MAILING LIST, OR IF THE ADDRESSEE IS NO LONGER EMPLOYED BY YOUR ORGANIZATION PLEASE NOTIFY AFRL/PRPG, WRIGHT-PATTERSON AFB OH 45433-7251 TO HELP MAINTAIN A CURRENT MAILING LIST.

COPIE OF THIS REPORT SHOULD NOT BE RETURNED UNLESS RETURN IS REQUIRED BY SECURITY CONSIDERATION, CONTRACTUAL OBLIGATIONS, OR NOTICE ON A SPECIFIC DOCUMENT.

REPORT DOCUMENTATION PAGE			Form Approved OMB No. 0704-0188	
Public reporting burden for this collection of information is estimated to average 1 hour per response, including the time for reviewing instructions, searching existing data sources, gathering and maintaining the data needed, and completing and reviewing the collection of information. Send comments regarding this burden estimate or any other aspect of this collection of information, including suggestions for reducing this burden to Washington Headquarters Services, Directorate for Information Operations and Reports, 1215 Jefferson Davis Highway, Suite 1204, Arlington, VA 22202-4302, and to the Office of Management and Budget, Paperwork Reduction Project (0704-0188), Washington, DC 20503.				
1. AGENCY USE ONLY (leave BLANK)		2. REPORT DATE October 1998		3. REPORT TYPE AND DATES COVERED Final Report, Jan. 93 to Oct. 98
4. TITLE AND SUBTITLE Advanced Cooling for High Power Electric Actuators			5. FUNDING NUMBERS C-F33615-91-C-2139 PE-62203F PR-3145 TA-29 WU-14	
6. AUTHOR(S) Michael G. Schneider Daniel P. Domberg				
7. PERFORMING ORGANIZATION NAME(S) AND ADDRESS(ES) Sundstrand Corp. PO Box 7002 Rockford IL 61125-7002			8. PERFORMING ORGANIZATION REPORT NUMBER	
9. SPONSORING / MONITORING AGENCY NAME(S) AND ADDRESS(ES) Propulsion Directorate Air Force Research Laboratory Air Force Materiel Command Wright-Patterson Air Force Base, OH 45433-7251 POC: Kirk Yerkes, AFRL/PRPG, 937-256-4428			10. SPONSORING / MONITORING AGENCY REPORT NUMBER AFRL-PR-WP-TR-1998-2147	
11. SUPPLEMENTARY NOTES				
12a. DISTRIBUTION / AVAILABILITY STATEMENT Approved for Public Release; Distribution Unlimited			12b. DISTRIBUTION CODE	
13. ABSTRACT (Maximum 200 words) The development of more electric technologies for future military aircraft promises to provide significant redundancy, reliability, maintainability, and performance benefits. Advanced Cooling For High Power Electric Actuators particularly address the use of electro-mechanical actuators (EMAs), and an approach for cooling EMAs using the combined concepts of passive reflux cooling and phase change materials (PCMs) for energy storage. This report presents results from tests on a motor cooler, and on two different motor drive coolers.				
14. SUBJECT TERMS Electric Actuators Thermosiphon Heat Exchanger Phase Change Material Thermal Management Reflux			15. NUMBER OF PAGES 71	
			16. PRICE CODE	
17. SECURITY CLASSIFICATION OF REPORT Unclassified		18. SECURITY CLASSIFICATION OF THIS PAGE Unclassified		19. SECURITY CLASSIFICATION OF ABSTRACT Unclassified
20. LIMITATION OF ABSTRACT SAR				

Table of Contents

Subject	Section
Report Summary	1.0
Reflux Cooling and Phase Change Thermal Storage for an Actuator Motor	2.0
2.1 Introduction	
2.2 Cooler Design	
2.2.1 SINDA Thermal Model Description	
2.2.2 Experimental Hardware	
2.2.3 Test Apparatus	
2.3 Test Results	
2.4 Conclusions	
Electronics Coolers	3.0
3.1 Small Cooler Report	
3.1.1 Introduction	
3.1.2 Small Cooler Design	
3.1.3 Thermal Testing	
3.1.3.1 Testing Summary	
3.1.3.2 Air Cooled Testing	
3.1.3.3 Reflux/PCM Cooled Testing	
3.1.4 Conclusions of a Small Cooler Test Program	
3.2 Large Reflux/PCM Cooler	
3.2.1 Introduction	
3.2.1.1 Technical Discussion	
3.2.2 Large Cooler Design	
3.2.3 Test Results	
3.2.4 Conclusions	
Program Conclusions	4.0

List of Figures

Figure No.	Title
2.2-1	Side View of Motor and Cooler
2.2-2	Cross Section of Reflux Layer
2.2-3	Cross Section of PCM Layer
2.2.1-1	SINDA Model Schematic
2.2.2-1	Parts Layout
2.2.2-2	Completed Cooler Assembly
2.3-1	Temperatures for Cycle Period of Ten Minutes
2.3-2	Thermal Constants for Cycle Period of Ten Minutes
2.3-3A	20 Second Harmonic on Six Minute Duty Cycles
2.3-3B	Motor Temperatures with a Step Input Power
2.3-4	Comparison of Natural and Reflux Cooling
2.3-5	Curve Fit of Winding Temperature Rise
2.3-6	Winding Temperature Response
2.3-7	
3.1.1-1	Reflux/PCM Design Concept
3.1.1-2	Typical Loading Percentage for Spoiler Electromotor-Actuator
3.1.2-1	Large Cooler Design Concept
3.1.2-2	PCM Research
3.1.2-3	Thermal Circuit Diagram Used in SINDA Analysis
3.1.2-4	Die Temperature for Differing PCMs
3.1.2-5	Die Temperature for Differing Air Velocities Using Triacontane PCM
3.1.2-6	Cooler Weight Comparison Chart
3.1.2-7	Cooler Orientation in Spoiler—During Descent
3.1.3.2-1	Test Equipment and Setup
3.1.3.2-2	Test Equipment and Setup
3.1.3.2-3	Test Article and Measurement Points
3.1.3.2-4	Junction and Case Temperature Rises for the High Power/High Air Flow Test
3.1.3.2-5	Junction Temperature Rise for Various Input Loads and Air Flows
3.1.3.3-1	Reflux Testing—Temperature Measurement Points
3.1.3.3-2	Comparison of Reflux and Air Cooled Switches
3.1.3.3-3	Plot Indicating Boiler Burnout
3.1.3.3-4	Plot Indicating Boiler Burnout and Elimination
3.1.3.3-5	Plot Indicating Condenser Limitations
3.1.3.3-6	Plot Indicating PCM Storage and Reflux Incipience
3.1.3.3-7	Case Temperature as a Function of Cooler Attitude (26 cc H ₂ O Fill)
3.1.3.3-8	Case Temperature as a Function of Cooler Attitude (44 cc H ₂ O Fill)
3.1.3.3-9	Case Temperature as a Function of Cooler Reflux Fill
3.2.1.1-1	Worst-Case Mission Duty Cycle, Present Power vs. Time
3.2.2-1	Large Cooler—Test Unit
3.2.2-2	Large Cooler—Test Measurement Points
3.2.2-3	Large Cooler—Test Apparatus
3.2.3-1	Cooler Temperatures for Step Power Input
3.2.3-2	Heat Balance for Cooler
3.2.3-3	Orientation Effects on Boiler Performance
3.2.3-4	Effect of Orientation on Case Temperature
3.2.3-5	Effect of Orientation on Case Temperature

List of Figures

Figure No.	Title
3.2.3-6	Case Temperature for Various Lateral Orientations
3.2.3-7	Effect on Being Above or Below the Liquid Level
3.2.3-8	Negligable Effect of Header Size
3.2.3-9	Power Level Effects on Cooler Response
3.2.3-10	Air Flow Effects on Performance
3.2.3-11	PCM Type Effect on Cooler Performance
3.2.3-12	Boiler Performance
3.2.3-13	Wall Superheats for Flame Sprayed and Non-Flame Sprayed Coolers
3.2.3-14	Boiler Temperature Rise for FS and nFS Coolers (SW Below Fluid Level)
3.2.3-15	Boiler Temperature Rise for FS and nFS Coolers (SW Above Fluid Level)
3.2.3-16	Comparison to Air-Cooler with Full Air Flow
3.2.3-17	Comparison to Air-Cooler with No Air Flow
3.2.3-18	Cooler Weight Comparison Chart
4-1	Flux Comparisons, Full Air Flow
4-2	Flux Comparisons, No Air Flow
4-3	Comparison of Time to Reach 100°C

List of Tables

Table No.	Title
2.2.1-A	Typical Nodal Values
2.2.1-B	Correlations Used in Thermal Analysis
3.1.3.2-A	Test Plan
3.1.3.2-B	Test Equipment Uncertainty Estimates
3.2.1.1-A	Correlations Used in Thermal Analysis

1.0 Report Summary

1.0 Report Summary

The development of more electric technologies for future military aircraft promises to provide significant redundancy, reliability, maintainability, and performance benefits. In particular, the use of electrically driven actuators for flight control surfaces allows elimination of the often leaky, maintenance intensive, and easily damaged actuator hydraulic circuits.

Many of these actuators, such as flaperons and stabilators, operate at high powers during certain flight segments such as takeoff, combat, and landing. Conventional hydraulic oil circuits remove the associated large waste heat loads from conventional hydraulic actuators, whereas, electrical actuators, such as electromechanical actuators (EMAs) and electrohydraulic actuators (EHAs), possess no inherent means of removing waste heat. The use of an active cooling loop for EMAs would reintroduce reliability, maintainability, and safety issues that are eliminated with the removal of conventional hydraulic circuits. Therefore, cooling becomes an issue for EMAs because of limited access and availability of appropriate heat sinks.

In the first phase of the present program, a cooling approach using reflux cooling and phase change thermal storage was designed, as detailed in WL-TR-93-2047. A development unit was subsequently built and tested as described in Section 2.0 of the present report. Overall thermal resistance of the motor/cooler system was 31 K/kW for the reflux/PCM cooler vs. 52 K/kW for a natural convection cooled motor at a load cycle frequency of 0.005 Hz. Due to the inherent thermal mass of the motor, there was not a significant difference in thermal performance between the two cooling approaches for load cycle frequencies less than .02 Hz (50 second load period.)

At the conclusion of the motor cooler test program, electronics cooling became a major thermal concern for EMAs because heat loads, especially in the converter, are approximately the same order as motor heat losses, and temperature limitations are more stringent for these electronics. Analysis showed that control and power electronics, with their low inherent thermal capacitance, would also benefit from a reflux cooling technique coupled with PCM energy storage. Therefore, a two-stage development was undertaken to apply reflux/PCM cooling technology to an EMA motor drive.

In the first stage of development of a reflux/PCM electronics cooler, small-scale coolers were designed, built, and tested, as described in Section 3.0 of the present report, to validate the operation and applicability of these technologies to electronics cooling. Tests on the small-scale coolers illustrated a thermal advantage over the state-of-the-art, air-only cooler, but also highlighted the need to improve boiler performance, increase reflux fluid hydrostatic head, and the need to increase the PCM mass in subsequent cooler designs. With this information, a full-scale cooler was designed, built, and tested for an entire 40-kVA motor drive, as described in subsection 3.2 of this report.

IGBT die and boiler surface fluxes exceeded 80 and 20 W/cm², respectively, during tests on the large cooler, with a boiler wall superheat of 16 K. Tests with an air-only cooler had 37 and 100 percent higher IGBT case to sink resistances for the high-air flow and no-air flow cases, respectively, for load durations of five to ten minutes. The maximum die heat flux for the no-air flow case on the air-only cooler was 32 W/cm². Across a range of attitudes, power levels, and air flow rates, the cooler performed robustly, with a system resistance of 0.32 K/W, on a per switch heat load basis, at the six minute point. The 51°C PCM provided a 0.04 K/W system resistance reduction compared to the 61°C PCM if the resistance at the four minute point is considered the basis for comparison. Future investigations should include additional parametric testing on reflux fluid fill level.

2.0 Reflux Cooling and Phase Change Thermal Storage for an Actuator Motor

2.0 Reflux Cooling and Phase Change Thermal Storage for an Actuator Motor

Abstract

A two-phase, thermosiphon cooler coupled with phase change material (PCM) energy storage was built to demonstrate a concept for cooling a 26-kW actuator motor. A Fluorinert® compound, FC75®, was used as the working fluid to transfer heat to the phase change material, acetamide. The PCM was contained in alternating layers of a plate-fin compact heat exchanger core. At the 90-percent power condition, the peak motor temperature was within 90°C of the heat sink, illustrating good source to sink thermal coupling by the thermosiphon. Conversely, when the motor was cooled by natural convection and conduction alone, the peak temperature was 170°C above sink temperature. Testing shows that the PCM material provides additional useful thermal inertia during the melting process. However, test data revealed that the melt temperature of the acetamide had been depressed from 80 to 68°C, due to absorbed water, highlighting the need to process the PCM in a dry atmosphere. The lower melt temperature did not affect the overall thermal test results, and the PCM heat of fusion was not affected by the water.

Nomenclature

- b = motor air gap radial thickness
- C = Boundary layer recovery factor
 - = $Pr^{1/2}$ - laminar boundary layer.
 - = $Pr^{1/3}$ - turbulent boundary layer.
- c_p = Specific heat of freestream (air)
- c_{pl} = Liquid specific heat
- C_{sf} = Fluid/surface pool boiling factor
- g = Local gravitational acceleration
- g_c = Gravitational proportionality constant
- h_{lam} = Laminar film condensation heat transfer coefficient
- h_{fg} = Fluid heat of vaporization
- k_l = Reflux fluid liquid thermal conductivity
- L = Characteristic length
- l = Condenser wall length (vertical)
- m = Fin efficiency parameter
- q'' = Boiler surface heat flux
- r = rotor radius
- s = Boiling Prandtl number exponent, $s=1$ for water, 1.7 for Fluorinert
- T_{BL} = Boundary layer temperature
- T = Local ambient temperature

1. Fluorinert is a Registered Trademark of 3M Co.
2. FC75 is a Registered Trademark of 3M Co.

T_s = Condenser wall temperature
 T_{sat} = Reflux fluid saturation temperature
 T_w = Boiler wall surface temperature
 U_r = rotor tip speed
 U = Freestream velocity

Dimensionless Groupings

Nu_b = Nusselt number for heat transfer across the motor air gap, hb/k
 Nu_L = Nusselt number for heat transfer from the wing surface, based on plate length, L
 Pr = Prandtl number, (use air value)
 Re_L = Reynolds number based on plate (wing) length, $U L/\nu$
 Re_b = Reynolds number based on motor air gap thickness, $U_r b/\nu$
 $Ta_b = Re_b (b/r)^{1/2}$
 Pr_f = Reflux fluid Prandtl number

Greek Letter Symbols

ϵ = Condenser fin efficiency
 μ_l = Liquid dynamic viscosity
 ν = kinematic viscosity of fluid
 ρ_l = Reflux fluid liquid density
 ρ_v = Reflux fluid vapor density
 σ = Fluid surface tension

2.1 Introduction

The development of more electric technologies for future military aircraft promises to provide significant redundancy, reliability, maintainability, and performance benefits. In particular, the use of electrically driven actuators for flight control surfaces, allows elimination of the often leaky, maintenance intensive, and easily damaged actuator hydraulic circuits.

Many of these actuators, such as flaperons and stabilators, operate at high powers during certain flight segments such as takeoff, combat, and landing. The development of inherently unstable aircraft, associated with improved maneuverability, particularly results in large actuator powers. Conventional hydraulic oil circuits remove the associated large waste heat loads from conventional hydraulic actuators, whereas, electrical actuators, such as electromechanical actuators (EMAs) and electrohydraulic actuators (EHAs), possess no inherent means of removing waste heat. The use of an active cooling loop for EMAs would reintroduce reliability, maintainability, and safety issues that are eliminated with the removal of conventional hydraulic circuits. Therefore, cooling becomes an issue for EMAs because of limited access and availability of appropriate heat sinks.

The aircraft structure and skin, and ultimately the ambient air, provide the most feasible heat sink for EMAs. Peak power levels for flaperons and other high power control surface actuators may reach 37 kW (50 hp) which, for a motor efficiency of 90 percent, imposes a peak heat load of 3.7 kW on the heat sink. However, these actuators typically operate at peak power for only brief durations, and will operate at significantly reduced power levels during most of a flight duty cycle. This characteristic of aircraft actuator duty cycles suggests the use of techniques that store energy during peak power periods and dissipate that stored energy during low power periods. Energy storage techniques allow the heat rejection system to be designed for the average heat loads rather than peak transient heat loads.

In the present concept demonstration, a two-phase fluid thermosiphon is used to provide the passive heat transfer, and a phase change material (PCM) provides energy storage. This technology depends upon submerging the heat source in a liquid that boils when heated. The generated vapor rises due to the density difference between the vapor and liquid phases and condenses on a cooler surface located above the heat source. Unlike a true reflux boiler the liquid condensate in a thermosiphon drains through dedicated and isolated channels to the pool of liquid surrounding the heat source to complete the cycle. Heat pipes operate in a similar fashion but are more like reflux boilers than thermosiphons, relying on surface tension in a wicking structure, rather than gravity, to provide the motive force for liquid circulation. In general, the allowable boiling heat flux at the heat source of a reflux type heat exchanger exceeds the allowable evaporative heat flux for a heat pipe using the same working fluid.

Preliminary steady-state analysis, using a SINDA (Systems Improved Numerical Differencing Analyzer) finite difference thermal model, revealed that the aircraft structure conductance, thermosiphon condenser area, and contact resistance between the motor stator and housing, were the driving resistances in the thermal network. Transient parametric trade studies indicated that reflux cooling, in combination with a PCM, were most beneficial when applied to actuators with low frequency duty cycles as was borne out in the present test program. Based on the results of these studies, a demonstration motor and cooler design was selected along with the optimum reflux working fluid and PCM. The analysis phase of this project led to the present laboratory test program.

2.2 Cooler Design

One of the difficulties encountered in designing a heat rejection system for EMAs involves defining the design specifications. One approach is to define a typical mission duty cycle and design the actuator to meet performance requirements for that particular application. Another approach is to gather thermal response data from motor/cooler assemblies, such as the present test unit, and use this information to analyze the response of the system to a duty cycle composed of a variety of loads. In this test program, frequency response data were gathered to serve as input tools for the latter approach. Recent studies have shown that duty cycles for many applications are approximately 0.6 to 1.0 Hz, but that high power mission segments can last for three minutes or longer. When integrated over time, the power levels are at least 30 to 40 percent of maximum load. In the present test program, duty cycles ranged from 0.0017 to 0.1 Hz, with an emphasis on the low frequency range to replicate the average power levels expected in an aircraft and to get high resolution frequency response data. Also, longer duty cycles are a better test of the robustness of the cooler because of the inherent stress they place on the motor cooler.

Figures 2.2-1 through -3, illustrate the implementation of this concept for motor cooling. Figure 2.2-1 shows a cross section of the motor and cooler. The liquid phase of the two-phase fluid wets the motor main housing, and waste heat from the motor boils the liquid, generating vapor. This vapor flows upward due to density difference through centrally located vapor channels called

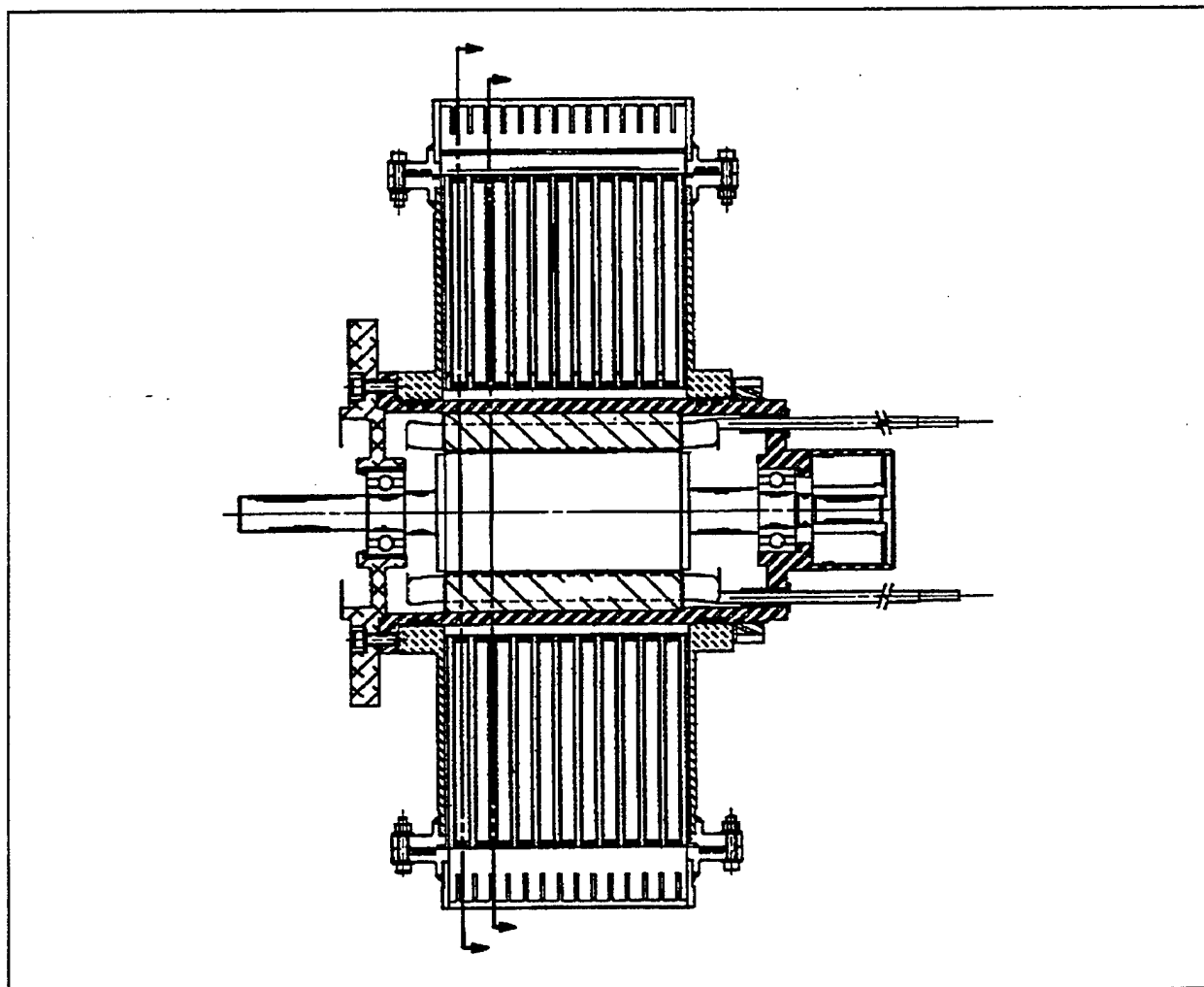


Figure 2.2-1 Side View of Motor and Cooler

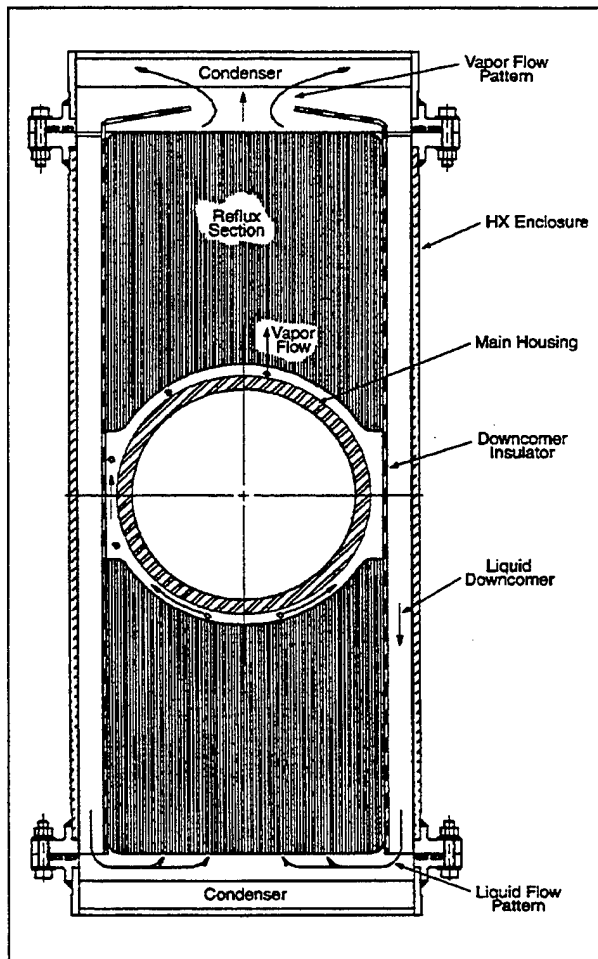


Figure 2.2-2 Cross Section of Reflux Layer

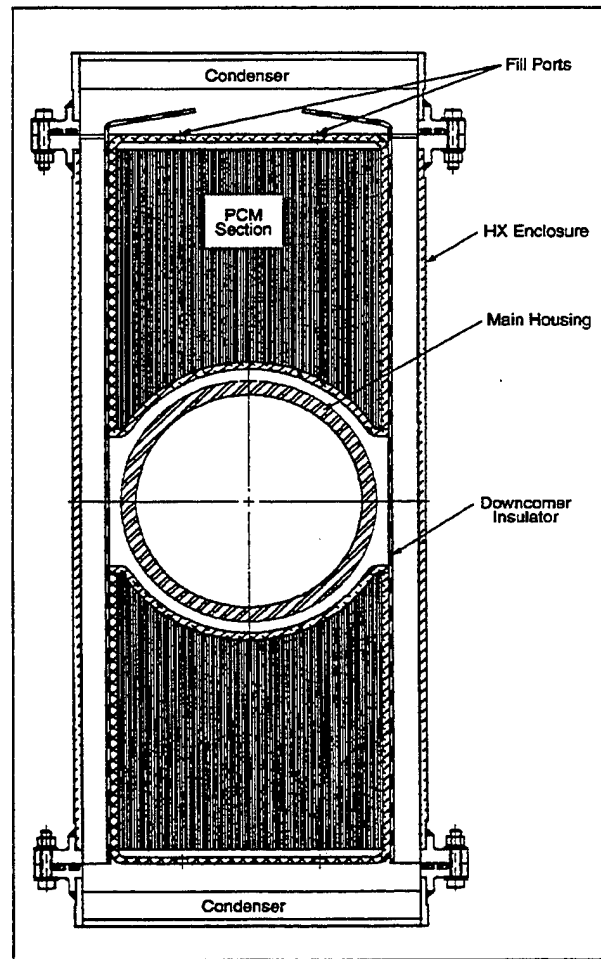


Figure 2.2-3 Cross Section of PCM Layer

"risers" or "reflux channels" and then condenses on the cooler surfaces simulating the aircraft structure or skin, as shown in Figure 2.2-2, a cross section of a reflux layer. Liquid condensate then drains in insulated "downcomers" to reenter the liquid pool surrounding the motor housing. During peak loads, the reflux fluid temperature (and pressure) rises, and energy is stored as latent heat due to the melting of the PCM, which is contained in the alternating layers of the plate-fin heat exchanger, shown in Figure 2.2-3. Because the actuator cooler must be gravity insensitive, the motor housing must be at least partially submerged in a liquid pool in all attitudes.

Heat load variations with this passive cooling approach result in changes in operating temperature and pressure for a given sink temperature. In its simplest form, the peak load defines the design condition for the cooling system, and the series thermal conductances between the motor and ambient air determine the steady-state motor temperatures. In transient load cases, the thermal capacitances of the motor and cooling system can significantly attenuate the motor temperature swings.

Enhancement of the system thermal capacitance through energy storage allows the heat rejection surfaces to be designed for the average load, reducing motor temperatures to those associated with the average heat load. Energy can be stored by the use of sensible storage, in the form of thermal mass which results in a temperature rise as heat is absorbed, and/or the use of a PCM that stores energy as latent heat at a relatively constant temperature. This latter approach, which was chosen for the present design, typically results in a system with minimum mass and volume.

2.2.1 SINDA Thermal Model Description

As mentioned earlier, a SINDA thermal model of an EMA motor incorporating a reflux cooler was developed to perform steady-state and transient analyses. The model includes all significant conductances between the motor (heat source) and ambient air (heat sink). Figure 2.2.1-1 schematically illustrates the node and conductor network that models the heat rejection system shown previously in Figures 2.2-1 through -3. Conductances include boiling, condensation, convection across the motor air gap, conduction through the reflux cooler, interface contact conductances, conduction through the aircraft structure, heat spreading across the aircraft wing and convection to the ambient air. Typical values for node temperatures and resistances are given in Table 2.2.1-A.

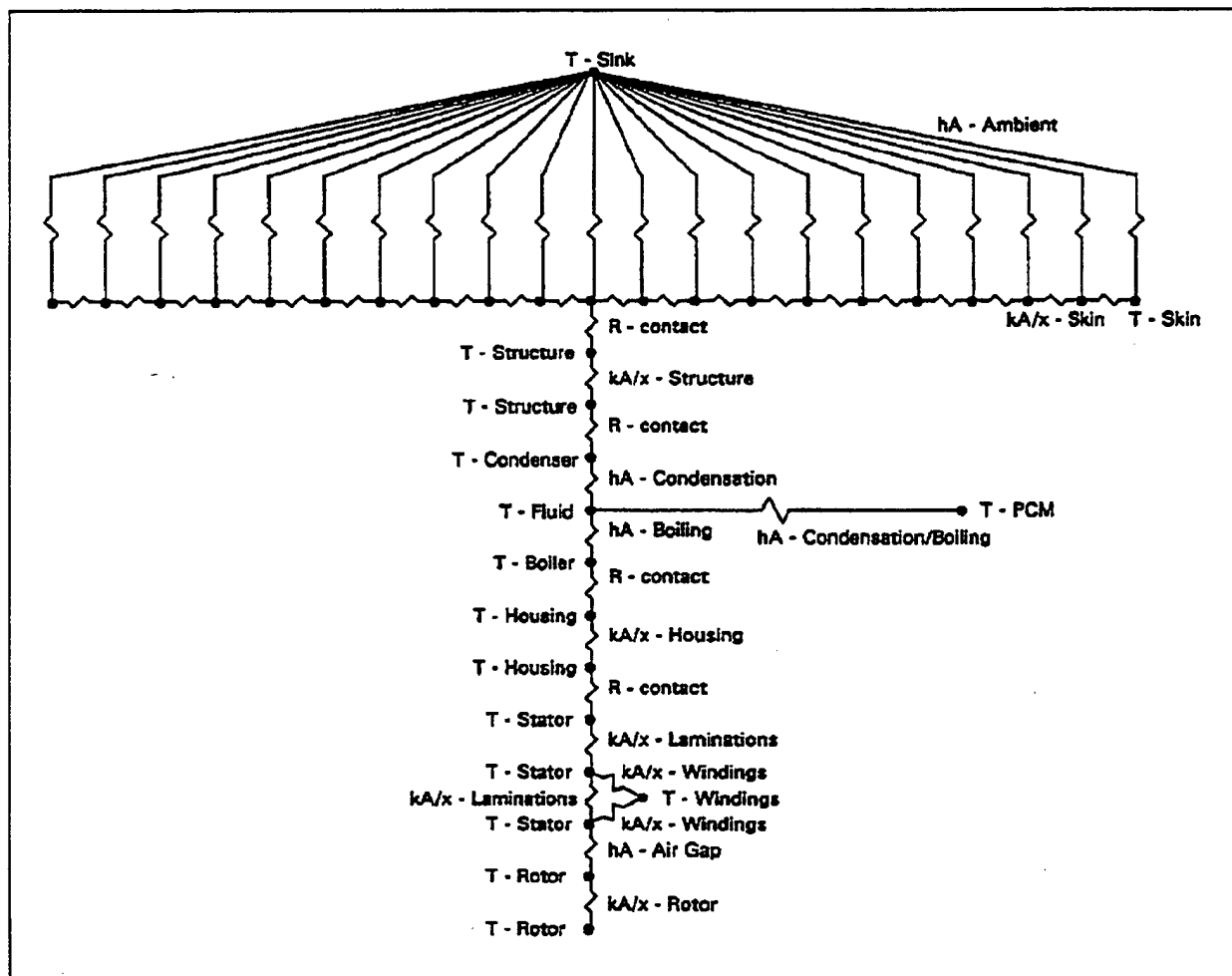


Figure 2.2.1-1 SINDA Model Schematic

Table 2.2.1-A Typical Nodal Values

Node	Temperature (°C)	Resistance (°C/W)
Sink (Boundary Layer) (0.5kW)	68.0	0.02
Skin	78.0	0.005
Structure (outer)	80.5	0.00018
Structure (inner)	80.6	0.0043
Condenser	82.7	0.0005
Reflux Fluid	83.0	0.0002
Boiler Surface (2.5 kW)	83.5	0.00042
Housing (inner)	84.6	0.00018
Stator (outer)	85.0	0.012
Stator (mid)	115.0	0.016
Windings	155.0	0.0087
Stator (inner) (0.25 kW)	157.2	0.25
Rotor (outer)	219.7	0.0011
Rotor (inner)	220.0	

The model estimates heat transfer coefficients on the working fluid side of the heat exchanger and calculates required conductance and capacitance values. This model does not perform a detailed thermal-hydraulic analysis of the reflux process, solving for recirculating flows, as forwarded by Schrage. Instead, the model estimates the boiling heat transfer coefficient using a pool boiling correlation and condensing heat transfer coefficient using a derivation for film condensation on a vertical flat plate. Outputs include motor and cooler temperatures as a function of operating conditions, including both steady state and transient conditions. Parametric analyses were performed with the model to identify controlling heat transfer conductances, characterize the effects of cooler geometry, study the effects of using PCM, and select the working fluid and PCM. A list of correlations used in the model is given in Table 2.2.1-B.

Table 2.2.1-B Correlations Used in Thermal Analysis

Correlation Description	Correlation	Reference
<u>Ambient Heat Transfer Coefficient</u> Correlation for turbulent flow over a flat plate	$Nu_L = Pr^{1/3} (0.037 Re_L^{0.8} - 850)$ L = Characteristic length (0.9m).	2
<u>Viscous Boundary Layer Heating on Aircraft Surface (Recovery Temperature)</u> Correlation for viscous heating within the boundary layer	$T_{BL} = T + CU^2/2c_p$ $C = Pr^{1/2}$ - laminar boundary layer. $= Pr^{1/3}$ - turbulent boundary layer.	3
<u>Air Gap Heat Transfer Coefficient.</u> Rotating, enclosed cylinder with zero axial flow	$Nu_b = 1.00; Ta_b < 41$ $Nu_b = 0.106 Ta_b^{0.63} Pr^{0.27}; 41 < Ta_b < 100$ $Nu_b = 0.193 Ta_b^{0.5} Pr^{0.27}; 100 < Ta_b$	4
<u>Boiling Heat Transfer Coefficient.</u> Nucleate pool boiling	$T_w - T_{sat} = C_{sf} (h_{fg} Pr_f^2 / c_{pf}) \{ (q'' / \mu_l h_{fg}) [g_c \sigma / g(\rho_l - \rho_v)]^{0.5} \}^{0.33}$	2
<u>Condensation Heat Transfer Coefficient</u> Laminar film condensation on a vertical flat plate	$h_{lam} = 0.943 \{ [\rho_l (\rho_l - \rho_v) g h_{fg} k_l^3] / [1 \mu_l (T_{sat} - T_s)] \}^{1/4}$	2

2.2.2 Experimental Hardware

The test unit consists of a 26 kW induction motor surrounded by a fluid containment vessel. Figure 2.2.2-1 shows an exploded view of the hardware and Figure 2.2.2-2 shows the motor and cooler assembly. FC75® is used as the reflux fluid, and acetamide, an organic compound, is the phase change material, with a melting point of about 80°C. The acetamide is contained in alternating layers of a plate-fin type compact heat exchanger, and the heat exchanger is located inside the fluid vessel. Waste heat from motor stator flows to the outer surface of the motor

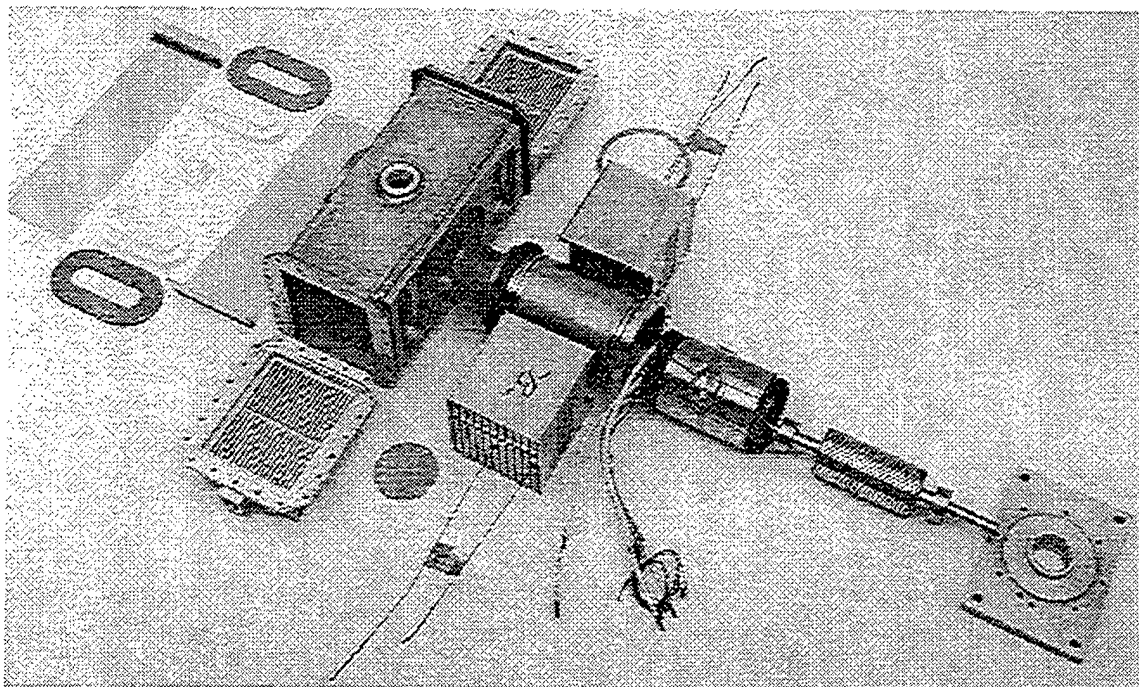


Figure 2.2.2-1 Parts Layout

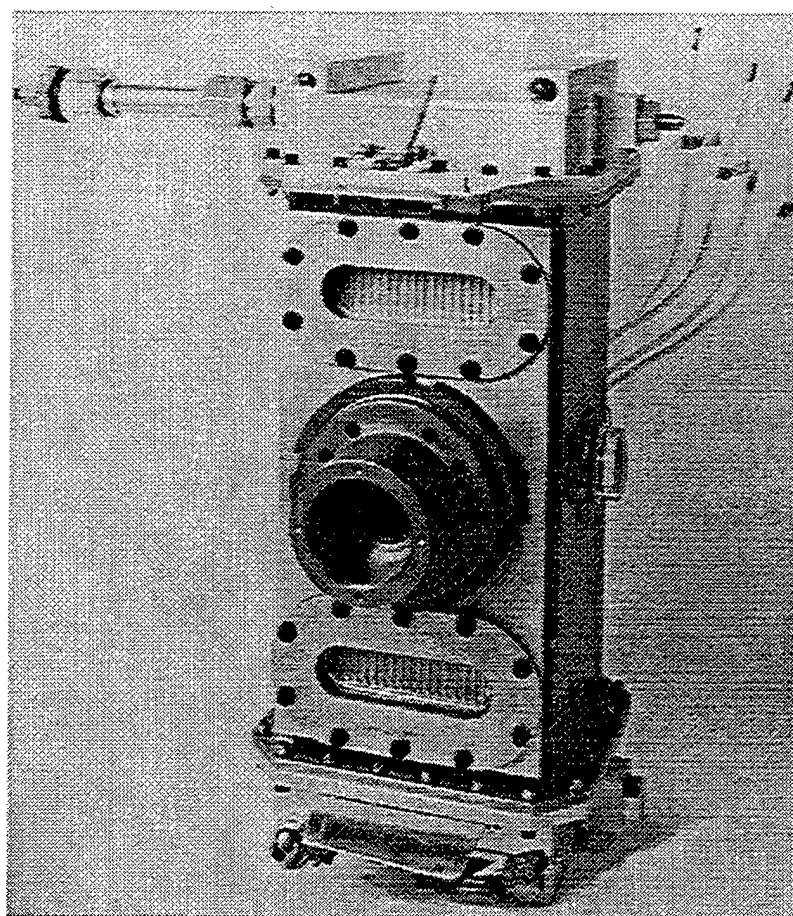


Figure 2.2.2-2 Completed Cooler Assembly

housing where it is transferred to the FC75® through boiling. The vapor bubbles then rise through open layers of the plate-fin heat exchanger to a condenser heat exchanger located above, which was cooled for these tests with temperature controlled oil. During peak power transients, when the fluid temperature exceeds the melting temperature of the acetamide, some thermal energy is transferred to the acetamide by latent heating. The remainder of the heat is rejected at the condenser surface. When the motor is operating at a low load and the acetamide temperature is higher than the working fluid, heat is transferred both from the acetamide and the motor to the FC75® which carries the heat to the condensing surface. Sight-glasses on the fluid vessel allowed visualization of the fluid flow, and thermal data were gathered for the reflux fluid, PCM, and for the motor.

2.2.3 Test Apparatus

The test unit was mounted on a single-axis articulating table to enable attitude testing. Because sufficient losses are generated in the motor at no-load to replicate partial loading conditions, the motor was not mechanically connected to a load during this phase of tests. Electrical power was supplied to the motor by a Behlman 120 kVA variable-frequency, variable-voltage power supply. A simple analog input signal controlled the power supply to provide square and sine wave duty cycles for the frequency response tests. A hydraulic cart provided a constant flow of MIL-L-23699 oil at a controlled inlet temperature to serve as the heat sink for the cooler assembly. All data were acquired by a PC-based data acquisition system with Notebook® data acquisition software. Electrical power was measured with a Yokagawa Model 2513 power meter and transmitted to the data acquisition system. Estimated uncertainties for the data are $\pm 1.2^{\circ}\text{C}$ for temperatures, ± 1.72 kPa for pressures, ± 0.54 kg/sec for cooler mass flow rates, and ± 30 W for electrical input power.

3. Notebook is a Registered Trademark of LabTech.

2.3 Test Results

Frequency response tests were performed with square wave and sinusoidal input power of 1.0 to 2.5 kW, representing losses for the motor operating at 35 to 90 percent power, with a variable load cycle period of 10 seconds to 10 minutes. Sink temperatures were varied from 20 to 68°C to replicate several operating conditions. For example, the 68°C case replicates hot day, Mach Number = 0.8, sea level flight conditions at the condenser surface. The first hardware configuration tested was with the reflux fluid level located at the top of the upper heat exchanger and the cooler was mounted in a vertical orientation. All data presented in Figures TBD.

Temperature profiles as a function of time for a test with a cycle time of ten minutes and input power of 1.3 kW are shown in Figure 2.3-1. Each time the motor was heated, the motor temperatures rose rapidly until boiling became the dominant mode of heat transfer at the housing surface. Likewise, as power was turned off, the boiling at the housing surface quickly reduced motor temperatures until boiling subsided. It is noteworthy that the boiling surface could not be instrumented to accurately measure heat flux, but calculated values are on the order of 5-7 W/cm². Figure 2.3-2, a detailed view of one of the cycles, illustrates how the motor lamination temperature profile can be broken into constituent exponential functions. Assuming a first order system, the time constant information embedded in these functions can be used to extrapolate the performance of this motor/cooler system to other duty cycles and operating conditions. The maximum temperature excursion for this test was about 123°C at the tip of the winding end turns.

Another set of tests, performed to learn about the effects of having one or both heat sinks operating, revealed that the performance of the cooler was virtually the same whether one or both of the condensers were operating as long as the upper condenser was used. If oil flow to the upper heat exchanger was interrupted, the lower cooler alone was not effective at removing heat and heat was stored in the PCM alone, and a thermal excursion could occur. It should be noted that aircraft applications would not require inverted operation for significant periods of

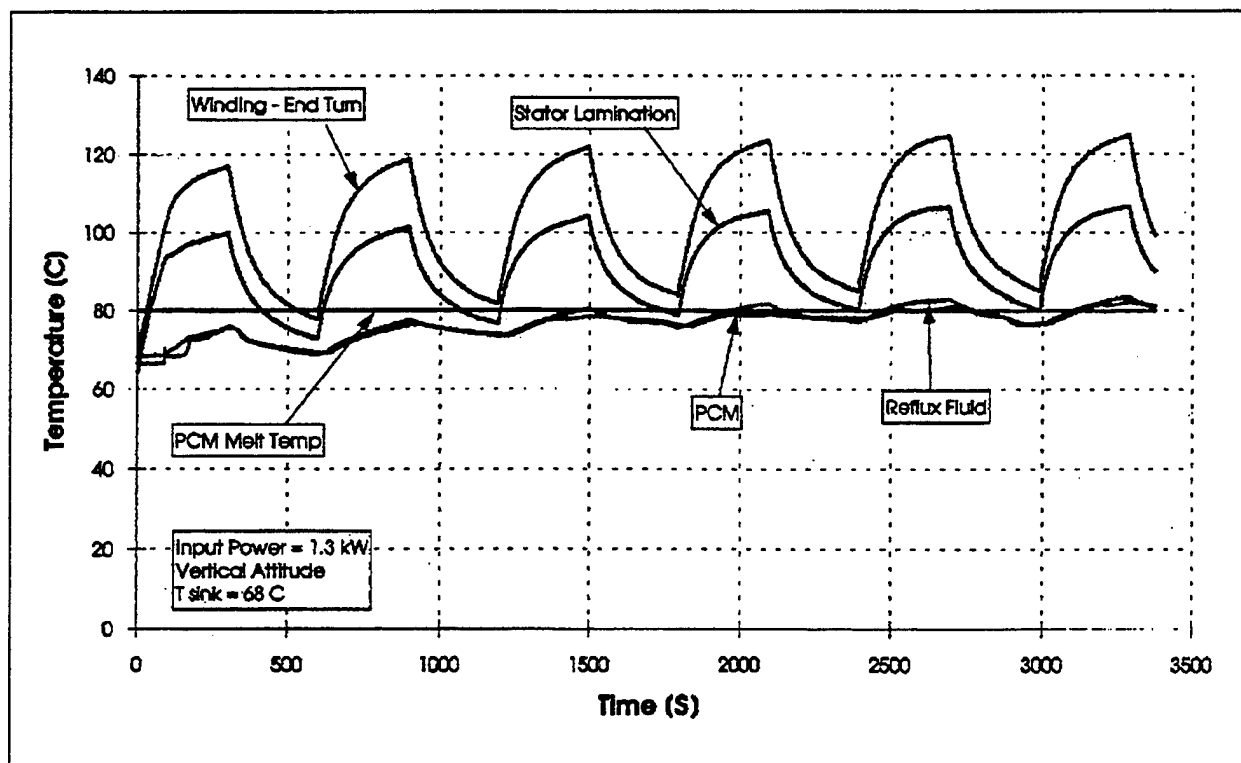


Figure 2.3-1 Temperatures for Cycle Period of Ten Minutes

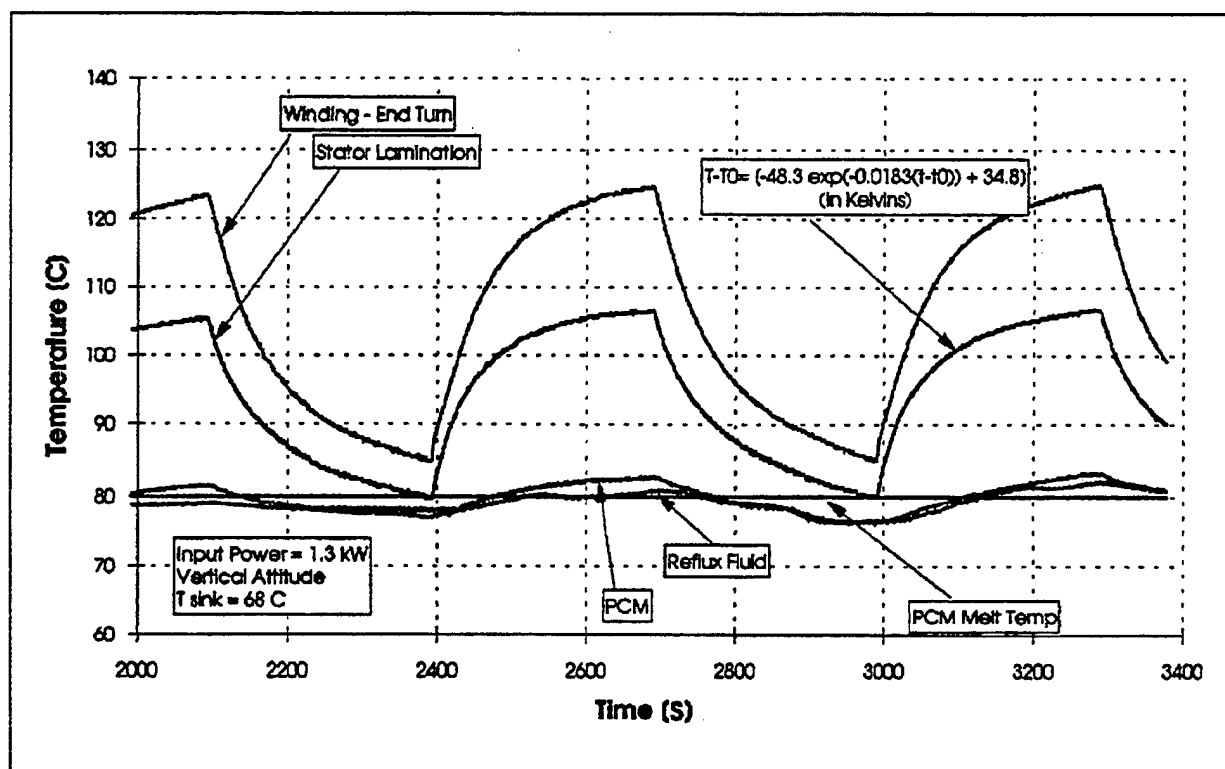


Figure 2.3-2 Thermal Constants for Cycle Period of Ten Minutes

time. When the reflux cooler was tested in a horizontal attitude with both condensers operational, it was just as effective at cooling the motor as in a vertical orientation, in spite of the relatively small available condensing area. This robust capability seemed to be due to recirculation patterns at each end of the cooler which rejected heat to both the PCM and the "condenser" through single-phase and two-phase heat transfer.

Next, the reflux fluid level was reduced such that the liquid level was at the top of the motor housing. Thermal performance, even in inverted and horizontal orientations, was equivalent to earlier tests indicating the potential to reduce weight by minimizing reflux fluid inventory.

Transient tests were also performed to simulate a typical mission duty cycle. The duty cycle consisted of a 2.5 kW sinusoidal input power at 0.05 Hz for bursts of three minutes, as shown in Figure 2.3-3. The effects of phase change, which are evident over the 1,000 to 2,200 second range, can be seen in the PCM temperatures, the motor peak temperatures, and in the output heat rate. (Although the transition temperature appears to be 69°C rather than the pure substance transition temperature of 80°C, the heat of fusion was confirmed to be unchanged at 242 kJ/kg in two ways: firstly, through digital scanning calorimetry, and secondly within the accuracy of the 12 percent heat balance measured over the course of the 42 minute test described in Figure 2.3-3. Apparently, the melt temperature was depressed by water contamination which occurred while processing the PCM.) Also, the onset of boiling can be seen at approximately 250 seconds.

Finally, the reflux cooler was removed, and the only means of heat transfer from the motor were conduction through the housing to the mounting pad and natural convection from the housing to ambient air. As expected, the temperature excursions were so high that the test had to be interrupted before winding temperature limits were exceeded as shown in Figure 2.3-4. For comparison, winding temperature rise data, defined as the difference between the winding and sink temperatures, from a reflux cooled test at the same power level are included in Figure 2.3-4, along with the SINDA model predictions for the reflux cooled case. The model predicts temperature rise within 9 K for this case, which is reasonable for a one-dimensional model.

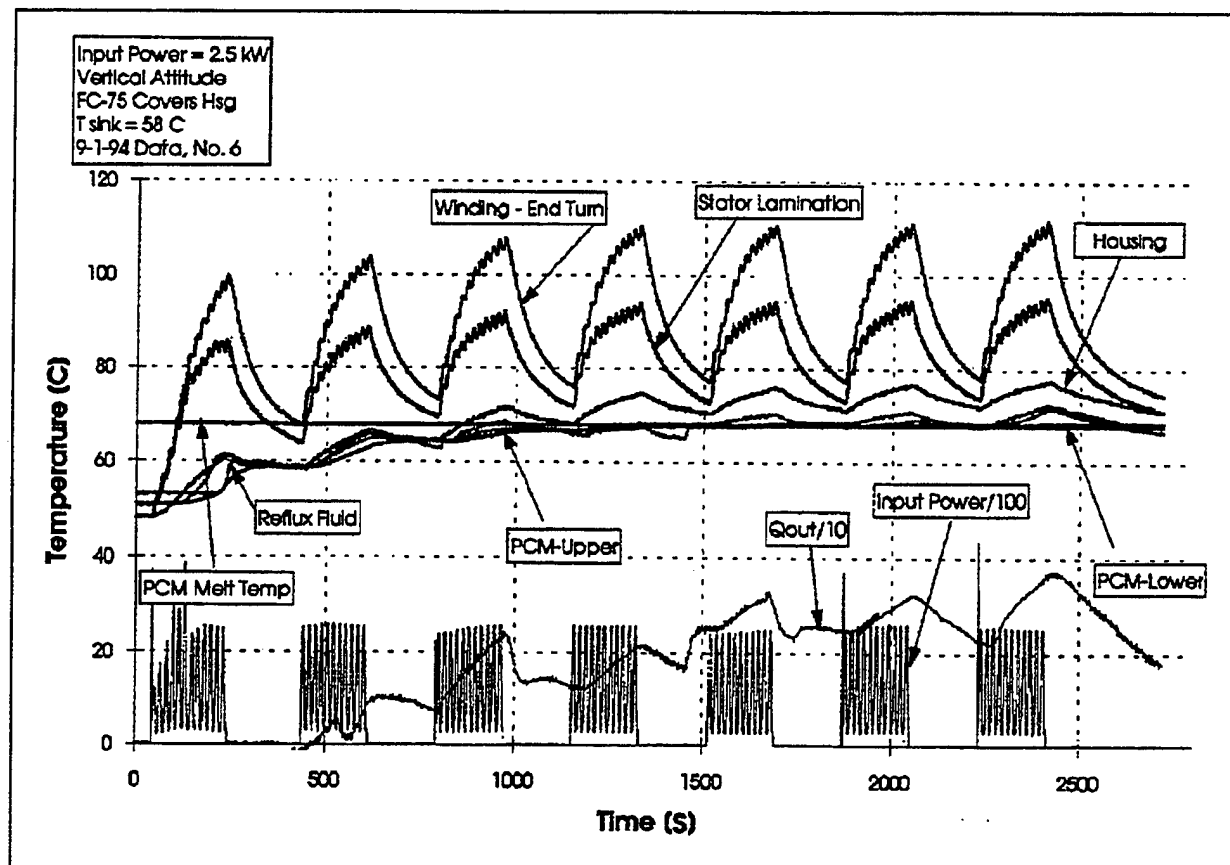


Figure 2.3-3A 20 Second Harmonic on Six Minute Duty Cycles

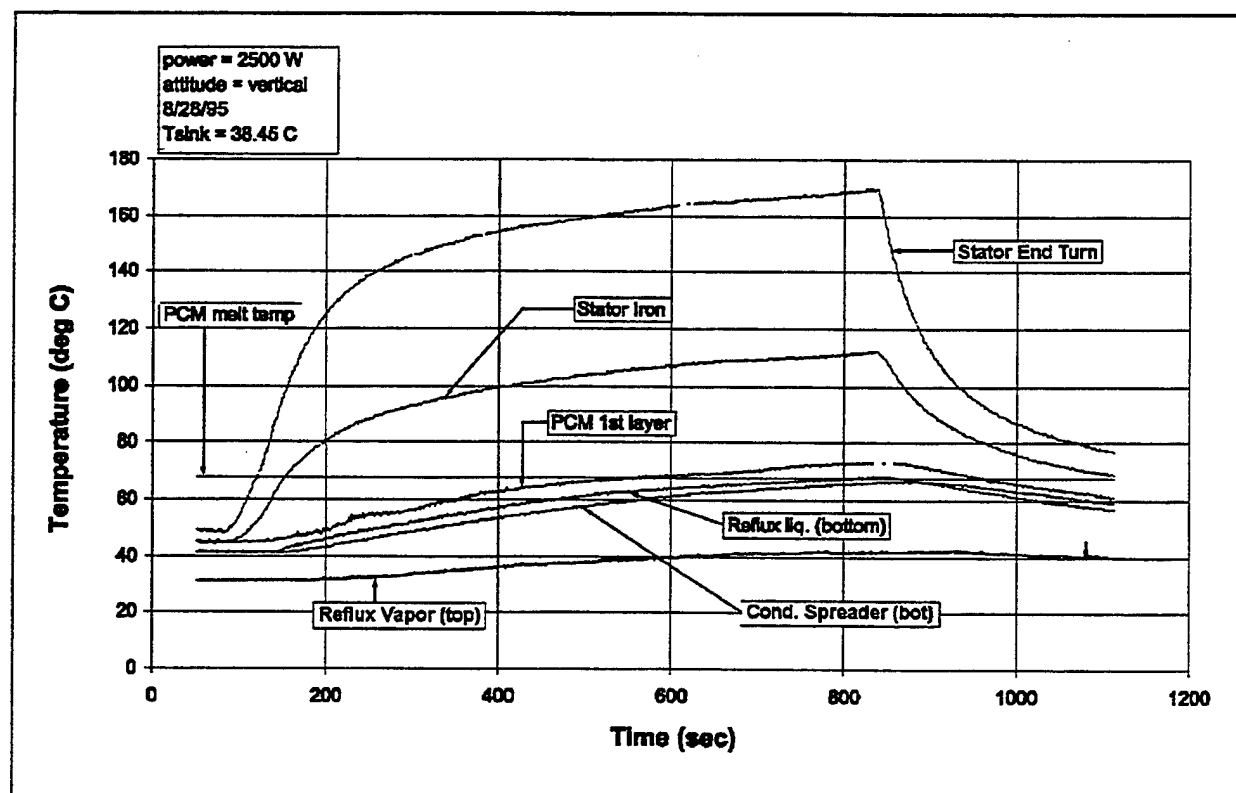


Figure 2.3-3B Motor Temperatures with a Step Input Power

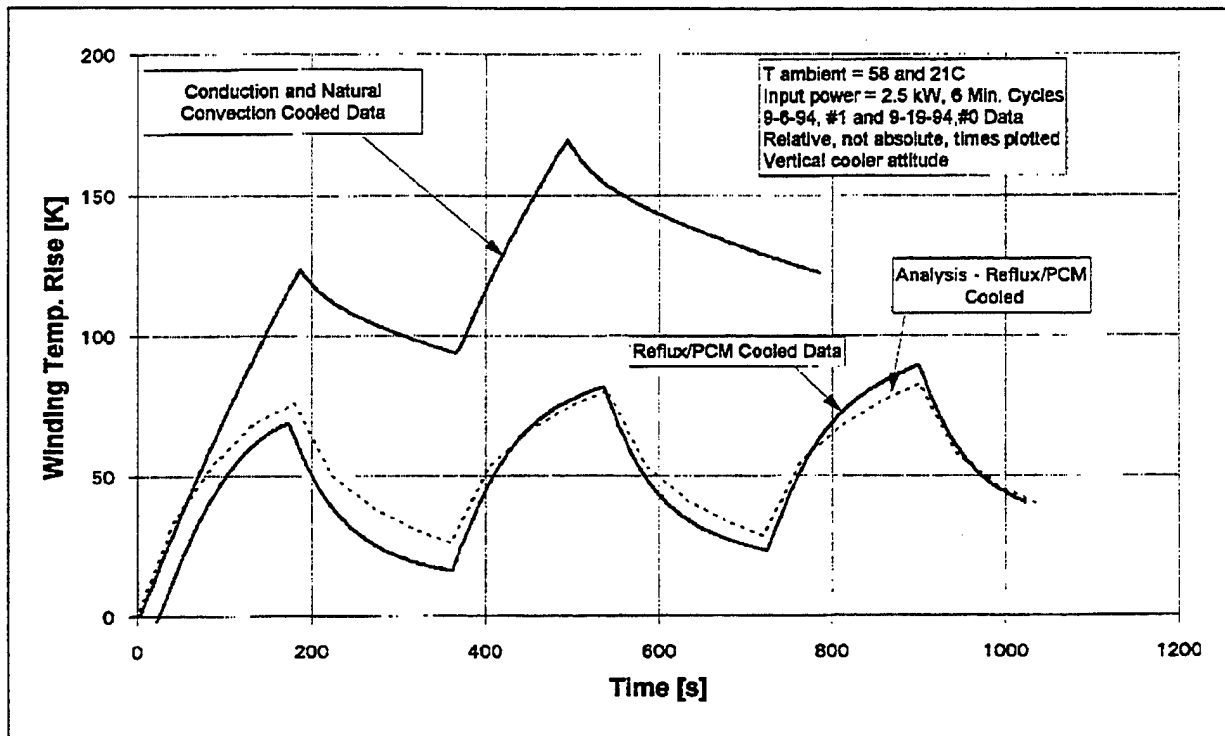


Figure 2.3-4 Comparison of Natural and Reflux Cooling

Figure 2.3-5 illustrates an exponential curve fit of test data from a reflux cooled test which illustrates that the cooling system has a time constant of 76 seconds with respect to the windings. These data, along with the data from the earlier tests, are shown in their curve-fit form in Figure

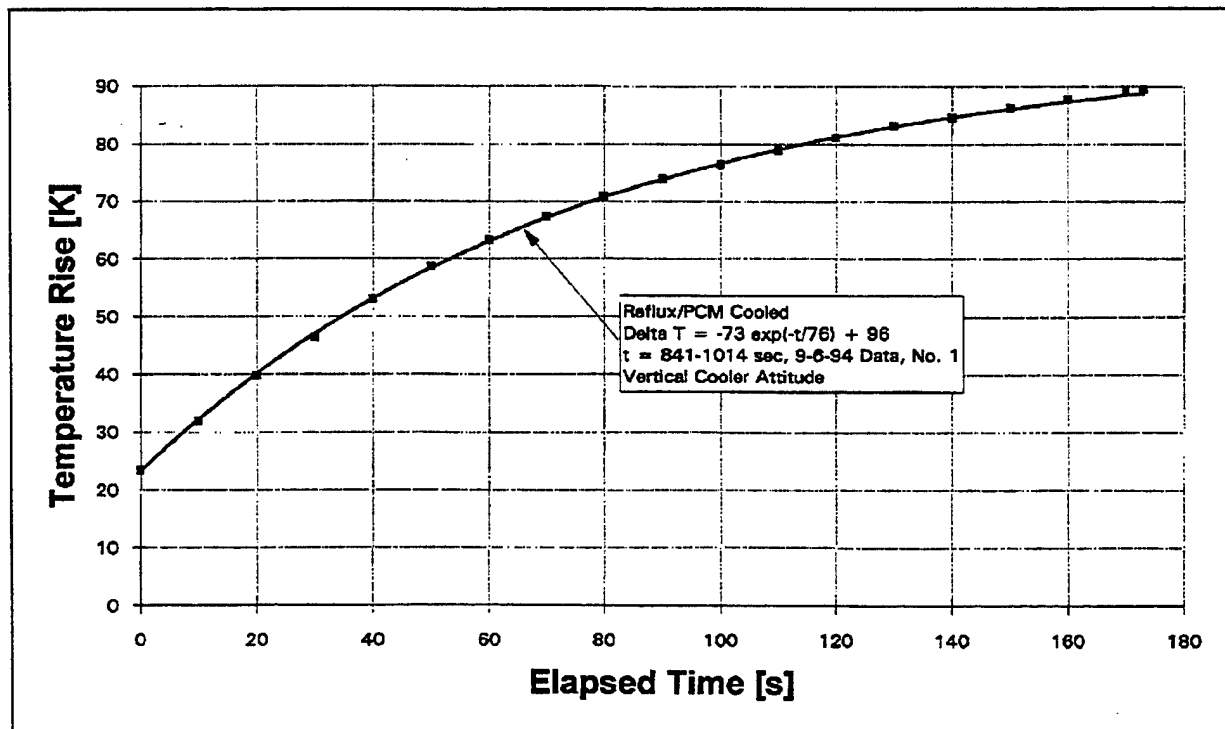


Figure 2.3-5 Curve Fit of Winding Temperature Rise

2.3-6, which shows a plot of the maximum winding temperatures, at the end of a heating cycle, as a function of load-cycle period. The temperature rise data from the natural convection cooled case is markedly higher than the reflux/PCM cooled cases. These data can be further normalized by the input power, as shown in Figure 2.3-7, to give the system response, which in this case is the winding temperature rise, to an input signal, the input signal being the motor input heat load. Three important observations can be drawn from these frequency response data.

1. The thermal system is overdamped, which is to be expected because of the large thermal masses present.
2. The system responds linearly to the input power signal, which implies that linear conductances dominate heat transfer from the motor. This linearity is evident because normalized temperature rise curves from the three reflux/PCM cooled cases essentially collapse onto a single curve.
3. Finally, the plot illustrates that reflux/PCM cooling provides significant thermal benefit for load cycles with frequencies less than 0.005 Hz (periods greater than 200 seconds.)

Due to power limitations of the power supply, the motor was not operated up to its magnetic limits, at which point heat input would be 4.8 kW and shaft power output would be nearly twice that at the 2.5 kW level (52 kW output.) SINDA model predictions indicate that the normalized temperature rise, for the reflux cooled case, would be on the same order as the 1.3 to 2.5 kW test data. Therefore, from the analysis, one might conclude that for a 0.005 Hz duty cycle, the winding temperature rise would be 149 K for the reflux cooled case vs. 250 K for the natural cooling mode. Thus, significant opportunities for increased power density accrue from using this cooling technology, especially for low frequency duty cycles.

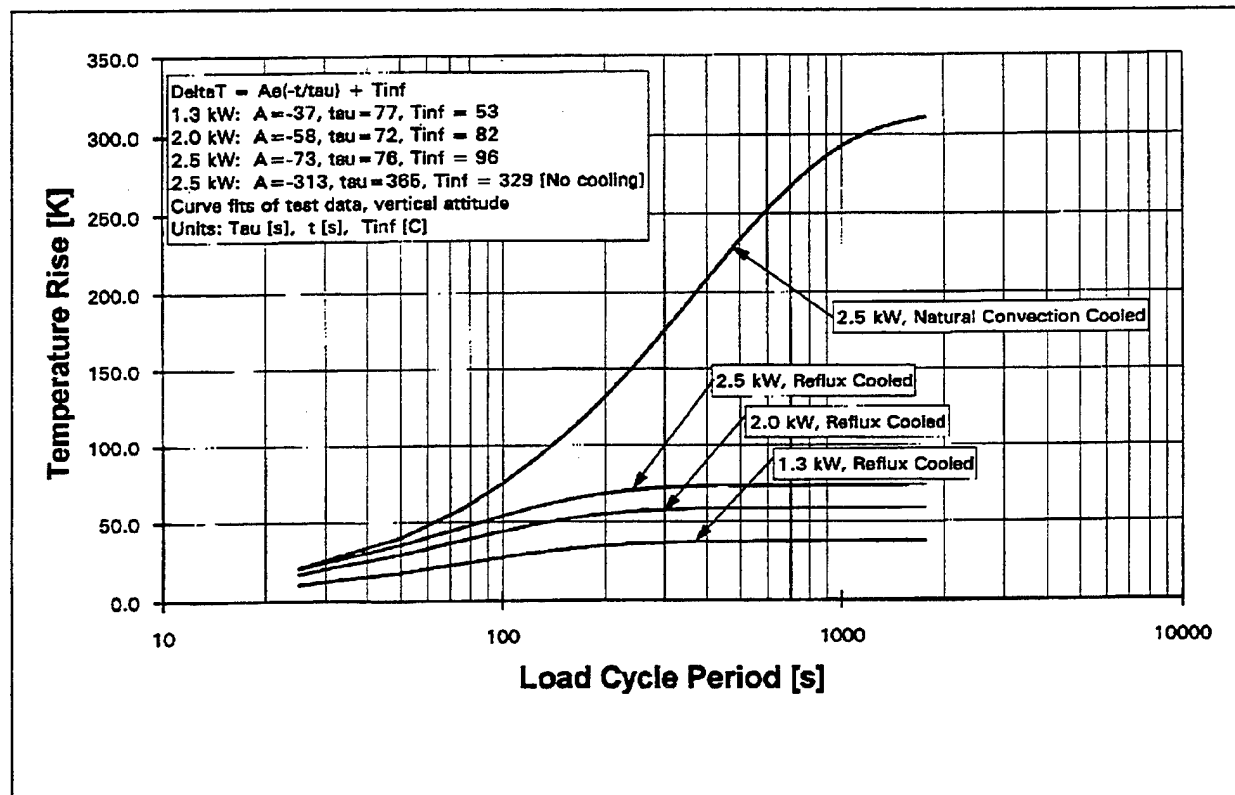


Figure 2.3-6 Winding Temperature Response

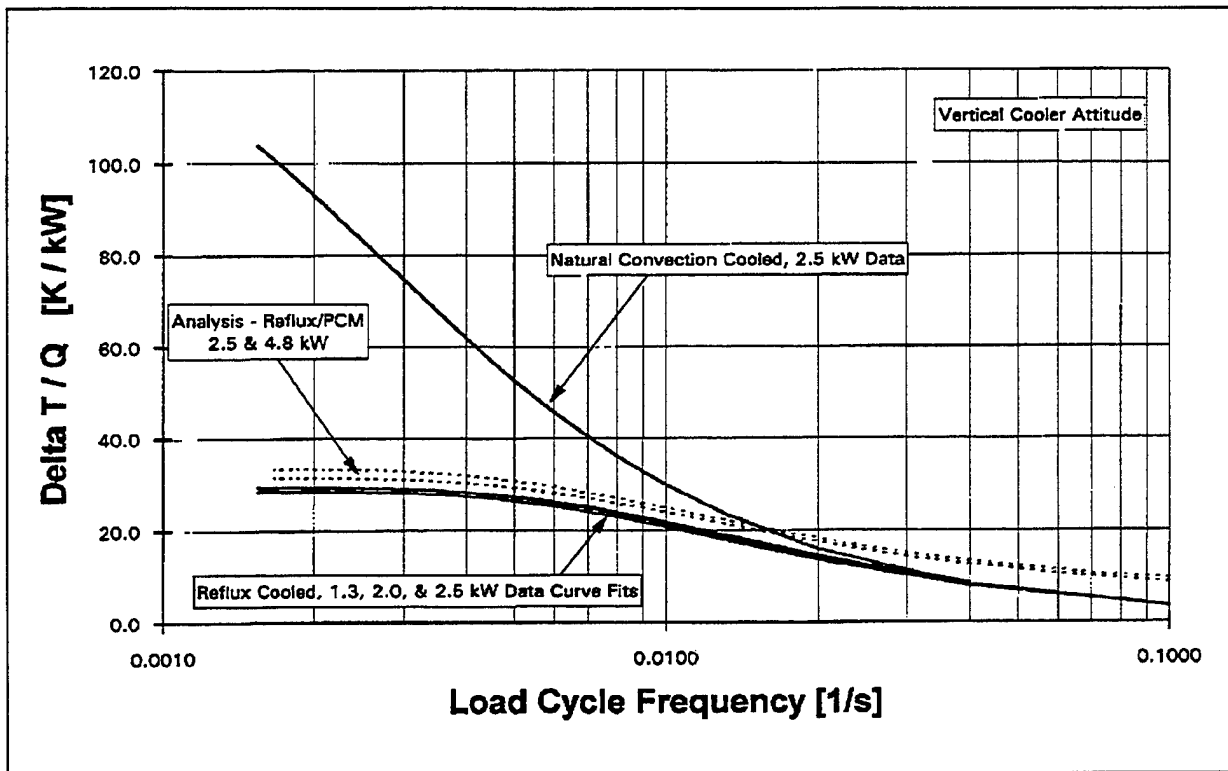


Figure 2.3-7

2.4 Conclusions

The large heat loads of EMAs and relative inaccessibility of heat sinks necessitates the use of novel cooling methods, such as reflux technology. In addition, the transient duty cycles of some actuators suggest weight and performance benefits will accrue from the use of thermal energy storage material to act as a thermal load leveler. Test results indicate the cooler is operating as anticipated, with good recirculation of the reflux fluid and effective access to the PCM. The maximum sink to motor temperature difference was 90°K as compared to over 170°K for the conductively cooled case, and the operation of the cooler was, in general, quite robust for the parameters tested.

The importance of process control when handling acetamide was highlighted by the water vapor contamination experienced in the test unit. Future filling operations will be performed in a dry atmosphere with a dried charge of PCM. It is noteworthy, however, that the PCM performed well at a slightly depressed melt temperature in spite of the contamination.

Finally, the plate-fin heat exchanger design concept has the flexibility to address issues such as survivability and the addition of motor control and power electronics. It is noteworthy that electronics cooling has arisen as a major thermal concern for EMAs because heat loads, especially in the converter, are approximately the same order as motor heat losses, and temperature limitations are more stringent for these electronics. Therefore, control and power electronics, with their low inherent thermal capacitance, would also benefit from a reflux cooling technique coupled with PCM energy storage.

3.0 Electronics Coolers

3.0 Electronics Coolers

3.1 Small Cooler Report

Abstract

Thermal analysis has shown that reflux/phase change material (PCM) cooling is superior to natural or forced convection cooling in certain applications. One such application is for cooling power electronics for a switched reluctance electromotor that is to be used in the spoiler of a large aircraft. A cooler was designed to dissipate over 850 W of heat from two integrated gate bipolar transistors (IGBTs) for a duration of six minutes. Fabrication drawings were created for the prototype design and five coolers were manufactured. Testing of the reflux/PCM cooler and an air only cooler was done and the results showed that neither the reflux/PCM cooler nor the air only cooler were adequate to reject the entire 850 W heat load. Additionally, the maximum switch temperature was 5°C warmer using the reflux cooler in comparison to the air only cooler. Reasons for the discrepancy between the thermal analysis and the test results include the SINDA model's inability to model boiler burnout beneath the switch and idealized assumptions about the thermosiphoning action in the analysis. Several improvements to the reflux/PCM design were identified. For instance surface treating the boiler with a painted coating could improve boiling by adding nucleation sites. Also, using a reflux fluid with a higher critical heat flux would yield improvements. Increasing the PCM section size and using a PCM with a higher density and heat of fusion would increase energy storage ability. And finally, using one large cooler instead of five small ones would provide a larger hydrostatic head and ensure a thermosiphoning effect.

3.1.1 Introduction

As industry progresses towards more electric vehicles, such as automobiles and aircraft, there is an increasing need for technologies and designs to keep these electronics cool. This is particularly true of the aircraft industry because the high altitude/thin air environment is not conducive to rapid heat transfer. One such cooling technology uses PCMs to absorb the latent heat that can be generated in these harsh environments. PCMs are specially suited to situations where the heat load is intense but short lived because the phase change absorbs a substantial amount of heat that can be dissipated slowly when the load is removed.

A technology developed at Sundstrand for cooling electronics is a combination of the reflux and PCM technologies. Figure 3.1.1-1 shows a typical reflux/PCM design concept. The switches (IGBTs) are mounted to a boiler plate. Above the boiler plate, in a sealed compartment, is the refluxing fluid. Above that, connected by pin fins, is the phase change material compartment. Above that are the reflux condenser and the air condenser. In normal refluxing operation, the fluid boils, transferring heat from the switches to the PCM and condenser. The fluid then condenses in the condenser and falls back to the boiler section. If the channels on either side of the PCM are different in size, or if the cooler is tilted slightly, an effect called thermosiphoning occurs. It can lead to much higher heat transfer coefficients than in normal refluxing operation.

One application where reflux/PCM technology can be used is to cool actuator electronics in the spoiler of an aircraft. The typical mission duty cycle for a motor in a spoiler is one that operates at a low power in normal flight and at high power only in emergency decent situations. Figure 3.1.1-2 shows the percentage of full loading that a spoiler might see for a takeoff, altitude climb, emergency decent, and landing scenario.

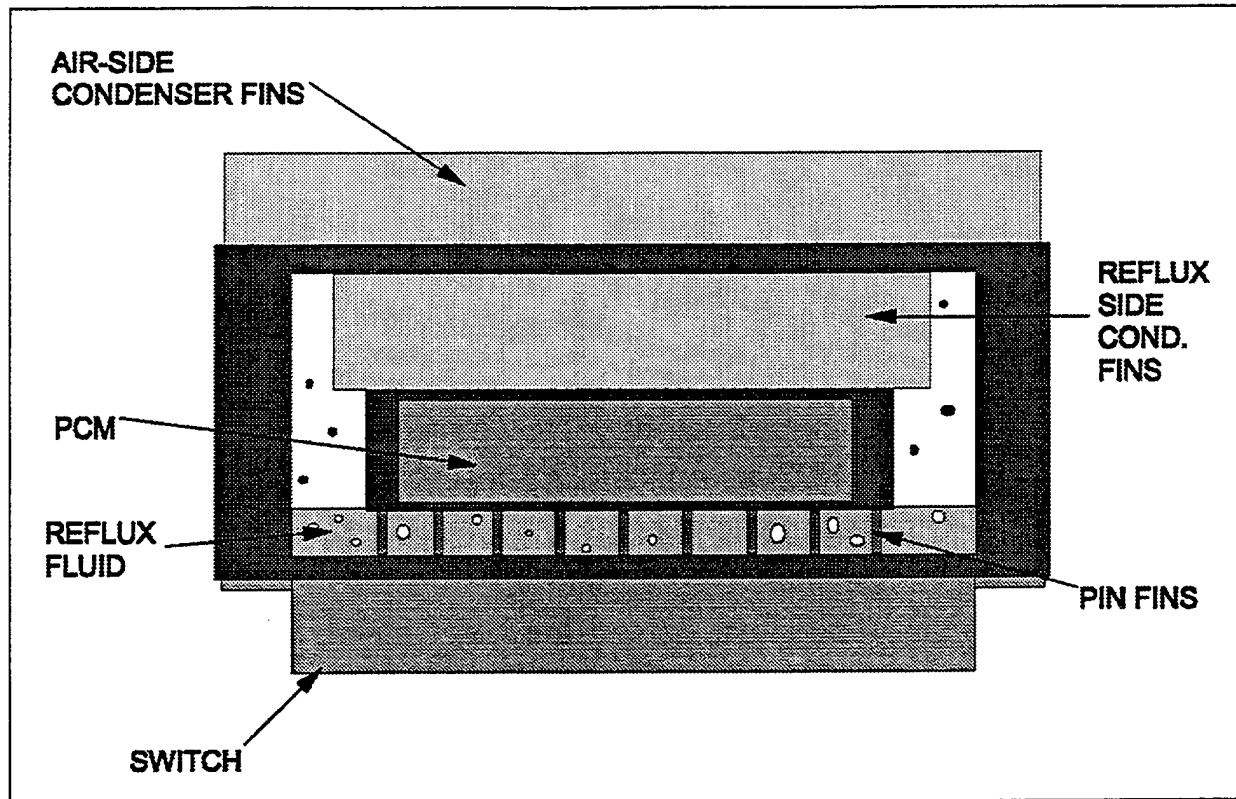


Figure 3.1.1-1 Reflux/PCM Design Concept

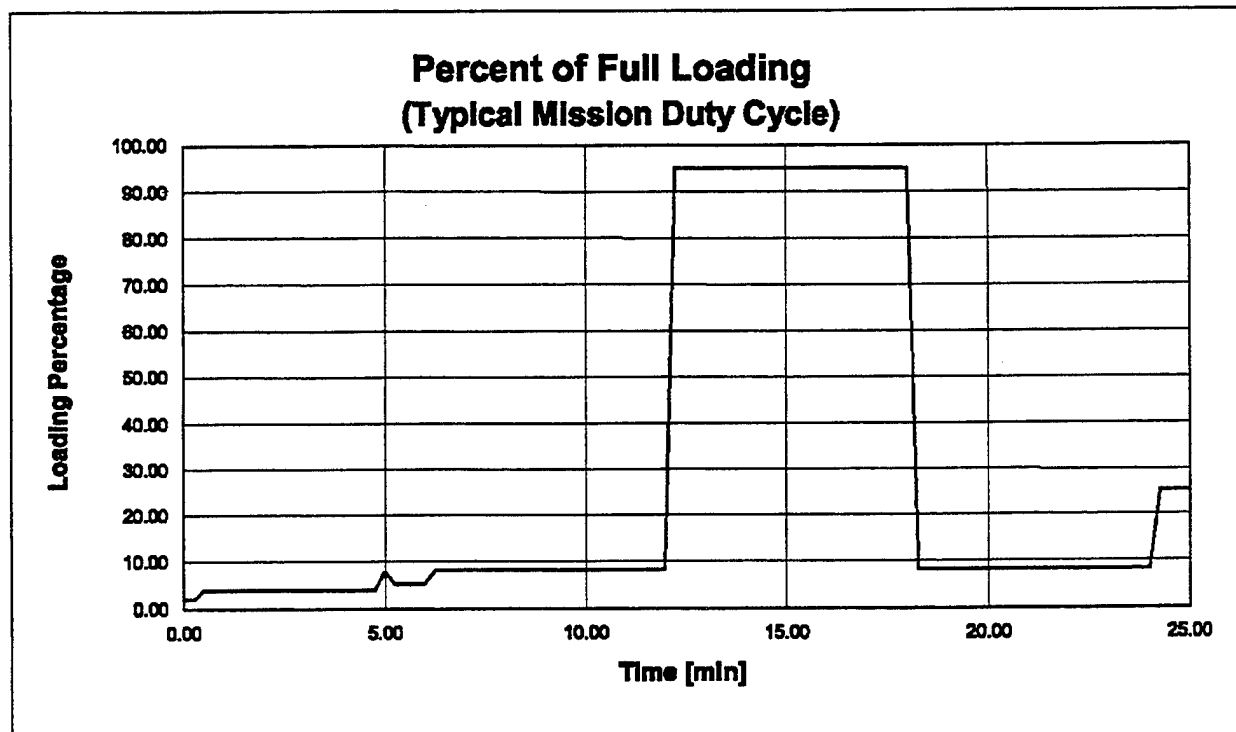


Figure 3.1.1-2 Typical Loading Percentage for Spoiler Electromotor-Actuator

3.1.2 Small Cooler Design

Problem Definition

The heat exchanger was designed to dissipate 870 W (two switches at 435 W) of continuous heat addition for a maximum of six minutes such that the temperature of the switching die junction would not exceed 125°C. In an EMA application, five of those coolers are required to cool ten switches dissipating 1,750 W (four switches at 435 W or 10 switches at 175 W). The volume of the heat exchanger(s) must be small enough to fit into the spoiler wing bay. In addition, the design must consider weight a prime driving factor.

Conceptual Design

One conceptual design for a reflux/PCM cooler is shown previously in Figure 3.1.1-1. Figure 3.1.1-1 shows a cross section of one small cooler (one cooler cools two switches). The switches measure about two in. square. Again, in the EMA application, ten switches will need to be kept cool. Therefore, five coolers of the cross section of Figure 3.1.1-1 are required.

Figure 3.1.2-1 shows the conceptual design of a large cooler. One large cooler would cool ten switches. The advantages of using one large cooler as opposed to five small ones are that it ensures better thermosiphoning action, it has a better load spreading capability in the boiler and PCM sections, and it has lower mass and cost.

The advantages of using five small coolers are that they are more fail-safe than one large cooler. If the large cooler were to leak, it would lose all of its reflux fluid. The small coolers would have the adjacent coolers to help dissipate the load. Testing and analysis were done on the small cooler design as a starting point for the test program.

Materials Selection

Aluminum was selected for the cooler casing and fins because of its brazability, machinability, cost, weight and thermal characteristics. The mounting surface on the cooler for the switches must be a material with a coefficient of thermal expansion (CTE) of approximately 7.0 ppm/°C in order to match the CTE of the switches. A 74 percent aluminum-silicon carbide MMC meets the requirements for this application. However, the prototype was made out of aluminum due to its lower cost and superior manufacturability.

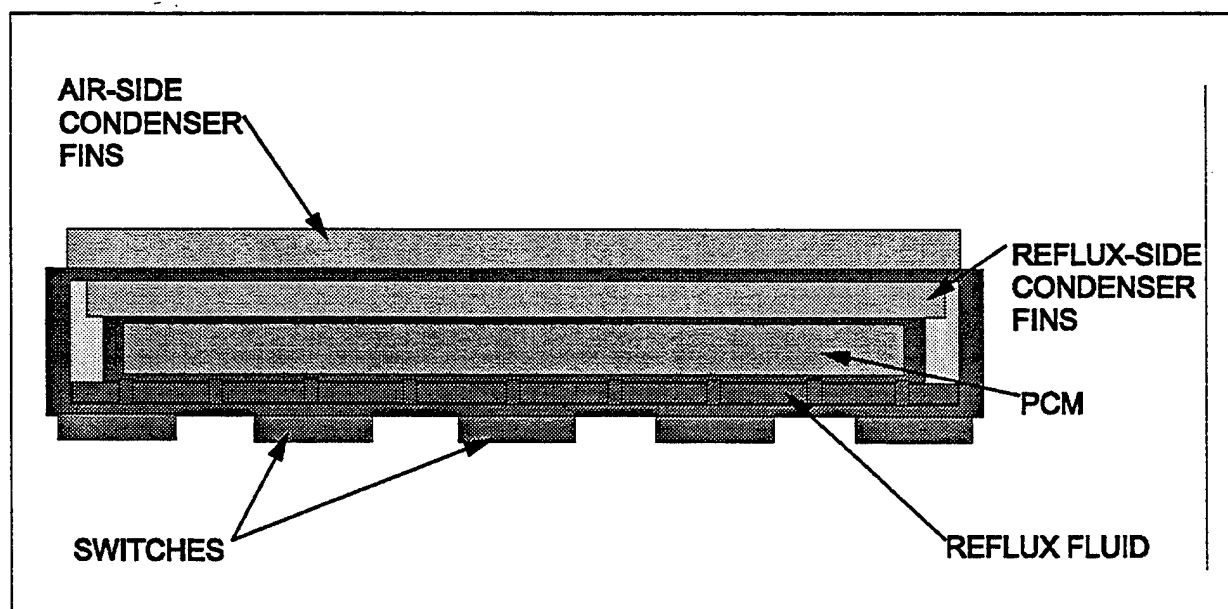


Figure 3.1.2-1 Large Cooler Design Concept

The reflux fluids used in the tests and analysis are Fluorinerts®. Specifically, FC72®, was tested. Additionally, water was tested as a reflux fluid to evaluate the effect of using a fluid with better boiling characteristics.

Research was done to determine the best PCM for the given application. Findings of the research and the design requirements are listed in Figure 3.1.2-2. Acetamide was selected as the best PCM due to its high heat of transition and ideal melt temperature. Testing was performed using T-50 however, due to its low cost, availability, and relatively simple handling and processing characteristics. Thermal analysis was performed using T-50, triacontane and acetamide.

Stress Analysis

When the reflux fluid is heated, it generates pressure. The maximum pressure that would be generated in the coolers with the reflux fluids being used is around 50 psia. A stress analysis using the finite element modeler, Ansys 5.1, was done on the small cooler design using an internal pressure of 100 psia (for a factor of safety).

The maximum stress in the cooler, which is just over 4 ksi, should not be excessive for brazed joints which can usually withstand about 10 ksi. In addition, cooler stress as a function of operating pressure is linear with operating pressure.

Thermal Analysis

In order to determine the possible benefits of using reflux/PCM technology over air cooling, a thermal analysis was done using SINDA (Systems Improved Numerical Differencing Analyzer and Fluid Integrator).

1. Fluorinert is a Registered Trademark of 3M Co.

2. FC72 is a Registered Trademark of 3M Co.

Compound Name	Stearic Acid	P-chlorostearic	T-50	Triacontane	Palmitic Acid	n-Octadecane	Sodium hydroxide Monohydrate	Diethylene Glycol	Camphor	Myristic Acid	Chloroacetic Acid
Chemical Formula	$\text{CH}_3(\text{CH}_2)_{16}\text{COOH}$	$\text{H}_3\text{C}(\text{CH}_2)_{15}\text{COOH}$		$\text{C}_{30}\text{H}_{62}$	$\text{CH}_3(\text{CH}_2)_{14}\text{COOH}$	$\text{C}_{18}\text{H}_{38}$	$\text{NaOH}\cdot\text{H}_2\text{O}$.5B, .27 Pb, .13 Sn, .1 Cd	$(\text{C}_{14}\text{H}_{27}\text{O}_2)_n$	
REQUIREMENTS:											
$80 < T_{\text{melt}} < 70^\circ\text{C}$	69.44	68.89	80	85	62	62	64	65	70	67.78	65.11
$(172^\circ\text{F} < T_{\text{melt}} < 160^\circ\text{F})$	157	158	122	149	143.8	143.6	147.2	154.4	158	138	133
$\rho_{\text{liq}} > 85 \text{ BTU/in}^3$	85.5	88.8	81.95	108	78.88	70.65	117.19	78.28	14.05	80.57	82.29
$(\rho_{\text{liq}} > 151 \text{ kJ/kg})$	188.46	198.88	188.37	250.67	185.4	164	272	184	32.6	187	191
$\rho_{\text{sol}} (\text{lb/in}^3)$	82.9	78.7	82.3	47.83	82.95	48.83	107.15		36.57	53.6	98.6
$(\rho_{\text{sol}} \text{ in } ^\circ\text{C})$	848.16	1215.15	1000	793	880	779	1720		587	880.39	1682.74
Specific Heat of Fusion $(\text{Btu} \cdot ^\circ\text{R}^{-1})$											
$> 4500 \text{ BTU/K}^2$	4,522.95	5,208.19	5,088.27	5,133.24	4,228.85	3,428.13	12,555.91		913.81	4,318.55	8,113.79
$> 168,000 \text{ kJ/K}^2$	108,515.80	124,035.15	128,370.00	121,261.21	157,680.00	127,755.00	467,840.00		18,135.20	100,832.93	302,303.34
$(K > 0.1 \text{ BTU/(in}^2\cdot^\circ\text{F)})$					0.09	0.09			10.85	0.05	
$(K > 0.178 \text{ W/m}^2\cdot^\circ\text{C})$					0.16	0.16			19	0.1	
$\Delta T_{\text{supercooling}} < 25^\circ\text{R}$ $(\Delta T_{\text{supercooling}} < 14^\circ\text{C})$	none				none				2R	none	
$\Delta T_{\text{melt}} < 30^\circ\text{C}$											
Compatible with Aluminum?	YES	YES	YES	YES	YES	YES	NO		YES	YES	
Sources:	1. Chemical Engineers' Handbook, Perry, R.H., Chilton, C.H. 1973, McGraw-Hill 2. Phase Change Materials Handbook, Hale, D.V., Lockheed Meats & Space Corp., 1971 3. National Society of Corrosion Engineers Handbook										

Figure 3.1.2-2 PCM Research

The mesh and its associated resistances/conductances are shown in Figure 3.1.2-3. Nodes 5004 and 5005 are just an extension of the switch mounting surface. This was done to see what kind of spreading might be achieved between adjacent coolers and switches. Figure 3.1.2-4 shows how switch temperature varies vs. time for various PCMs. Heat loading in the analysis follows the profile shown in Figure 3.1.1-2. Figure 3.1.2-5 shows how the cooler's performance changes with airflow. As expected, the higher the airflow, the better the cooling.

Another analysis was performed to determine if spreader thickness had any effect on switch temperature. The results were that no significant temperature decrease occurred due to changing the spreader thickness. The spreading ability of the spreader was also found to be only marginally superior in the case where a thicker spreader was put to use. The addition of material and weight in using a thicker spreader is not worth the small benefit of added spreading. Laboratory testing would later prove that a thicker spreader was necessary to prevent boiler burnout.

Cooler Weight

Figure 3.1.2-6 shows an analysis of various cooler and hardware mounting schemes. From purely a weight standpoint, it appears that using an air-cooled cooler with directly mounted switches is the best design. When thermal and switch life considerations are taken into account, the reflux/PCM coolers are superior. Analysis has shown the benefits of using reflux/PCM schemes to cool the electronics. The benefits of having colder switches and longer switch lives are necessary, therefore a reflux/PCM cooler should be chosen.

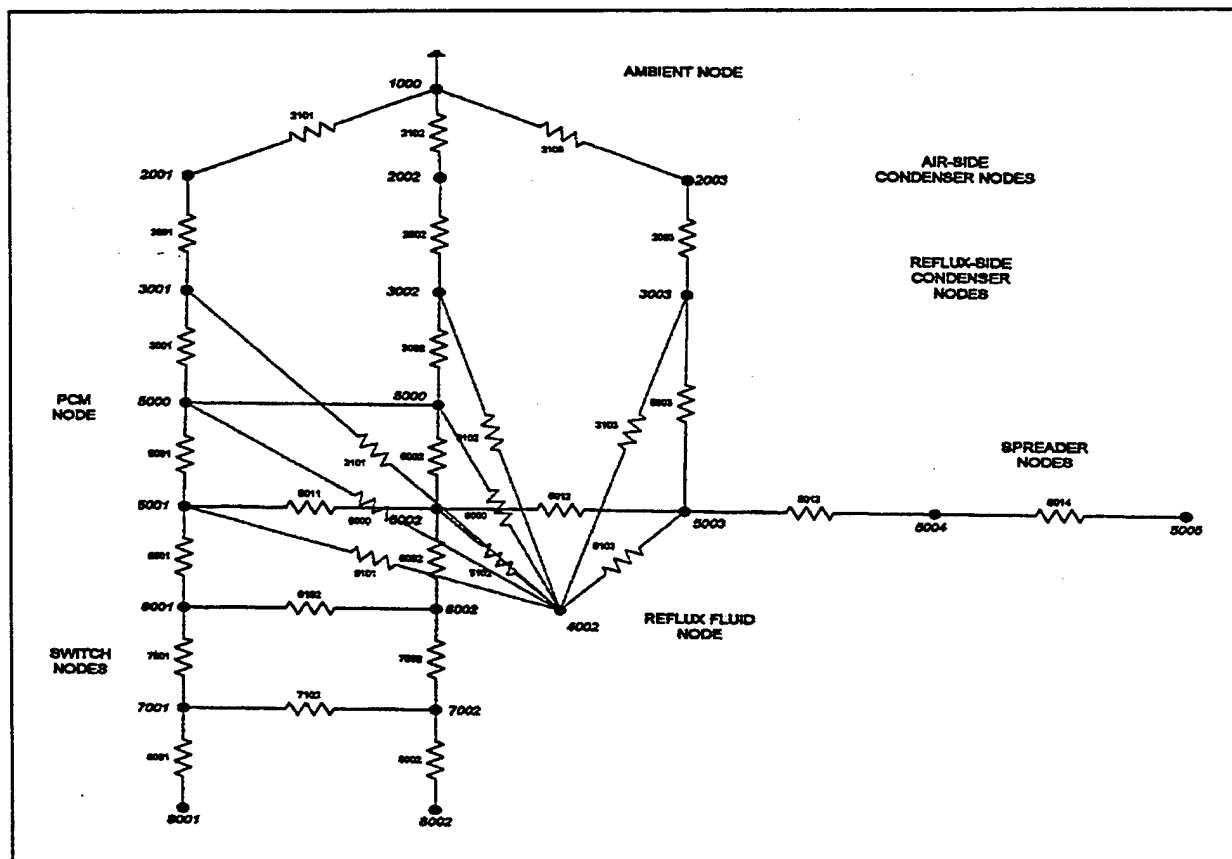


Figure 3.1.2-3 Thermal Circuit Diagram Used in SINDA Analysis

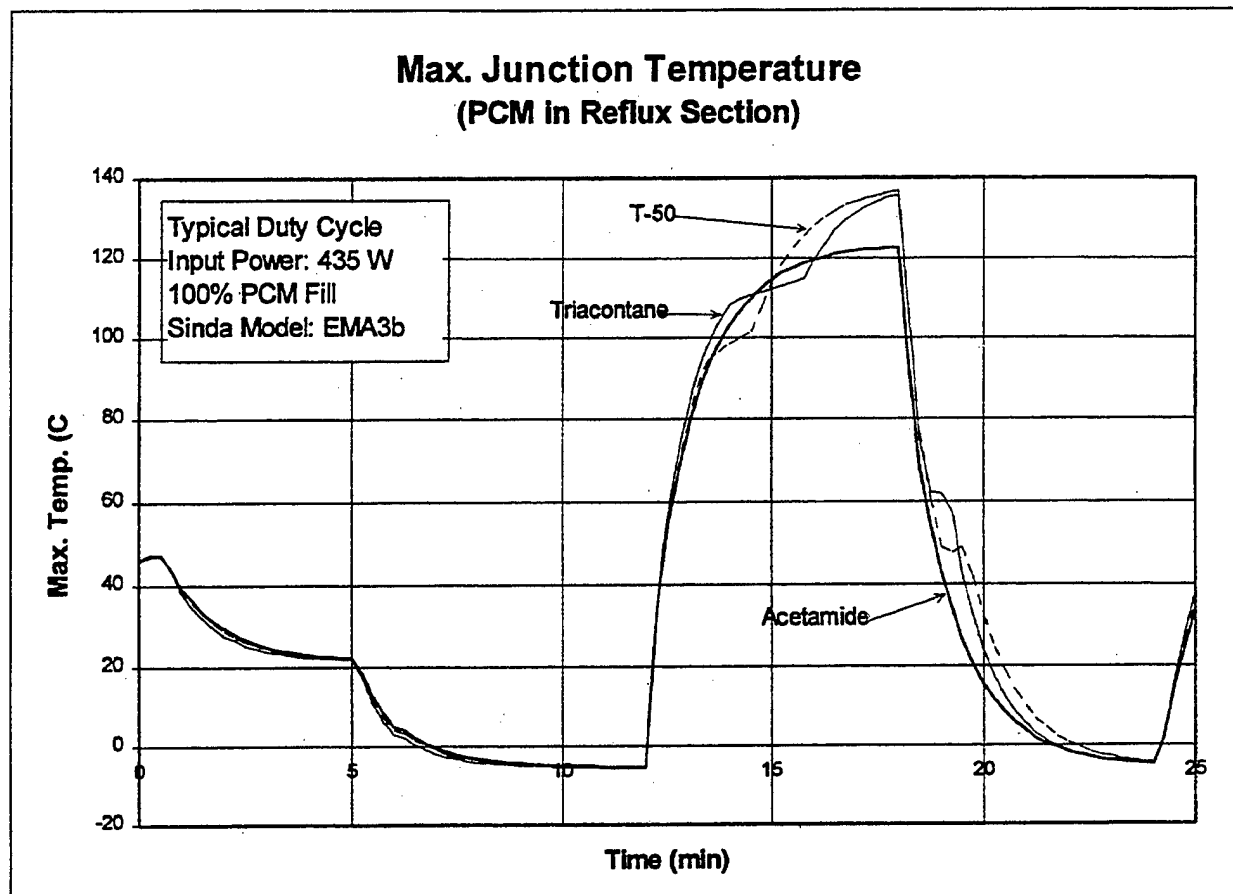


Figure 3.1.2-4 Die Temperature for Differing PCMs

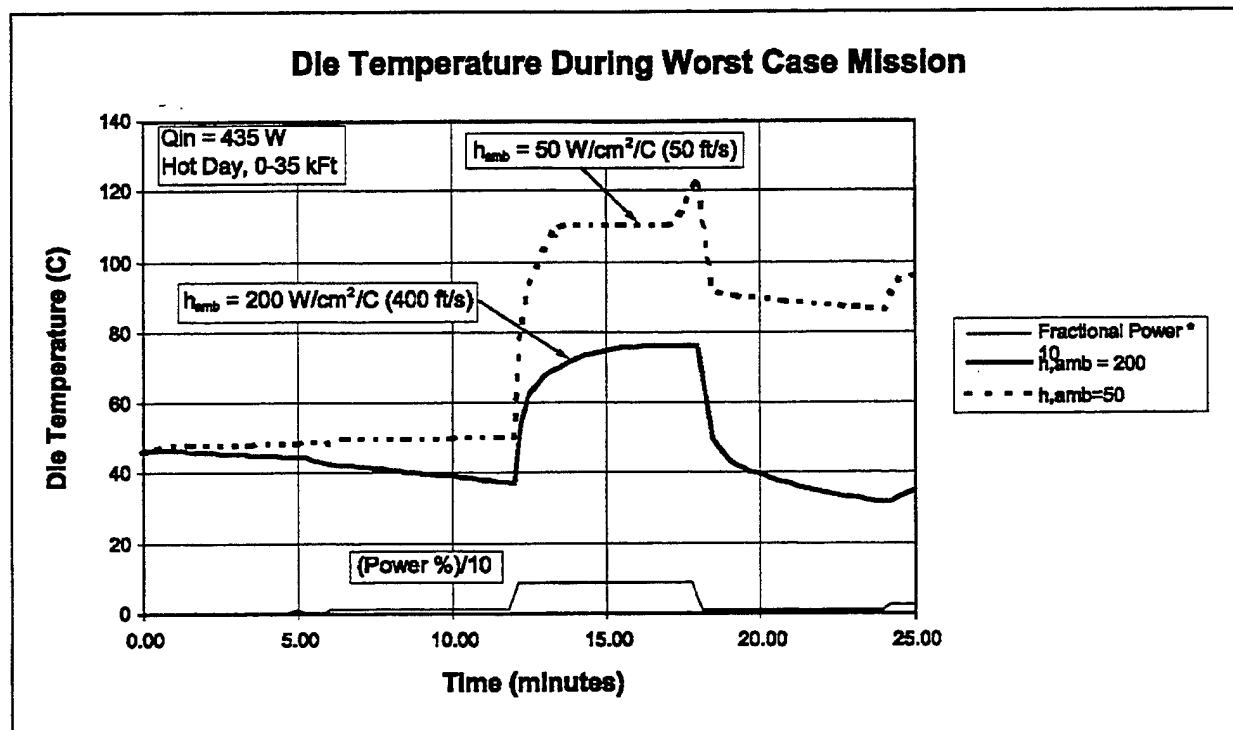


Figure 3.1.2-5 Die Temperature for Differing Air Velocities Using Triacontane PCM

Cooler Weight Comparison Chart							
	Single Plate 10 M-packs	Single Plate - 10 direct mounts	5 Plates - 2 M-packs each	5 Plates - 2 dies each	10 Plates - 1 M-pack each	Direct air cooled - 10 M-packs **	Direct air cooled - 10 direct mounts**
Cooler Volume * [in^3]	82.5	82.5	90.0	90.0	112.5	42.0	42.0
Cooler Weight w/o fluid (lbm)	2.20	2.20	2.88	2.88	3.60	1.78	1.78
PCM (lbm)	2.15	1.40	2.15	2.15	2.15	0.00	0.00
Reflux Fluid (lbm)	0.23	0.15	0.23	0.23	0.23	0.00	0.00
Electronics weight (lbm)	1.98	0.72	1.98	0.72	1.98	1.98	0.72
Total Weight	6.56	4.47	7.24	5.98	7.96	3.76	2.50
* Includes volume of air side fins and enclosed void spaces ** Air cooled versions reach 120C after 25 seconds @ full load, hot day.							

Figure 3.1.2-6 Cooler Weight Comparison Chart

Practical Design

Thermal and stress analysis have shown that the reflux/PCM design meets the operating requirements. Therefore, a detailed design of the cooler was done. Figure 3.1.2-7 shows the probable orientation of the cross section for a cooler in an emergency decent (this cross section is at 90 degrees to the cross section shown in Figure 3.1.1-1). The cooler is tilted such that only half of the switches will be below the reflux liquid level. As boiling occurs in the liquid, the liquid and vapor will rise and wet the surfaces of the other five switches. The condenser efficiency is governed largely by the quality of the vapor going through it. A quality of one (all vapor) yields higher efficiencies than lower qualities. By leaving a large enough gap in the upper bend of the cooler (where the vapor rises), the carryover rate of liquid in the liquid/vapor stream entering the condenser should be small. The condenser will then condense the vapor and the fluid will drain back down to the lower switches.

3.1.3 Thermal Testing

3.1.3.1 Testing Summary

Thermal tests were done on M-packs with #108 IGBT dies using convective air cooling and reflux/PCM cooling. The air cooled tests were done to serve as benchmarks to compare with the reflux/PCM tests. Thermstrate® was used at the switch to cold plate interface for all testing.

For the air only tests, two M-packs were mounted to a plate-fin air cooler and then mounted to fan ducting. DC power was run through the switches and various temperature measurements (i.e., junction temperature, case temperature, flange temperature, and air temperature) were made. Power and air flow were the test parameters. Air flow was ran from 7.5 lbm/min to 0 lbm/min and power was ran from 50 W per switch to 170 W per switch. Thermocouples, an infrared (IR) camera and a Luxtron probe were all used to measure temperatures. Results

3. Thermstrate is a Registered Trademark of Power Devices, Inc.

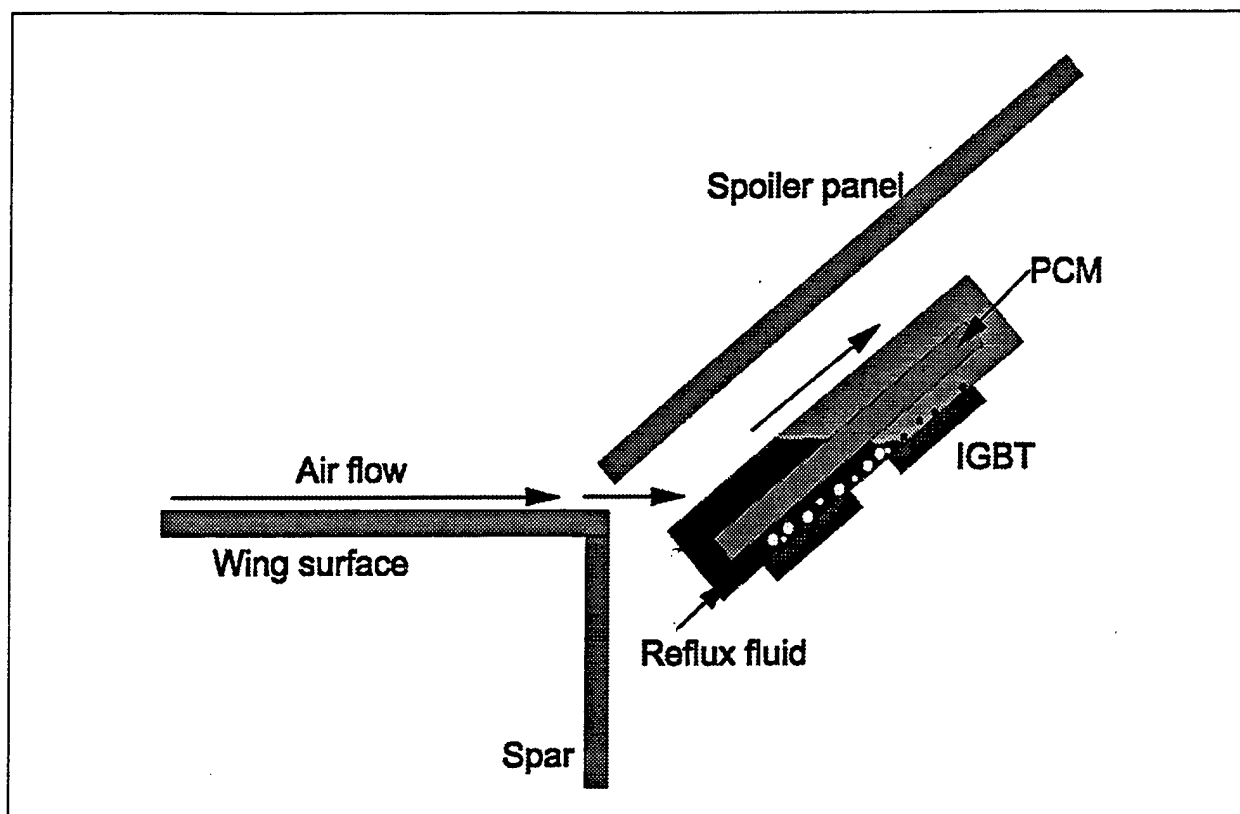


Figure 3.1.2-7 Cooler Orientation in Spoiler—During Descent

revealed a maximum junction temperature of 114°C during the high power/high flow test and a max. junction temperature of ~ 100°C for the low power low flow case.

For the reflux/PCM tests, the same two M-packs were mounted to the small cooler design which was then mounted to the fan ducting. DC power was then run through the switches and various temperature measurements (i.e., junction temperature, case temperature, PCM temperature, boiler temperature, condenser temperature, flange temperature, and air temperature) were made. Power, reflux fluid type and fill amount, cooler attitude and air flow were the test parameters. Input power was ran at 170 and 225 W per switch. Air flow was ran at 0 lb/min and 4.7 lb/min. Cooler attitude was ran at 0 degrees (horizontal), 30 degrees, 90 degrees (vertical), and 40 degrees laterally. FC72® and water were the reflux fluids used with 35 grams and 75 grams of FC72® being tested and 26 cc's and 44 cc's of H₂O being tested. Thermocouples, an infrared (IR) camera and a Luxtron probe were all used to measure temperatures. Results of reflux/PCM tests show poor performance compared to thermal analysis. A maximum junction temperature (using FC72®) of 115°C during the 340 W and 4.7 lbm/min test was achieved. Reasons for the cooler performing below predictions include boiler burnout due to a heat flux beneath the die exceeding the critical heat flux of the fluid and questionable thermosiphoning action occurring in the small cooler.

3.1.3.2 Air Cooled Testing

Introduction

In order to determine quantitatively benefits of using a Reflux/PCM cooler, a benchmark air-cooled test was performed.

The objectives of the tests were:

- To determine quantitatively the ability of an air only heat exchanger to cool M-pack switches.

- Determine input power/airflow/junction temperature relationships.
- To debug the test equipment and improve testing techniques.

Test Parameters

The main test parameters for the air-cooled tests were input power and air flow rate. A supplementary parameter of contact interface between the switch and the cold plate was also looked at with the interface either being a bare contact or a Thermstrate® interface. The Thermstrate® interface data is more relevant to the overall test plan because the reflux/PCM coolers will also be tested with this interface material. Therefore, the bare contact interface data will not be discussed.

The fans that were used to create air flow had a maximum mass flow rate of 7.5 lbm/min for this cooler, therefore it is the upper bound. Mass flows of 7.5, 4.5, and 0 lbm/min were used. Input power was limited to a value that did not bring the die junction temperature above 120°C. This was done to protect the switches for further tests and it dictated the maximum power input for a particular air flow. The exact test plan is shown in Table 3.1.3.2-A.

Table 3.1.3.2-A Test Plan

Input Power (per Switch)	Mass Flow		
	7.5 lbm/min	4.5 lbm/min	0 lbm/min
50 W	X	X	X
100 W	X	X	X
150 W	X	X	
200 W	X	X	

It should be noted that the actual values of input power and air flow vary slightly from the values in the test plan. For instance, for the 4.5 lbm/min case, an input power of 187 W was used while in the 7.5 lbm/min case an input power of 205 W was used. This was done to try to get the junction maximum temperature to be as close to 120°C as possible without going over.

Test Equipment

The following equipment was used to measure temperatures and pressures of the test article:

- Hughes Probeye Thermal video system model # 7300
- Luxtron model #755 fluoroptic thermometer
- Dwyer manometer
- Hewlett Packard model 6011A power supplies (2)
- Sorenson model QRD 20-P power supplies (2)
- Type T thermocouples (6)
- Video cassette recorder

All thermocouple data were acquired by a PC-based data acquisition system with Notebook® data acquisition software. Electrical input power was measured from the digital displays on the power supplies. IR camera data were recorded using the VCR.

Table 3.1.3.2-B shows the estimated uncertainties for the data. An emissivity calibration was done for the Hughes IR camera.

4. Notebook is a Registered Trademark of LabTech.

Table 3.1.3.2-B Test Equipment Uncertainty Estimates

Measuring Device	Uncertainty
Hughes IR Camera	$\pm 4^{\circ}\text{C}$
Luxtron Probe	$\pm 4^{\circ}\text{C}$
Manometer	$\pm .1 \text{ in. H}_2\text{O}$
Power supplies	$\pm 20 \text{ W}$
Thermocouples	$\pm 1.2^{\circ}\text{C}$

Accuracy of the mass flow rate is estimated at $\pm .75 \text{ lbm/min.}$

Test Setup

The test equipment was setup as shown in Figures 3.1.3.2-1 and -2. The switches were mounted to the heat exchanger with a torque of 10 in.-lb. The heat exchanger was then mounted to the fan ducting and the power supplies were connected to the switches. Thermocouples were mounted at the air inlet and exit, as well as the switch locations shown in Figure 3.1.3.2-3. The manometer was connected to a fitting on top of the air ducting so that it read the static inlet pressure and the IR camera was positioned to read (quantitatively) the junction temperature of the upper switch. Qualitative readings of the temperatures over both switch surfaces were also recordable.

Test Procedure

Once all of the test equipment was hooked up, items such as ambient temperature and die junction initial temperature were measured using the Luxtron probe (junction temperature was measured at the location shown in Figure 3.1.3.2-3. In addition, the air flow fans were set to the desired value and the heat exchanger pressure drop was measured. Next, the data acquisition

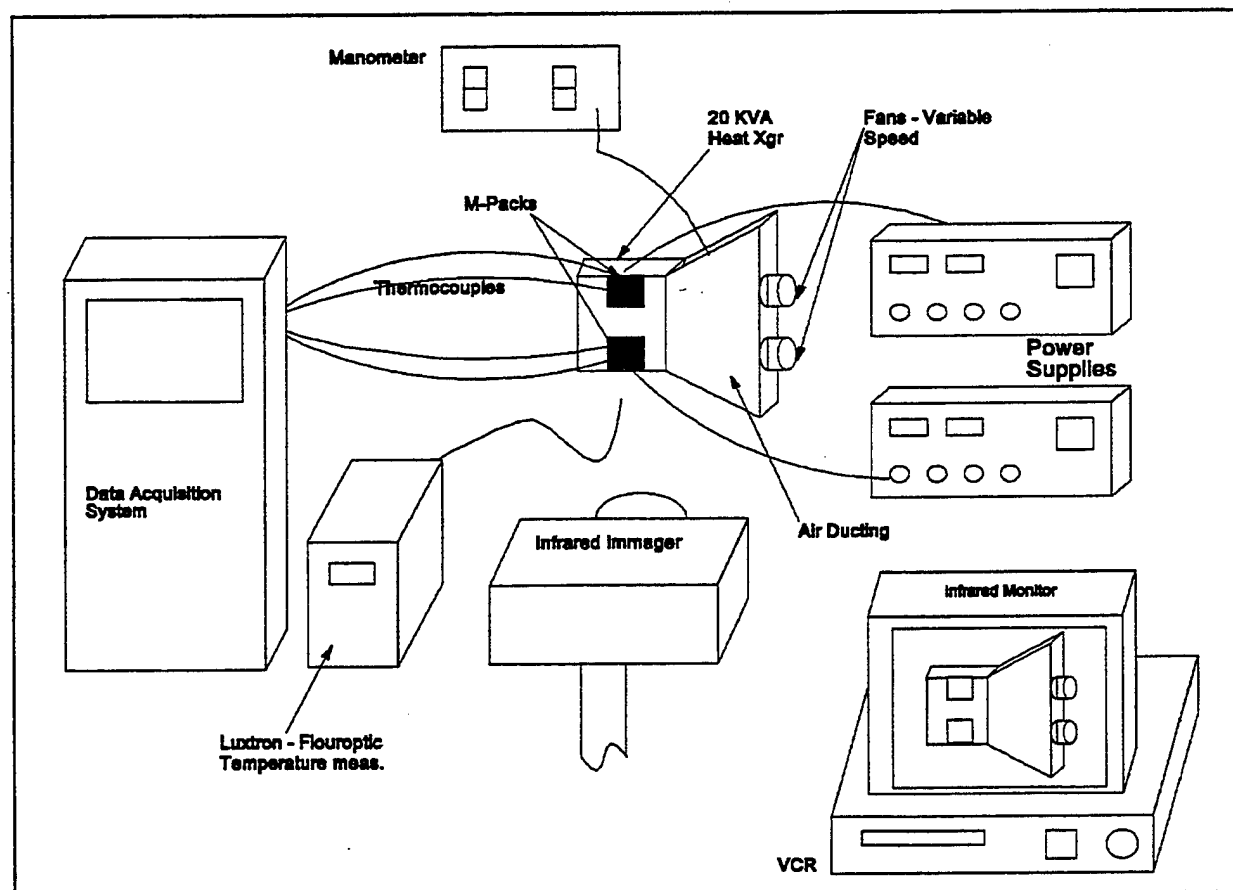


Figure 3.1.3.2-1 Test Equipment and Setup



Figure 3.1.3.2-2 Test Equipment and Setup

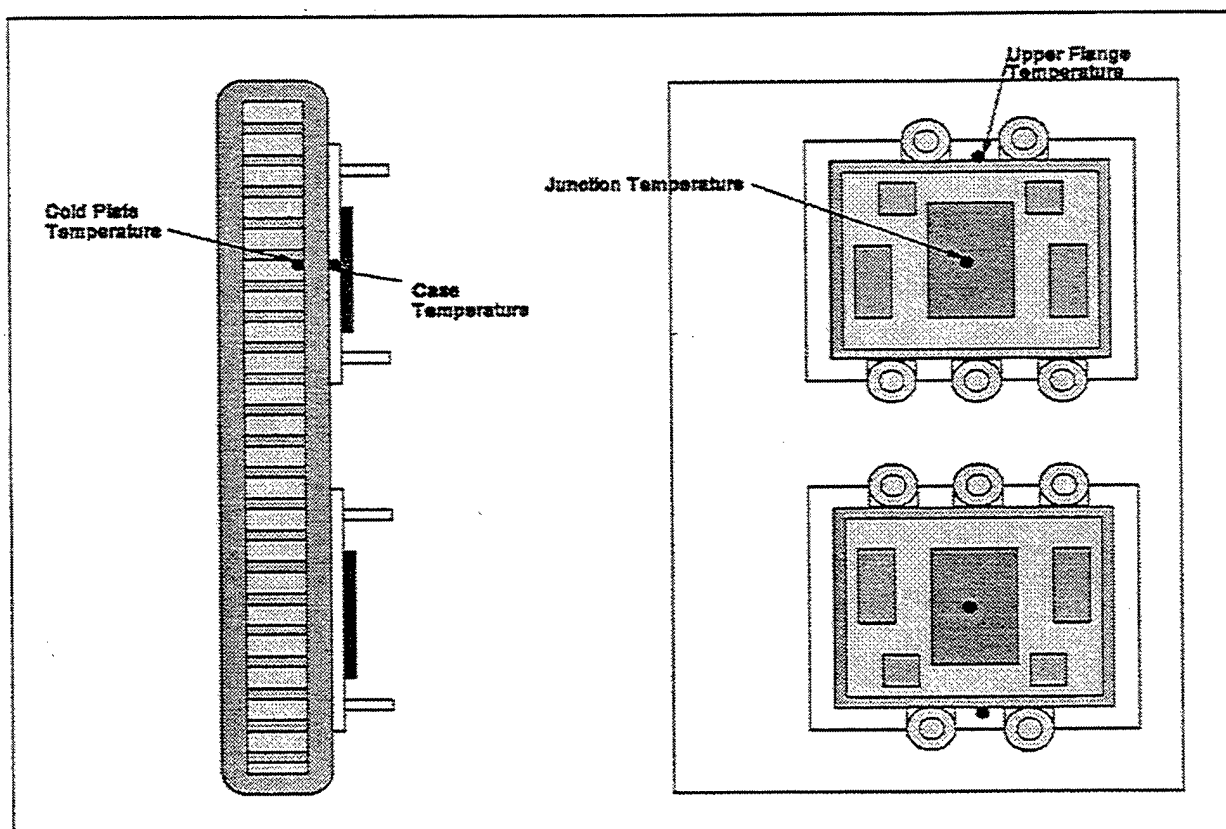


Figure 3.1.3.2-3 Test Article and Measurement Points

system and VCR were started and dc power was applied to the switches. After the IR camera and case thermocouple temperatures reached steady-state, a measurement of the upper and lower switch junction temperatures were made using the Luxtron probe. Power was then disconnected from the system and temperatures were allowed to reach ambient. All of the above was then repeated for the power inputs and air flow rates listed in the test parameters subsection of this report.

Test Results

Figure 3.1.3.2-4 shows junction temperature (recorded with the IR Camera) and case temperature (recorded with a thermocouple) for a high power/high flow test. It shows that the temperatures are tracking well with a resistance of about $0.025^{\circ}\text{C}/\text{W}$. In addition, the initial and final temperatures are shown as measured with the Luxtron probe. Figure 3.1.3.2-5 plots IR camera junction temperature data for the highest input loading for each of the three air flow cases. For the 7.5 lbm/min and 4.5 lbm/min cases, a steady state was reached after about two to three minutes. The 0 lbm/min case however, did not reach steady state even after 5 minutes and the test had to be terminated due to elevated junction temperatures.

Test Conclusions

The air tests performed serve well as a baseline comparison to the reflux/PCM testing. The results of the tests indicate that unless a high heat transfer coefficient (air velocity) can be achieved, then air cooling will not be sufficient to cool the switches. Even in the high air velocity tests, a power input of only 170 W per switch was attained for a junction temperature of 120°C . This is much lower than the 430 W of heat input that has been projected for the switches. Junction temperature/input power/airflow relationships were all quantitatively defined.

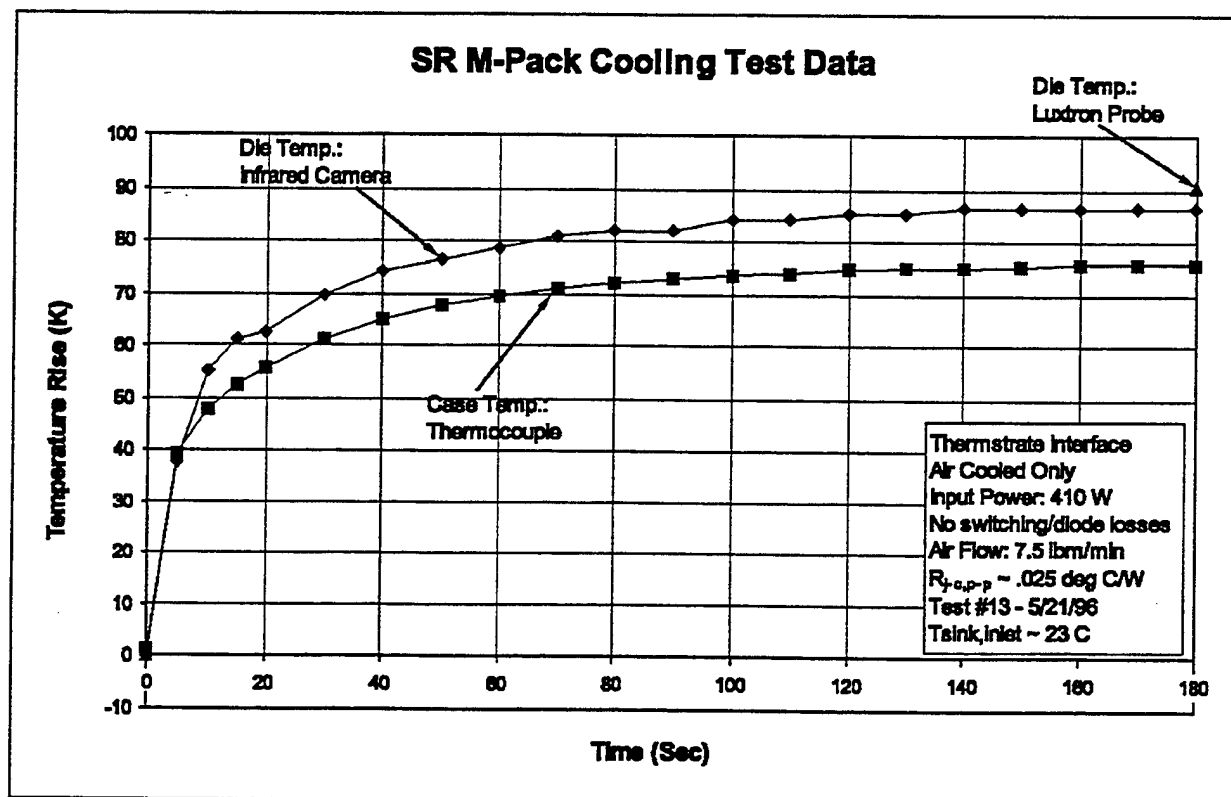


Figure 3.1.3.2-4 Junction and Case Temperature Rises for the High Power/High Air Flow Test

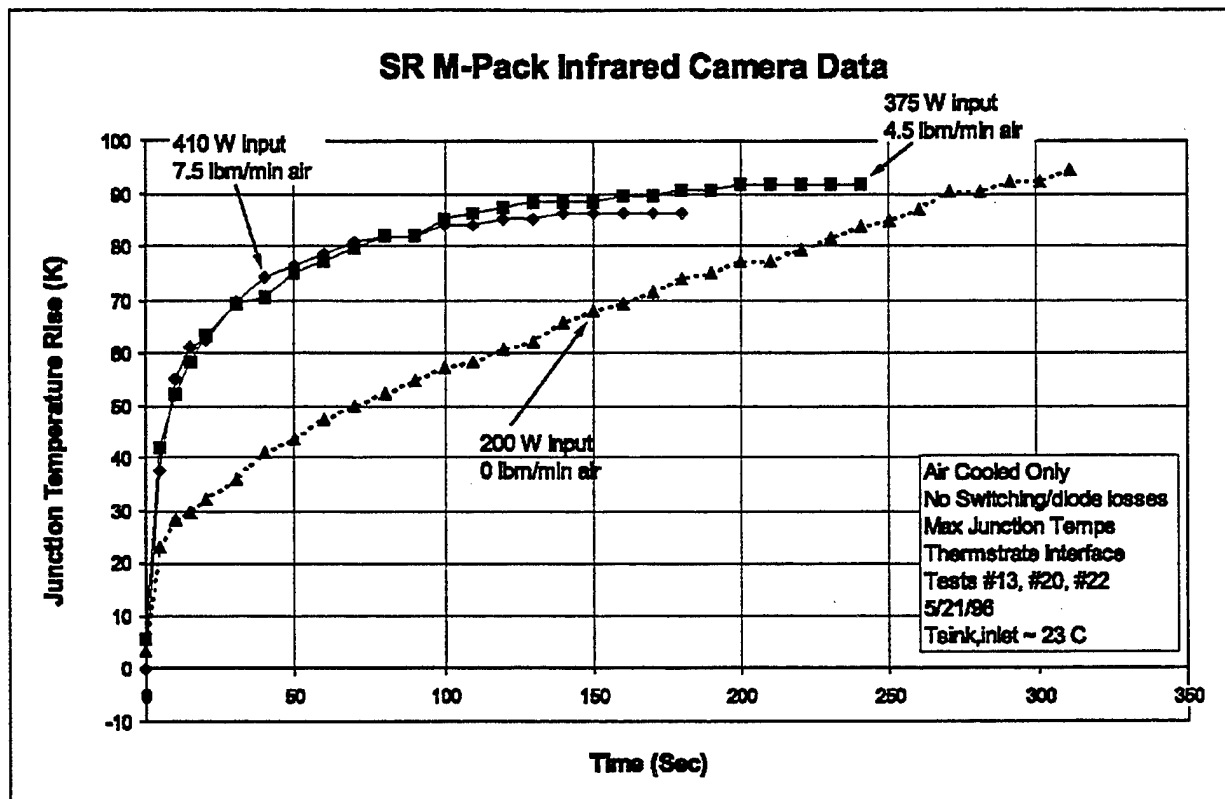


Figure 3.1.3.2-5 Junction Temperature Rise for Various Input Loads and Air Flows

3.1.3.3 Reflux/PCM Cooled Testing

The objectives of the reflux/PCM cooled tests are:

- To determine quantitatively the ability of a reflux/PCM heat exchanger to cool M-pack switches
- Determine input power/airflow/cooler attitude/reflux fill and type/junction/temperature relationships

Test Parameters

The main test parameters for these tests are input power, reflux fluid type and quantity, air flow rate and cooler attitude. Thermstrate was used at the switch to cooler interface just as it was used for the air cooler testing.

The fans that were used to create air flow had a maximum mass flow rate of 4.7 lbm/min for this cooler, therefore, it is the upper bound. Mass flows of 4.7 and 0 lbm/min were used. Input power was varied from 170 W per switch to 225 W per switch. Cooler attitudes were 0, 30, and 90 degrees rotated about a point in the center of the cooler as shown in Figure 3.1.1-1. An additional attitude of 40 degrees was tested rotated as shown in Figure 3.1.3.3-1. FC72® is the initial reflux fluid used with quantities of 35 grams and 75 grams. Later testing is done using water with 26 cc and 44 cc quantities.

Test Equipment

The same test equipment and uncertainties were used in this testing as were used in the air cooled testing. The only addition is that reflux fluid pressure was measured using an Endevco model 8510b pressure transducer with an uncertainty of ± 1.5 percent of full scale reading (full scale is 200 psia).

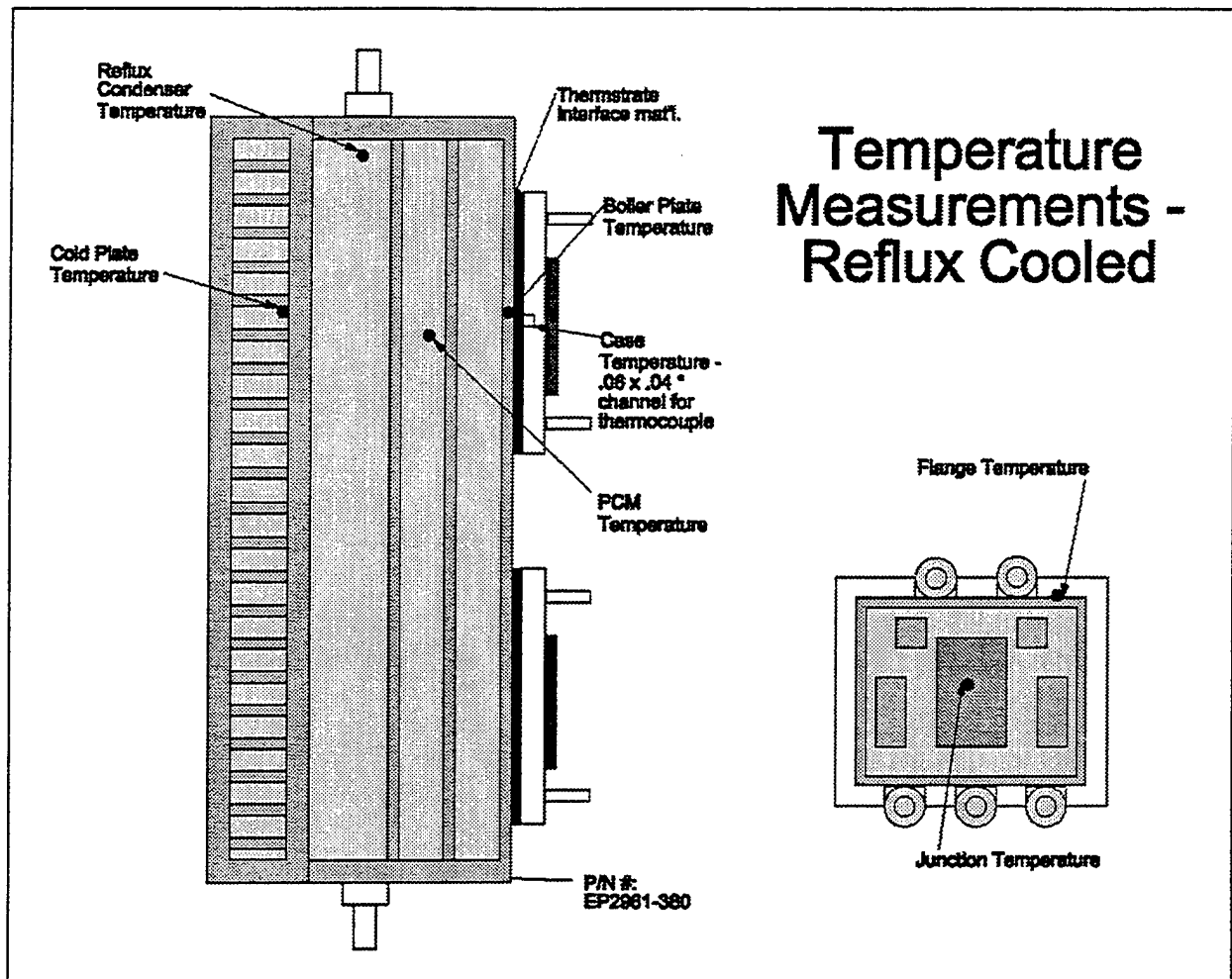


Figure 3.1.3.3-1 Reflux Testing—Temperature Measurement Points

Test Setup

The test setup for the reflux/PCM testing is identical to the test setup shown in Figure 3.1.3.2-1 and -2 for the air cooled testing. The attitude articulation of the cooler was achieved using a large mill head. Figure 3.1.3.3-1 shows the various points at which temperature measurements were made.

Test Procedure

Once all of the test equipment was hooked up, items such as ambient temperature and die junction initial temperature were measured using the Luxtron probe (junction temperature was measured at the location shown in Figure 3.1.3.3-1). In addition, the air flow fans were set to the desired value and the heat exchanger pressure drop was measured. Next, the data acquisition system and VCR were started and dc power was applied to the switches. After the IR camera and case thermocouple temperatures reached steady-state, a measurement of the upper and lower switch junction temperatures were made using the Luxtron probe. Power was then disconnected from the system and temperatures were allowed to reach ambient. All of the above was then repeated for the power inputs, air flow rates, cooler attitudes and reflux fluids listed in the test parameters section of this report.

Test Results

Figure 3.1.3.3-2 shows a plot of the junction temperature rise normalized by input power vs. time for air and reflux cooled switches. The results are not what was expected from the thermal analysis. This plot suggests that the air cooled switches are cooler than the reflux cooled switches, by about 5°C , after 250 seconds. Figure 3.1.3.3-3 suggests why this is occurring. The delta temperature from the boiler to the condenser is 50 degrees for this plot using 75 grams of FC72® Fluorinert®. This is almost half of the total temperature drop through the whole cooler. Typical boiler to condenser temperature drops are around 10 to 20 percent of the total drop. This indicates that the critical heat flux of the FC72® ($\sim 17 \text{ W}/\text{cm}^2$) has been exceeded and burnout is occurring at the boiler. Burnout occurs when boiling is so rapid that the fluid cannot rewet the surface. This results in very poor heat transfer coefficients.

Figure 3.1.3.3-4 also shows boiler burnout occurring when only 26 cc's of water (critical heat flux $\sim 150 \text{ W}/\text{cm}^2$) are used. It also shows burnout being eliminated when 44 cc's of water are used. The temperature delta is only 15°C in this case. Unfortunately, Figure 3.1.3.3-5 shows that once burnout is eliminated, the cooler becomes condenser limited (the delta temperature rises) for the fluid type and amount used.

On a better note, Figure 3.1.3.3-6 shows a plot of case, reflux, PCM, and switch flange temperatures over time for a typical case. This plot illustrates that the PCM is being used for thermal storage (see the flattening of the PCM curve from 40 to 60 seconds). Unfortunately, this flattening is of too short a duration for it to have much effect on the junction temperature. Increased PCM mass would increase this effect.

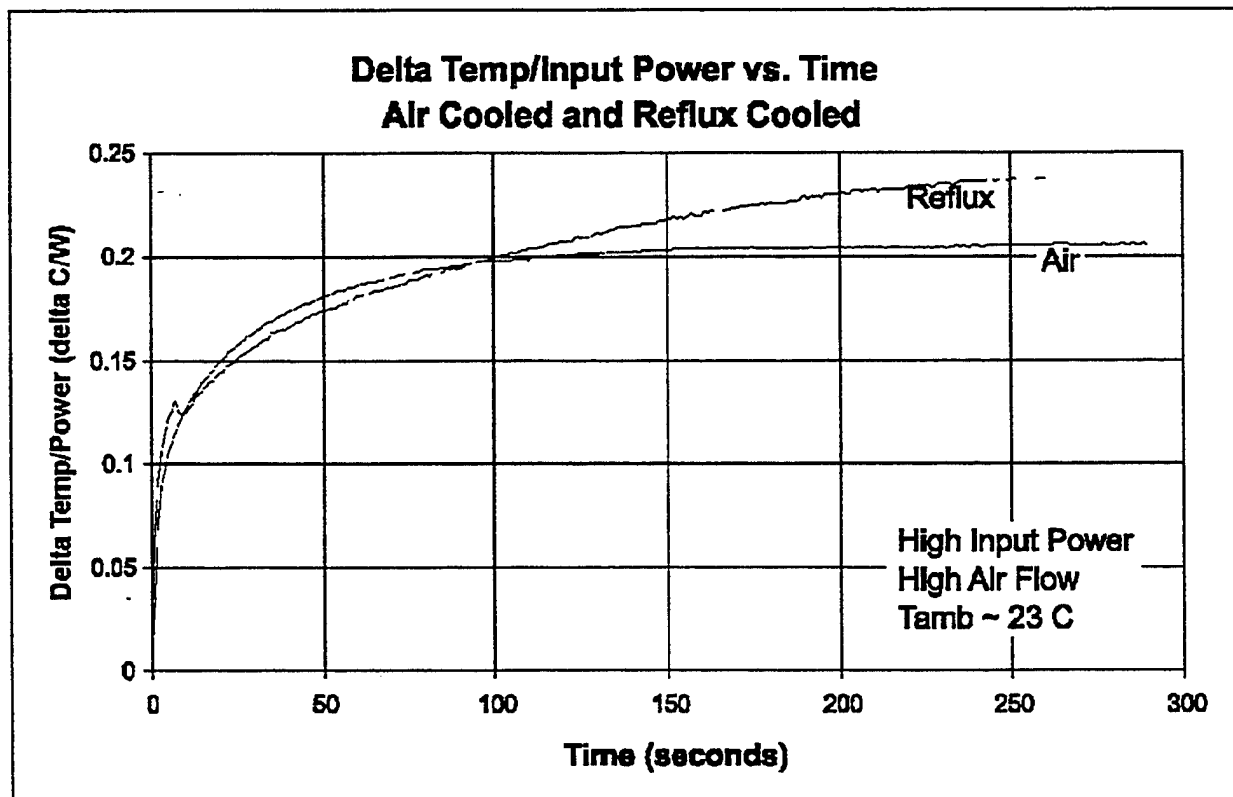


Figure 3.1.3.3-2 Comparison of Reflux and Air Cooled Switches

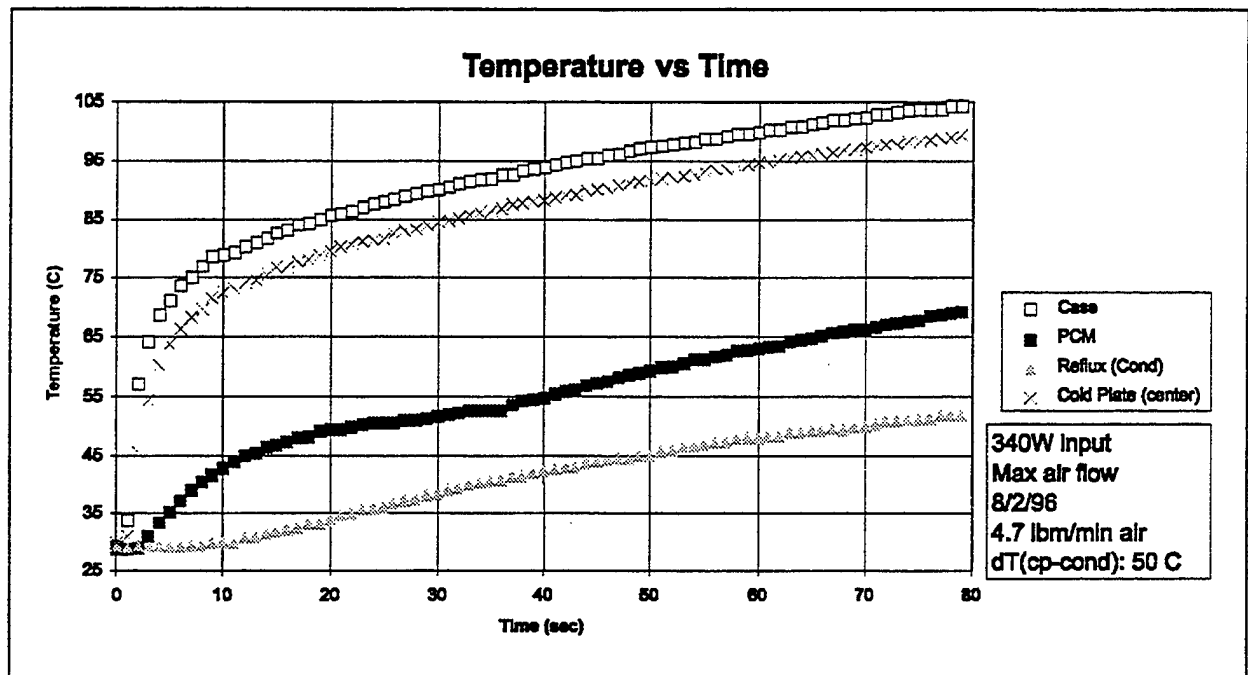


Figure 3.1.3.3-3 Plot Indicating Boiler Burnout

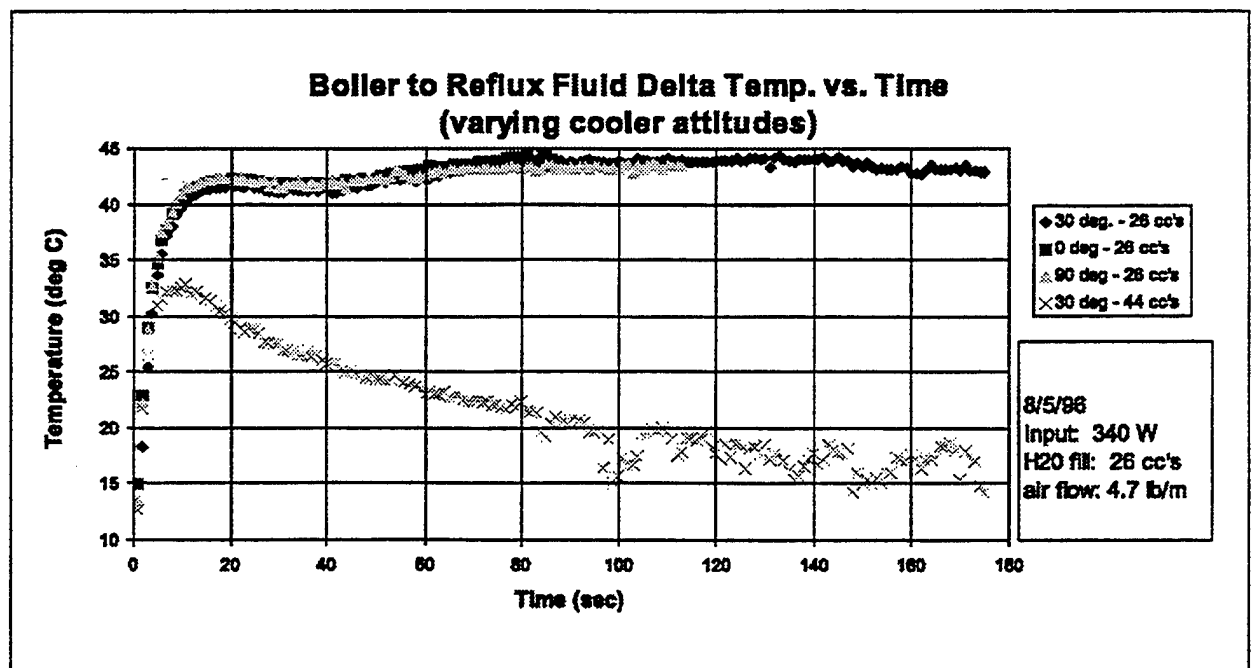


Figure 3.1.3.3-4 Plot Indicating Boiler Burnout and Elimination

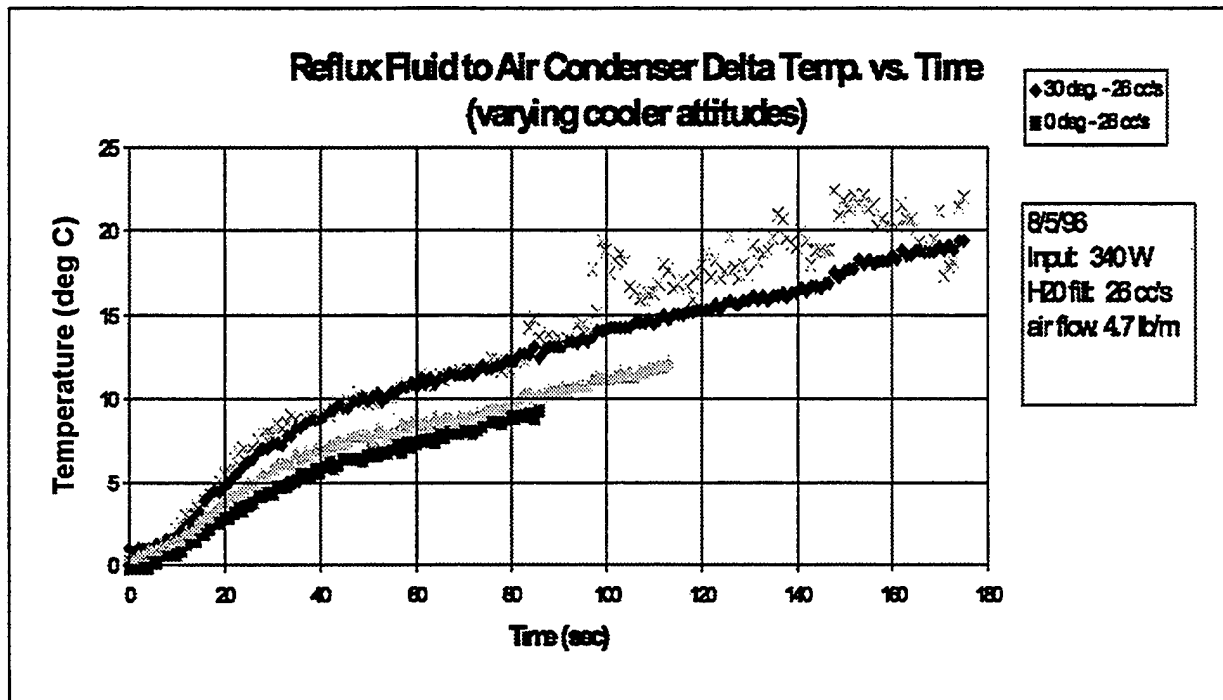


Figure 3.1.3.3-5 Plot Indicating Condenser Limitations

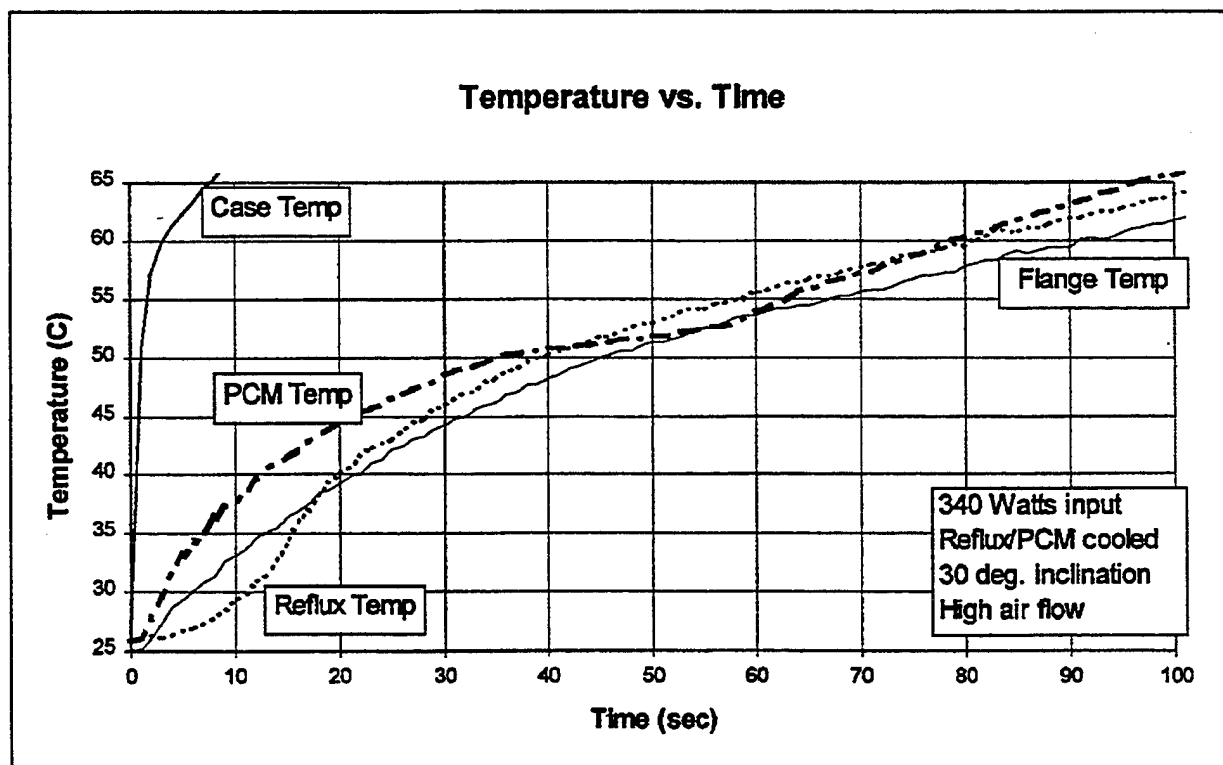


Figure 3.1.3.3-6 Plot Indicating PCM Storage and Reflux Incipience

Figure 3.1.3.3-7 shows that at a fill level of 26 cc's of H₂O, there is no discernible difference in case temperature rise as a function of cooler attitude. Figure 3.1.3.3-8, however, shows that at 44 cc's of H₂O, there is a change in the case temperature rise for a given attitude change. The lack of a difference in the 26 cc fill case is due to boiler burnout. Judging by Figure 3.1.3.3-8, the cooler operates best in a 90 degree (vertical) orientation, probably due to thermosiphoning action.

Figure 3.1.3.3-9 shows that the fill volume affects the performance of the cooler. The case temperature, and hence the die temperature, is kept more than 20°C cooler in the 44 cc fill volume test vs. the 26 cc fill volume test.

Not shown here is a test using no air flow. Performance in this case was greatly reduced yielding die temperatures up to 30°C higher than if 4.7 lbm/min of air was flowing. This is expected because an energy balance shows that over 200 W of energy were being rejected through the condenser during a steady state run.

Test Conclusions

Although reflux/PCM cooler performance was not what was expected, it is believed that the problems with the design have been identified. Those problems are boiler burnout, condenser limitations and inadequate PCM section size. Improvements to these areas should yield performance benefits that will approach the idealized thermal analysis.

Parametric studies using water have been carried out and cooler operation as a function of attitude, fluid fill and air flow have been determined. Additional studies regarding fluid fill percent as a function of boiler and condenser performance should be done, if a redesign is made.

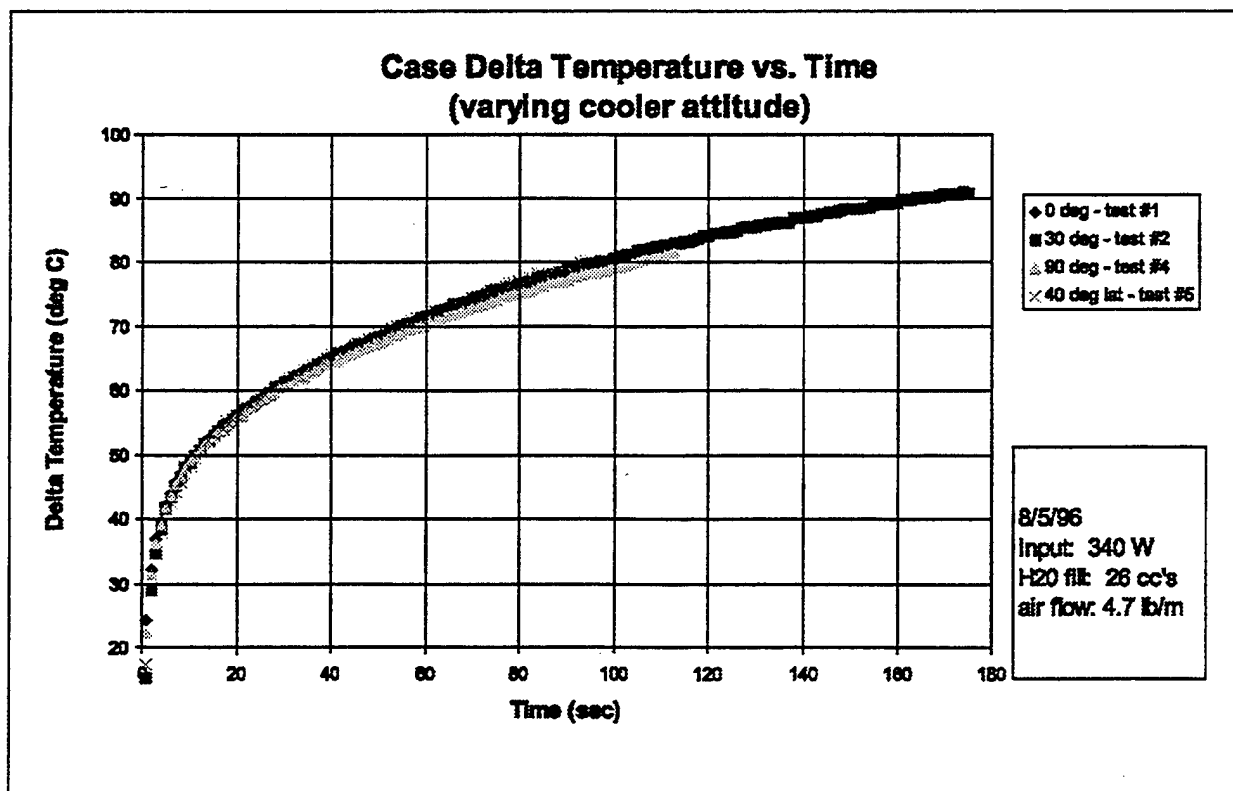


Figure 3.1.3.3-7 Case Temperature as a Function of Cooler Attitude (26 cc H₂O Fill)

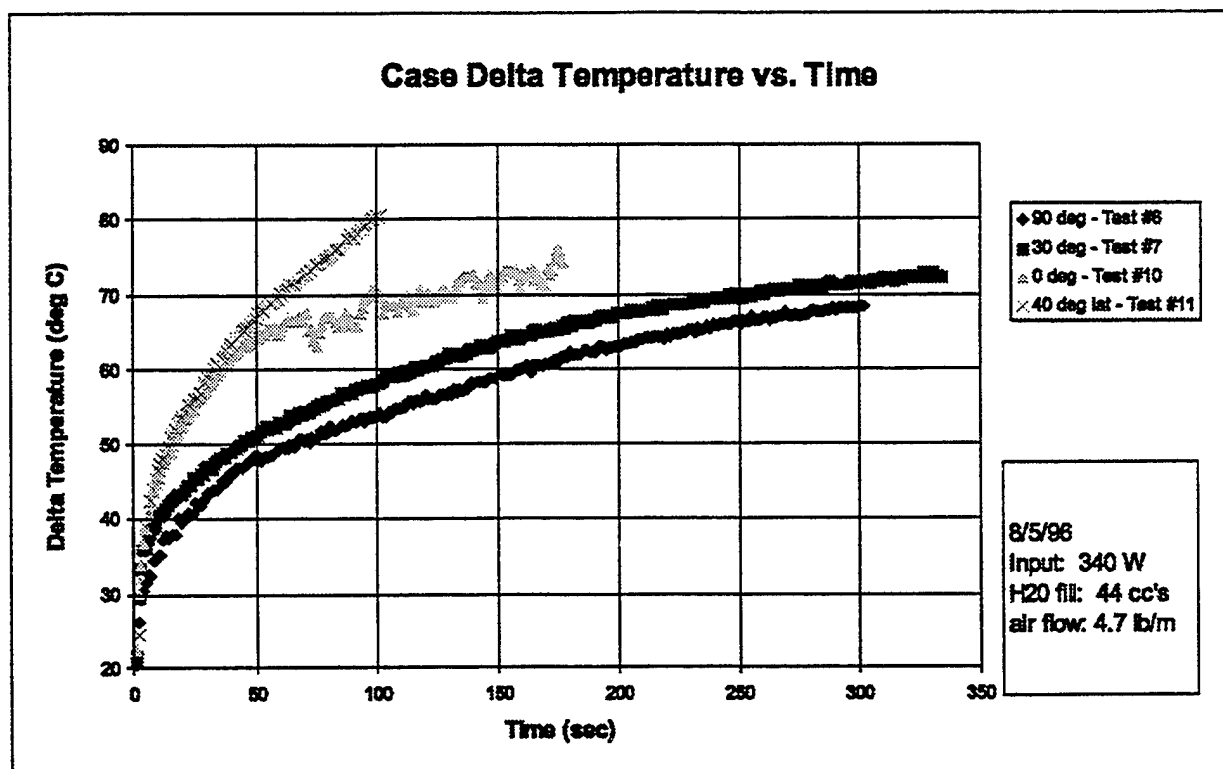


Figure 3.1.3.3-8 Case Temperature as a Function of Cooler Attitude (44 cc H₂O Fill)

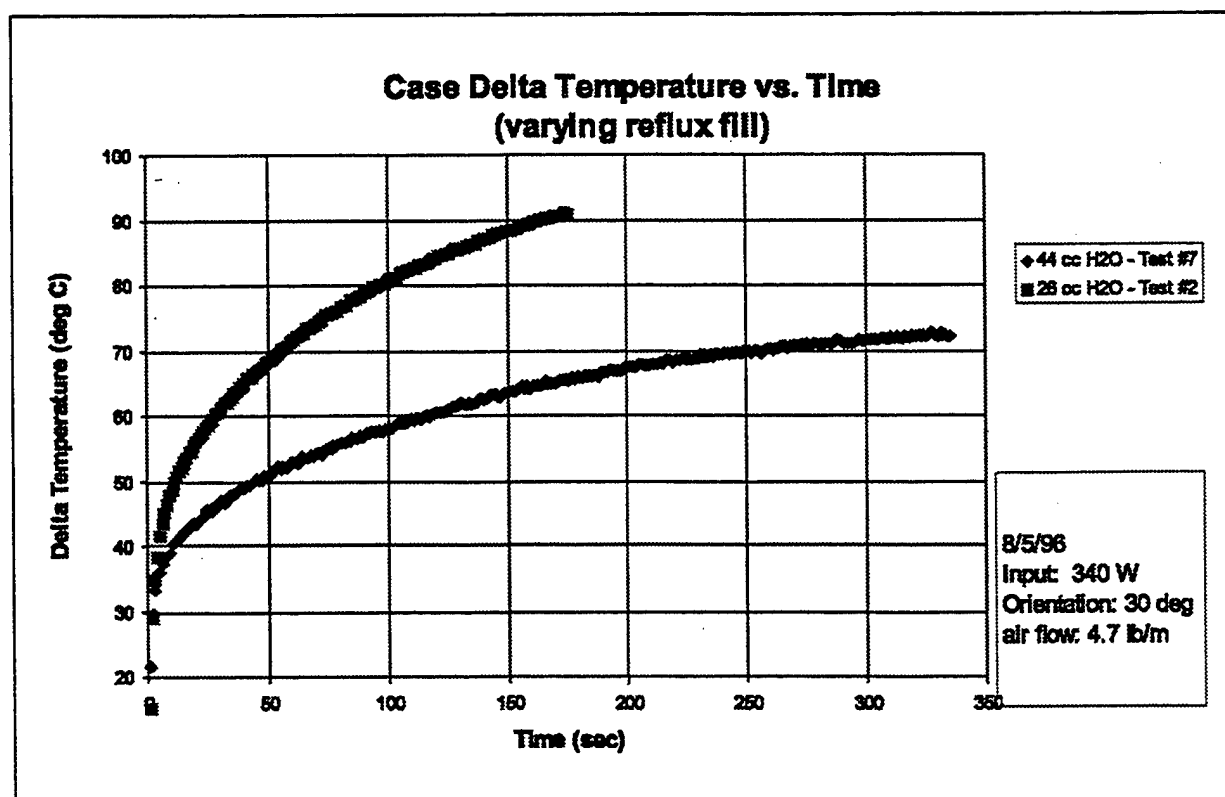


Figure 3.1.3.3-9 Case Temperature as a Function of Cooler Reflux Fill

3.1.4 Conclusions of Small Cooler Test Program

Although the reflux/PCM test results were not what was expected, it is believed that improvements to the design can be made that will enhance the cooler performance so that it more closely resembles the thermal analysis. Boiler surface enhancements and new boiling fluids should improve boiler performance.

The condenser section should be changed slightly to enhance its performance, as well. Widening the gap between the fins and going to a perforated fin design would help this problem area. Additionally, determining the minimum reflux fluid amount that is needed for adequate boiler operation would help to reduce the likelihood of two-phase flow entering into the condenser.

Increasing the volumetric size of the PCM section, as well as using a PCM with a higher density and heat of fusion would add valuable capacitance to the system. Testing showed that T-50 is not dense enough and does not have enough storage capacity for this application. In order to increase the melt time of the PCM by an order of magnitude, a PCM like acetamide should be used in a PCM section that has a 50 to 100 percent larger volume than in the current design. This should add enough thermal storage capacity to allow the system to perform at an acceptable level.

Finally, the use of one large cooler instead of five small ones is recommended in order to increase the hydrostatic head in the cooler. This will ensure that the thermosiphoning or reflux effect is occurring and will enhance the heat transfer rate of the cooler. In addition, it gives the added benefits of lighter weight and lower cost.

3.2 Large Reflux/PCM Cooler

Abstract

Subsequent to the test program with small reflux/PCM coolers, a large electronics cooler using reflux heat rejection and phase change material (PCM) energy storage has been built and tested. The cooler provides thermal control for an electromechanical actuator motor drive. These aircraft actuator motor drives do not have an available high performance heat sink, and thus must rely on the quiescent air in an actuator bay or the aircraft structure as heat sinks. Thermal loads on the power electronics of these motor drives can be quite high for short durations, suggesting the use of phase change energy storage to store the heat until it can be rejected to the available heat sinks. The present experiment used Fluorinert® compound FC72®a for the refluxing fluid, and Shellwax® paraffin wax with either a 51°C and 61°C melt temperature as a PCM for high power transients. Critical heat flux was not detected in the present test series, although the peak fluxes at the base of the power die and at the boiler surface were 80 and 20 W/cm², respectively, with a boiler wall superheat of 16°C. The motor drive peak heat load of 1,000 W was applied for six minute intervals. For transient loads with a duration of less than six minutes, the reflux/PCM cooler provided a significant performance benefit relative to the baseline air-only cooler.

Nomenclature

- c_{pl} = Liquid specific heat
- C_{sf} = Fluid/surface pool boiling factor
- g = Local gravitational acceleration
- g_c = Gravitational proportionality constant
- h_{lam} = Laminar film condensation heat transfer coefficient
- h_{fg} = Fluid heat of vaporization
- k_l = Reflux fluid liquid thermal conductivity
- l = Condenser wall length (vertical)
- m = Fin efficiency parameter
- q'' = Boiler surface heat flux
- s = Boiling Prandtl number exponent, $s=1$ for water, 1.7 for Fluorinert®
- T_{BL} = Boundary layer temperature
- T = Local ambient temperature
- T_s = Condenser wall temperature
- T_{sat} = Reflux fluid saturation temperature
- T_w = Boiler wall surface temperature

Dimensionless Groupings

- Pr_f = Reflux fluid Prandtl number

5. Shellwax is a Registered Trademark of Shell Oil Corp.

Greek Letter Symbols

- η_f = Condenser fin efficiency
- μ_l = Liquid dynamic viscosity
- ν = Kinematic viscosity of fluid
- ρ_l = Reflux fluid liquid density
- ρ_v = Reflux fluid vapor density
- σ = Fluid surface tension

3.2.1 Introduction

The development of more electric technologies for future military aircraft promises to provide significant redundancy, reliability, maintainability, and performance benefits. In particular, the use of electrically driven actuators for flight control surfaces allows elimination of the often leaky, maintenance intensive, and easily damaged actuator hydraulic circuits.

Many of these actuators, such as flaperons and stabilators in fighter aircraft, operate at high powers during certain flight segments such as takeoff, combat, and landing. Spoiler actuators in transport aircraft, which are also potential sites to apply electromechanical actuators (EMAs), too experience highly cyclic duty cycles with the majority of the work occurring over a short portion of a flight. The development of inherently unstable aircraft, associated with improved maneuverability, particularly results in large actuator powers. Hydraulic oil circuits remove the associated large waste heat loads from conventional hydraulic actuators, whereas, electrical actuators, such as EMAs and electrohydraulic actuators (EHAs), possess no inherent means of removing waste heat. The use of an active cooling loop for EMAs would reintroduce reliability, maintainability, and safety issues that are eliminated with the removal of conventional hydraulic circuits. Therefore, cooling becomes an issue for EMAs because of limited access and availability of appropriate heat sinks.

Previous studies have shown that EMA motors have sufficient inherent thermal mass to attenuate most high power transients (Schneider, et al, 1995), but that the power electronics, which have innately lower thermal capacitance and which have lower temperature limitations, would benefit from a reflux cooling technique coupled with PCM energy storage.

The aircraft structure and skin, and ultimately the ambient air, provide the most feasible heat sink for EMAs. Peak power levels for flaperons, spoilers, and other high power control surface actuators may reach 40 kW (54 hp) which, for a motor drive efficiency of 96 percent, imposes a peak heat load of 1.6 kW on the heat sink. However, these actuators typically operate at peak power for only brief durations, and will operate at significantly reduced power levels during most of a flight duty cycle. This characteristic of aircraft actuator duty cycles suggests the use of techniques that store energy during peak power periods and dissipate that stored energy during low power periods. Energy storage techniques allow the heat rejection system to be designed for the average heat loads rather than peak transient heat loads.

In the present motor drive cooler concept demonstration, a two-phase fluid thermosiphon is used to provide the passive heat transfer, and a PCM provides energy storage. A thermosiphon is a device in which heat is transferred to a liquid pool causing the liquid to boil. The generated vapor rises due to the density difference between the vapor and liquid phases and condenses on a cooler surface located above the heat source. Unlike a true reflux boiler the liquid condensate in a thermosiphon drains through dedicated and isolated channels to the pool of liquid adjacent to the heat source to complete the cycle (Bland and Funke, 1992). Heat pipes operate in a similar fashion, but are more like reflux boilers than thermosiphons, relying on surface tension in a wicking structure, rather than gravity, to provide the motive force for liquid circulation. In

general, the allowable boiling heat flux at the heat source of a reflux type heat exchanger exceeds the allowable evaporative heat flux for a heat pipe using the same working fluid (Bland and Funke, 1992).

Preliminary steady state analysis, using a SINDA (Systems Improved Numerical Differencing Analyzer) finite difference thermal model, revealed that air-side convection, junction to case resistance, and boiler heat transfer were the driving resistances in the thermal network. Transient parametric trade studies indicated that reflux cooling, in combination with a PCM, were most beneficial when applied to actuator motor drives with low frequency duty cycles as was borne out in the present test program. Based on the results of these studies, a demonstration motor and cooler design was selected along with the optimum reflux working fluid and PCM. The analysis phase of this project led to the present laboratory test program.

3.2.1.1 Technical Discussion

Passive Cooling Approach for EMAs

A power electronics device, such as an IGBT, is mounted to a heat spreader which transfers the heat to a boiler surface. The liquid phase of the two-phase fluid, which wets the boiler surface, is boiled by the waste heat, generating vapor bubbles. This vapor flows upward due to density difference through a channel called a "riser" or "reflux channel" and then condenses on the condenser fins. Liquid condensate then drains in the "downcomer" to reenter the liquid pool. The PCM, with its low thermal conductivity, serves to insulate the downcomer channel from the riser channel, thus preventing formation of vapor bubbles in the downcomer channel. Vapor bubbles in the downcomer reduce the overall heat rejection capability of the thermosiphon because they block the recirculation of liquid condensate back to the boiler surface. During peak loads, the reflux fluid temperature (and pressure) rises, and energy is stored as latent heat due to the melting of the PCM, which is contained in the interior layer of the plate-fin heat exchanger. Also, some heat is directly conducted into the PCM layer by pin-fins which cross-link the boiler surface to the PCM layer. Even though the entire boiler is not submerged, effective cooling will also occur in the upper portion due to carryover of liquid from the lower portion of the riser channel.

Heat load variations with this passive cooling approach result in changes in operating temperature and pressure for a given sink temperature. In its simplest form, the peak load defines the design condition for the cooling system, and the series thermal conductances between the IGBT and ambient air determine the steady state device temperatures. In transient load cases, the thermal capacitances of the switches and cooler can significantly attenuate the motor temperature swings.

Enhancement of the system thermal capacitance through energy storage allows the heat rejection surfaces to be designed for the average load, reducing the IGBT temperatures to those associated with the average heat load. Energy can be stored by the use of sensible storage, in the form of thermal mass which results in a temperature rise as heat is absorbed, or the use of a PCM that stores energy as latent heat at a relatively constant temperature. This latter approach, which was chosen for the present design, typically results in a system with minimum mass and volume.

Typical Mission Specifications and Installation

One of the difficulties encountered in designing a heat rejection system for EMAs involves defining the design specifications. A worst-case mission duty cycle, which was developed for a transport aircraft spoiler EMA as part of the Advanced Motor Drive Program sponsored by Wright Laboratories, was chosen as the target heat load for the present program. The aircraft takes off and climbs with minimal spoiler EMA loads until twelve minutes into the flight when it is suddenly commanded to execute an emergency descent. Hot day conditions are assumed at takeoff. In the present test program, duty cycle data were gathered over a variety of period lengths up to 10 minutes to assure that the cooler can cool the motor drive for the six minute high power duty illustrated in Figure 3.2.1.1-1. At the same time, the general duty cycle data which

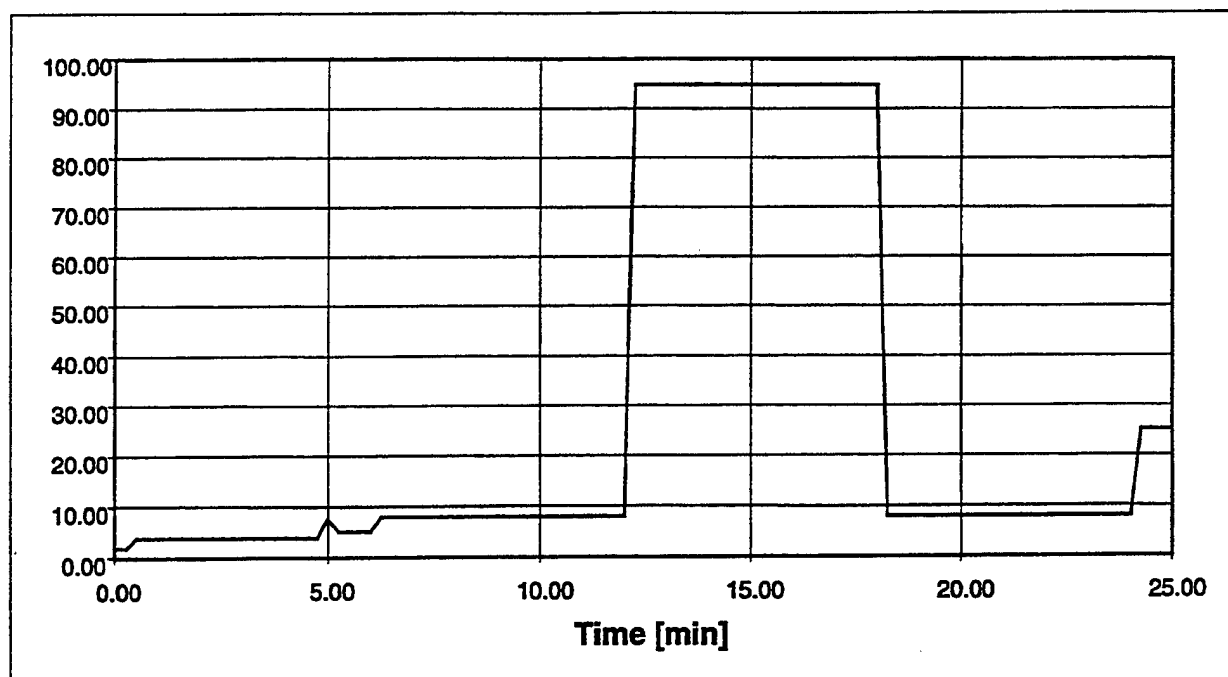


Figure 3.2.1.1-1 Worst-Case Mission Duty Cycle, Present Power vs. Time

were gathered can apply to other actuators with a variety of duty cycles. The longer duty cycles are a good test of the device robustness because of the inherent stress they place on the electronics cooler.

SINDA Thermal Model Description

As mentioned earlier, a SINDA thermal model of an EMA motor incorporating a reflux cooler was developed to perform steady-state and transient analyses. The model includes all significant resistances between the power electronics switch, or heat source, and ambient air, which is the ultimate heat sink.

The model estimates heat transfer coefficients on the working fluid side of the heat exchanger and calculates required conductance and capacitance values. This model does not perform a detailed thermal-hydraulic analysis of the reflux process, solving for recirculating flows, as forwarded by Schrage (1990). Instead, the model estimates the boiling heat transfer coefficient using a pool boiling correlation and condensing heat transfer coefficient from a Nusselt-type film condensation correlation on a vertical flat plate. However, a separate steady state thermal-hydraulic analysis was performed to size the thermosiphon channel geometries. Outputs of the SINDA analysis include IGBT and cooler temperatures as a function of operating conditions, including both steady state and transient conditions. Parametric analyses were performed with the model to select the working fluid and PCM, identify controlling heat transfer resistances, characterize the effects of cooler geometry, and quantify the effects of using PCM versus no PCM. A list of correlations used in the model is given in Table 3.2.1.1-A.

Table 3.2.1.1-A Correlations Used in Thermal Analysis

Correlation Description	Correlation	Reference
Viscous Boundary Layer Heating on Aircraft Surface (Recovery Temperature) Correlation for viscous heating within the boundary layer	$T_{BL} = T_w + CU^2/2c_p$ $C = Pr^{1/2}$ —laminar boundary layer. $= Pr^{1/3}$ —turbulent boundary layer.	1
Boiling Heat Transfer Coefficient. Nucleate pool boiling	$T_w - T_{sat} = C_{sf}(h_{fg} Pr_f^2 / c_{pf}) \{ (q'' / \mu_f h_{fg}) [g_c \sigma / g(\rho_f - \rho_v)]^{0.5} \}^{0.35}$	2
Condensation Heat Transfer Coefficient Laminar film condensation on a vertical flat plate	$h_{film} = 0.943 \{ [\rho_f (\rho_f - \rho_v) g h_{fg} k_f^3] / [1 \mu_f (T_{sat} - T_s)] \}^{1/4}$	2

1. Holman, 1981.
2. Rohsenow, 1982.

3.2.2 Large Cooler Design

Given the results of the small reflux/PCM cooler performance, a large (5 phase) cooler was designed to mitigate many of the problems mentioned above.

In order to eliminate boiler burnout, the spreader plate thickness was increased to 0.46 cm (0.18 in.). Additionally, boiler surface treatments were looked into as a possible solution to the burnout problem. Also, an aluminum sputtering, or flame spray treatment was added to one of the boiler surfaces to test whether boiling would be enhanced to help lower wall superheats.

The PCM section was thickened to give this cooler a greater percentage of latent mass for energy storage. The air-side condenser fins were changed from perforated to lanced offset—which yields a twofold increase in the overall airside conductance.

The test unit shown in Figure 3.2.2-1, has a brazed plate-fin aluminum heat exchanger structure, (nearly identical to the small cooler structure). The motor drive for which the cooler was designed drives a 40 kW motor for the spoiler EMA. The cooler was designed for four IGBTs conducting simultaneously to simulate an emergency descent condition.

Dry weight of the cooler is 2,307 g, and an additional 216 g of Shellwax® 100 and 384 g of FC72® were added to the cooler, totaling 2,907 g. The Shellwax® PCM was chosen because of its high

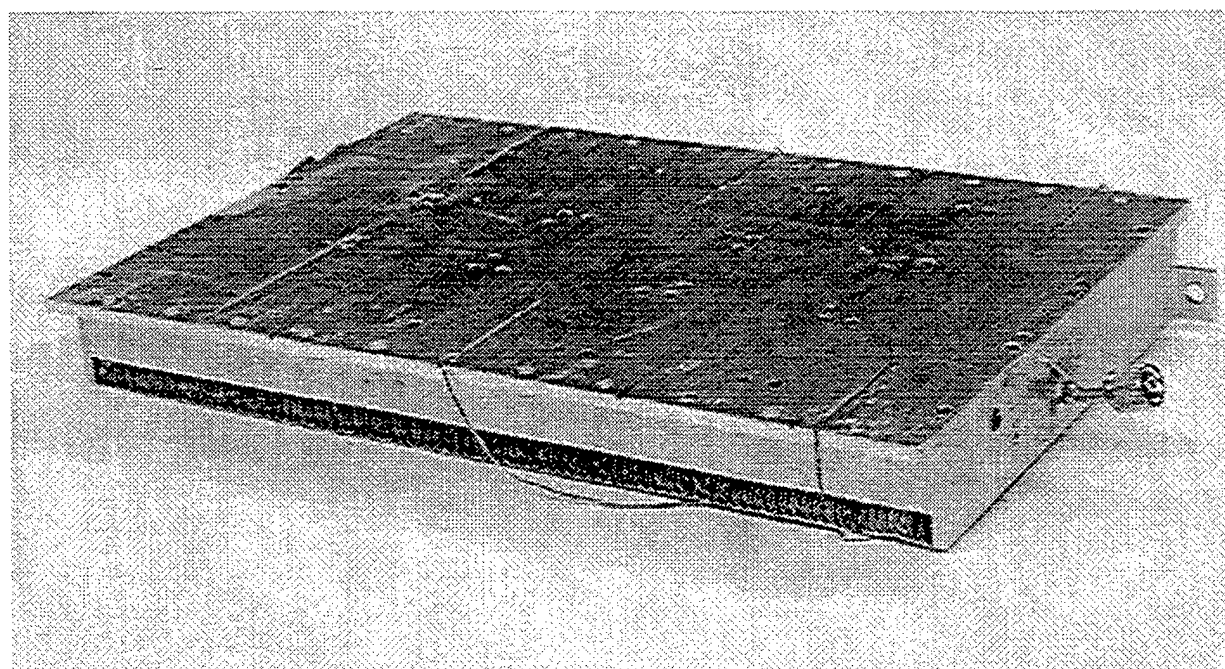


Figure 3.2.2-1 Large Cooler—Test Unit

hfs of 227.5 kJ/kg, its appropriate melt temperature of 51°C, specific gravity of 0.81, and because it is compatible with the aluminum containment material. A higher melt temperature PCM might be necessary for some applications if hot day, low altitude, high Mach number, high power duty is anticipated. The 384 g of Fluorinert® represents a 50 percent volume fill of the thermosiphon volume. The cooler measures 29.5 by 19.8 cm, and has an overall thickness of 3.30 cm. Thickness of the PCM layer is 0.89 cm. Detailed thermal analysis dictates that the spreader plate be 0.51 cm thick to prevent heat fluxes at the boiler surface from exceeding critical heat flux. Air side fins are 0.94 cm high lanced-offset, 5.7 fins per cm, 0.15 mm thick, with a flow length of 17.4 cm.

The IGBTs, which measured 5.1 by 6.4 cm, and weighed 98 g, were bolted to the cooler with a torque of 1.1 N-m, with a layer of Thermstrate® contact conductance enhancement material mounted between. To simplify testing, the IGBTs were operated in a dc mode, with losses occurring only in the 2.52 cm² IGBT die itself. Most tests were terminated when the IR camera indicated that the IGBT die temperature had exceeded 125°C, although some tests were stopped before that temperature, if steady-state had been achieved. Also, during some high power tests, brief excursions above 125°C were allowed.

Test Objectives

The objectives of the reflux/PCM cooled tests are:

- To determine quantitatively the ability of a reflux/PCM heat exchanger to cool M-pack switches.
- Determine input power/airflow/cooler attitude/reflux fill and type/junction/temperature relationships.

Test Parameters

The main test parameters for the reflux/PCM tests are input power, air flow rate, cooler attitude, PCM type and header size. Thermstrate was used at the switch to cooler interface just as it was used for the previous testing. The blower that was used to create air flow had a maximum mass flow rate of 6 lbm/min for this cooler, therefore it is the upper bound. Mass flows throughout this range were used. Input power was varied from 250 W per switch to 0 W per switch. Cooler attitudes were 0, 45, and 90 degrees rotated about both the length and width axes. FC72® is the reflux fluid used with quantities of 200 cc's and 240 cc's. PCM type is either Shellwax® 100 (50°C melt) or Shellwax® 200 (61°C melt).

Test Equipment

All test equipment used during this phase of the program is identical to that used in the small cooler testing, the only exception being that a larger variable speed blower was introduced because of the additional head required to force air through the new air-side fins. Air-mass flow was measured using the manometer and a square-edged orifice in the blower ducting. Please refer to the small cooler test equipment section for a description of the remaining test equipment.

Test Setup

The test setup for the large cooler testing was identical to that of the small cooler testing. Temperature measurements for the large cooler are shown in Figure 3.2.2-2. Figure 3.2.2-3 shows the large cooler, with four IGBTs attached to it, mounted to an articulating test bed. Additionally, one can see the power supplies and PC data acquisition system used during testing.

Test Procedure

Once all of the test equipment was hooked up, items such as ambient temperature and die junction initial temperature were measured using the Luxtron probe (junction temperature was measured at the location shown previously in Figure 3.2.2-2). In addition, the air flow fans were set to the desired value and the heat exchanger pressure drop was measured. Next, the data acquisition system and VCR were started and dc power was applied to the switches. After the

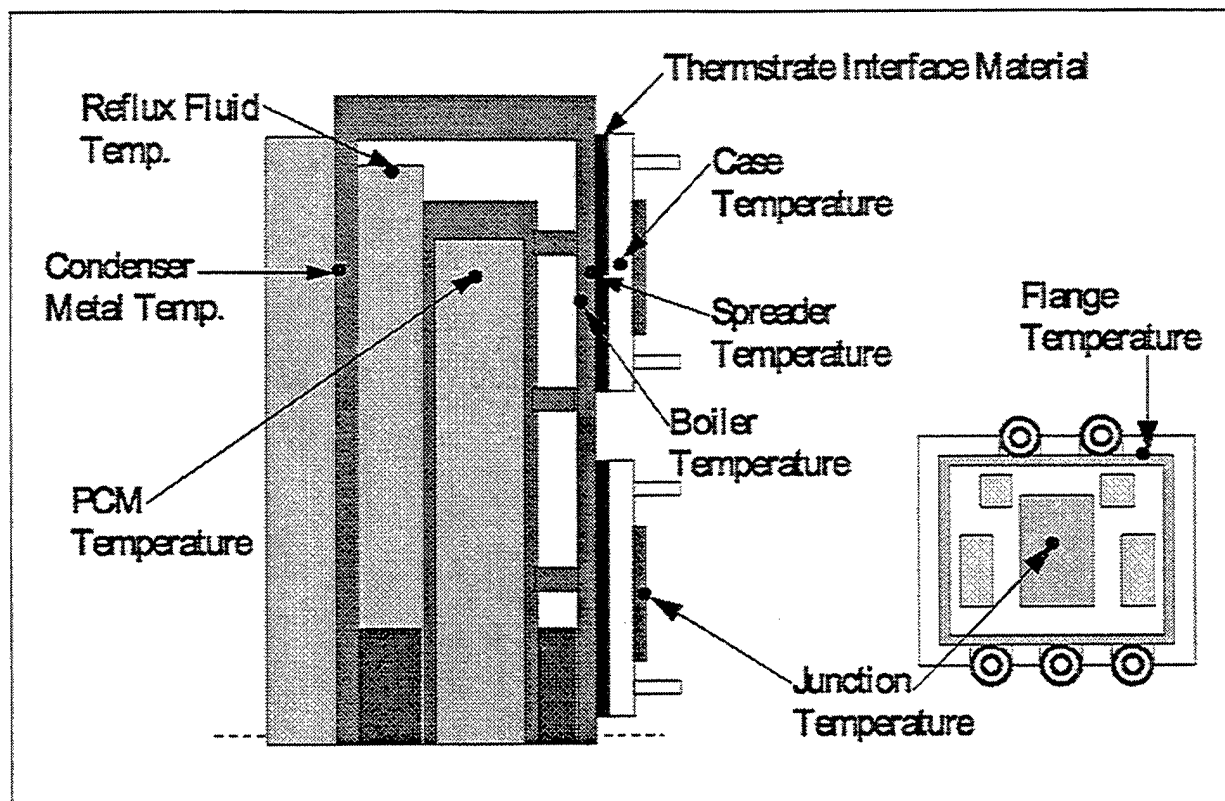


Figure 3.2.2-2 Large Cooler—Test Measurement Points

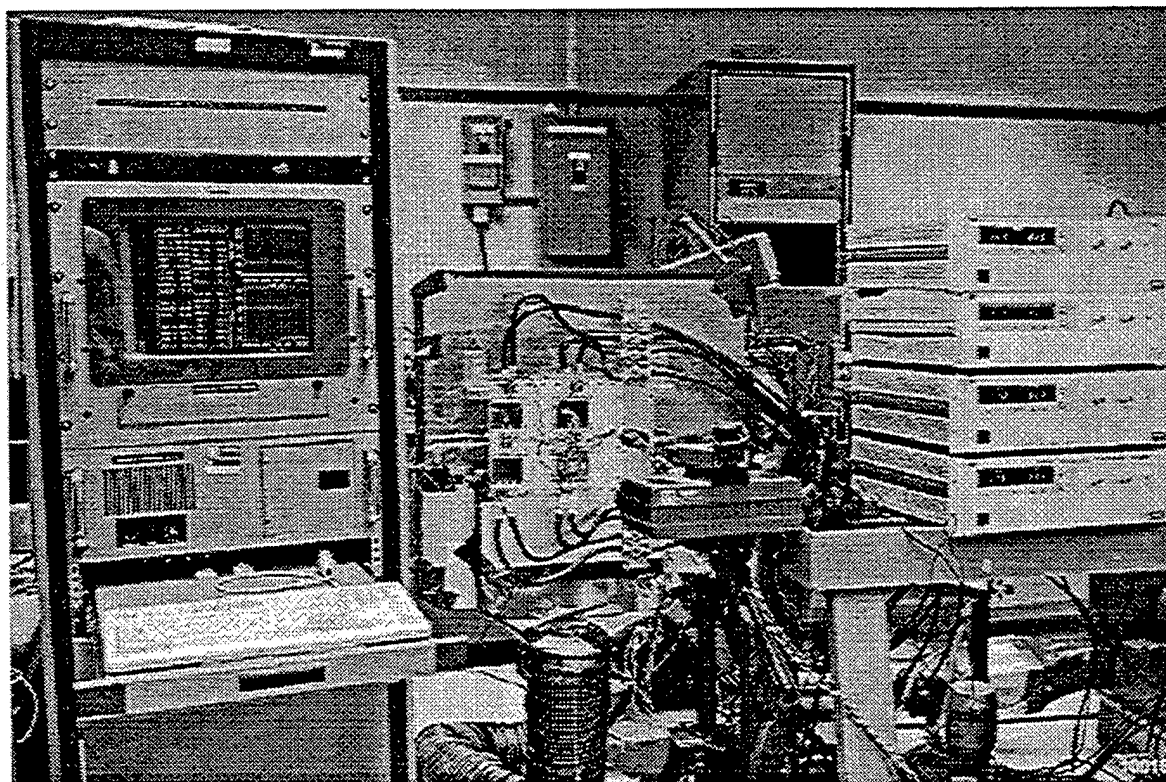


Figure 3.2.2-3 Large Cooler—Test Apparatus

IR camera and case thermocouple temperatures reached steady-state, a measurement of the upper and lower switch junction temperatures were made using the Luxtron probe. Power was then disconnected from the system and temperatures were allowed to reach ambient. All of the above was then repeated for the power inputs, air flow rates, cooler attitudes and reflux fluids listed in the test parameters section of this report.

3.2.3 Test Results

Step response tests were performed on the cooler over a variety of power levels, attitudes, air flow rates, and with different PCMs. For example, Figure 3.2.3-1 shows a typical test in which a heat load of 200 W is imposed on all four switches. Die temperature is not shown on this plot because it was not as accurately measured using the infrared camera, as the other temperature channels. Case temperature for IGBT #1 is plotted, along with the adjacent spreader, boiler, and reflux fluid temperatures. It is noteworthy that no single resistance in the thermal network dominates the response of the system. But it is also noteworthy that the temperature drop from the case to the boiler is at least half of the total. When you consider that this drop occurs over a small portion of the cooler (shown previously in Figure 3.2.2-2), it leads you to the conclusion that this small area, from the switch junction to the boiler surface, should be a focus of future work.

For comparison, the SINDA model prediction for case temperature is shown previously in Figure 3.2.2-2, as well. The 20 percent overprediction is caused by the low resolution in the simplified IGBT model. Also, note that the model underpredicts the initial transient which implies that thermal capacitances or conductances were overestimated.

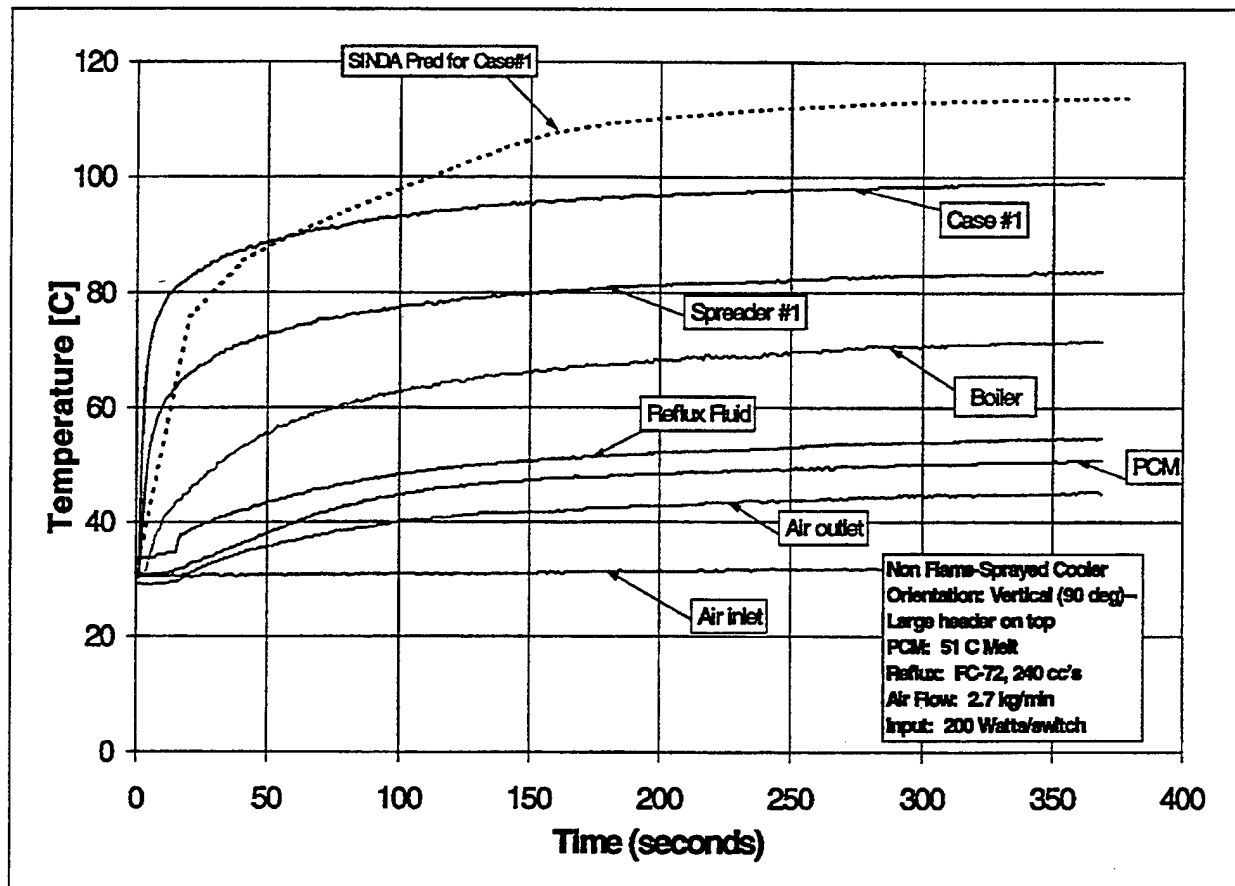


Figure 3.2.3-1 Cooler Temperatures for Step Power Input

Heat balances at the end of the six minute duty were within 5 percent, with heat input allotted to the cooling system approximately as follows (Figure 3.2.3-2): 15 percent to sensible heating of the heat exchanger metal, 15 percent to latent heating of the PCM, 10 percent to heating the Reflux fluid, 55 percent removed in the cooling air flow, and the balance in sensible heating of the switches and in natural convection losses to the laboratory air.

Tests were performed in several orientations to determine the sensitivity of the cooler to orientation. Figure 3.2.3-3 shows boiler to sink resistance data for a single switch in the horizontal and vertical orientations. Little difference in cooler performance was evident across the spectrum of testing. Note the sudden temperature drop in the 15-to-25 second range for this channel, especially in the vertical orientation. This step could be due to boiling incipience or the onset of flow boiling or thermosiphon action or wetting of the # 4 boiler area, which would cause a sudden increase in the boiler-side conductance. Also, note that switch # 4 was located at the top of the cooler for the vertical test, and thus would have been adjacent to the vapor space in the reflux section. One would anticipate that the onset of flow boiling would have a pronounced effect on the temperature response of that switch.

Figure 3.2.3-4 illustrates the effect of cooler orientation on performance. These orientations are attained by rotating the cooler about an axis parallel to the cooler's longest dimension (length). In it, case temperature rises are plotted for the various orientations. When the small header is up, the switch is below the fluid level and incipience overshoot can be seen. When the large header is up, the switch runs hotter because it is relying on the thermosiphon action to cool its boiler.

Figure 3.2.3-5 shows the effect of lateral orientations on cooler performance. In this case, the cooler was rotated about an axis parallel to its middle dimension (width). The added hydrostatic head created by rotating it in this direction creates added flow boiling and thermosiphon action which decrease the switch temperatures in these orientations.

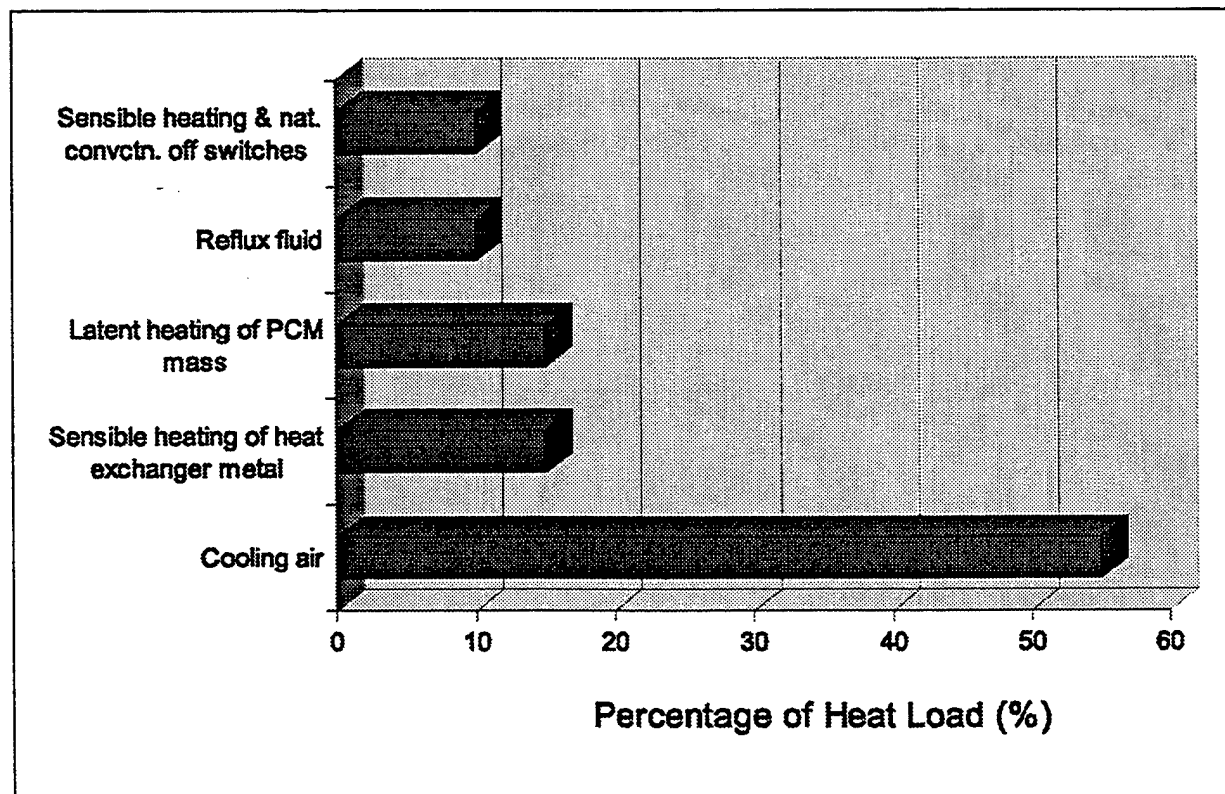


Figure 3.2.3-2 Heat Balance for Cooler

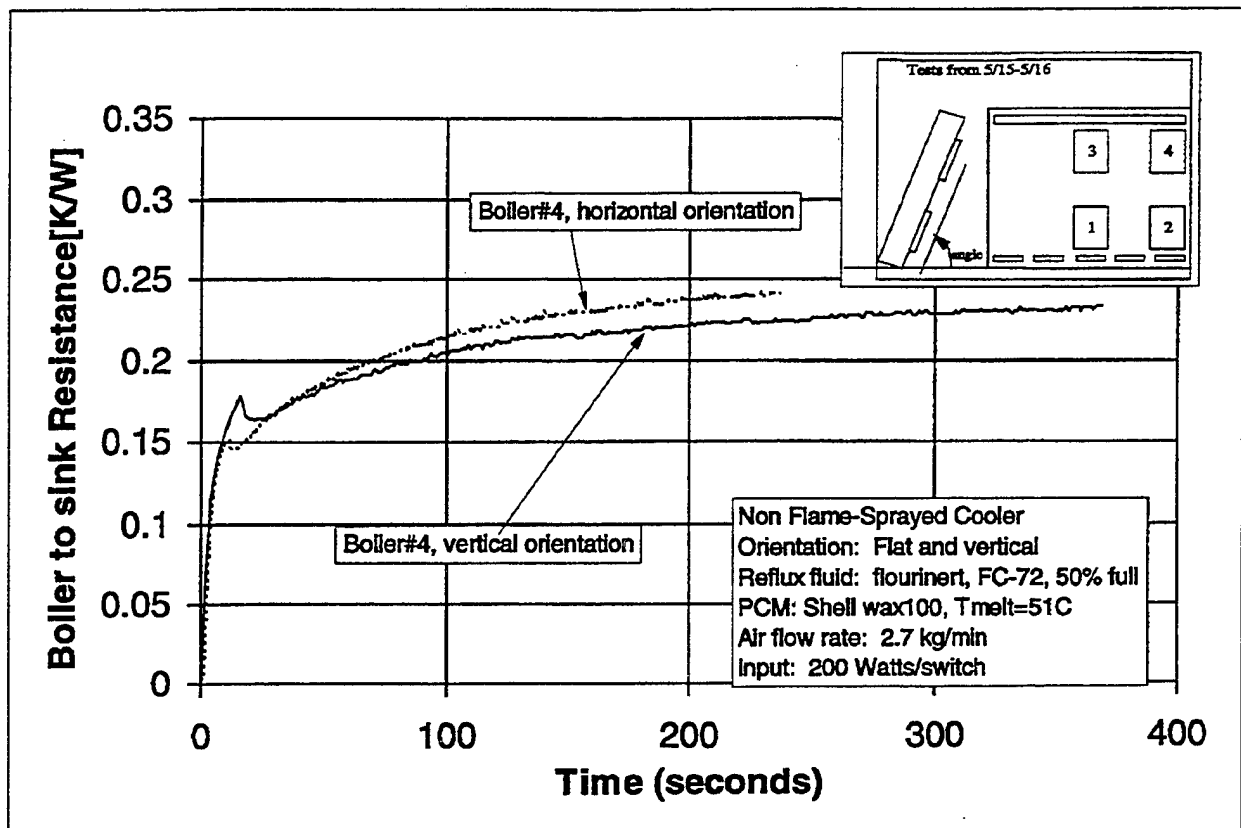


Figure 3.2.3-3 Orientation Effects on Boiler Performance

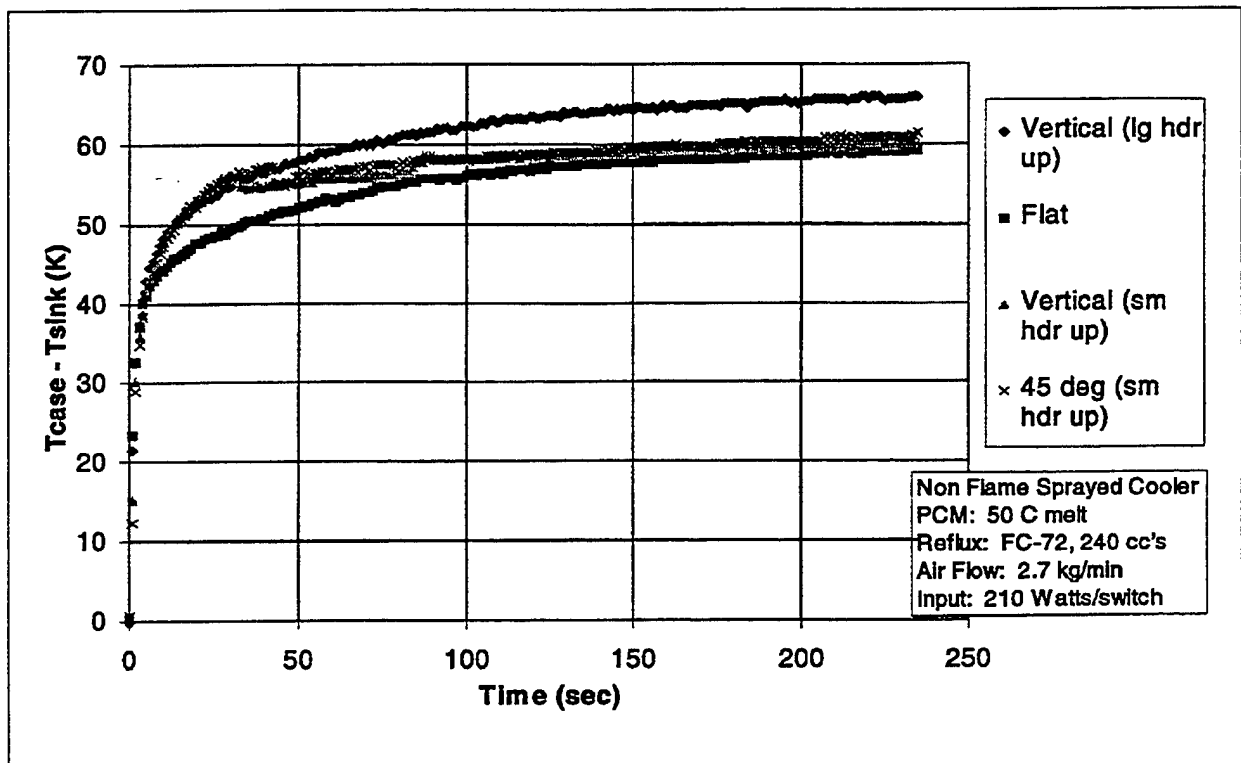


Figure 3.2.3-4 Effect of Orientation on Case Temperature

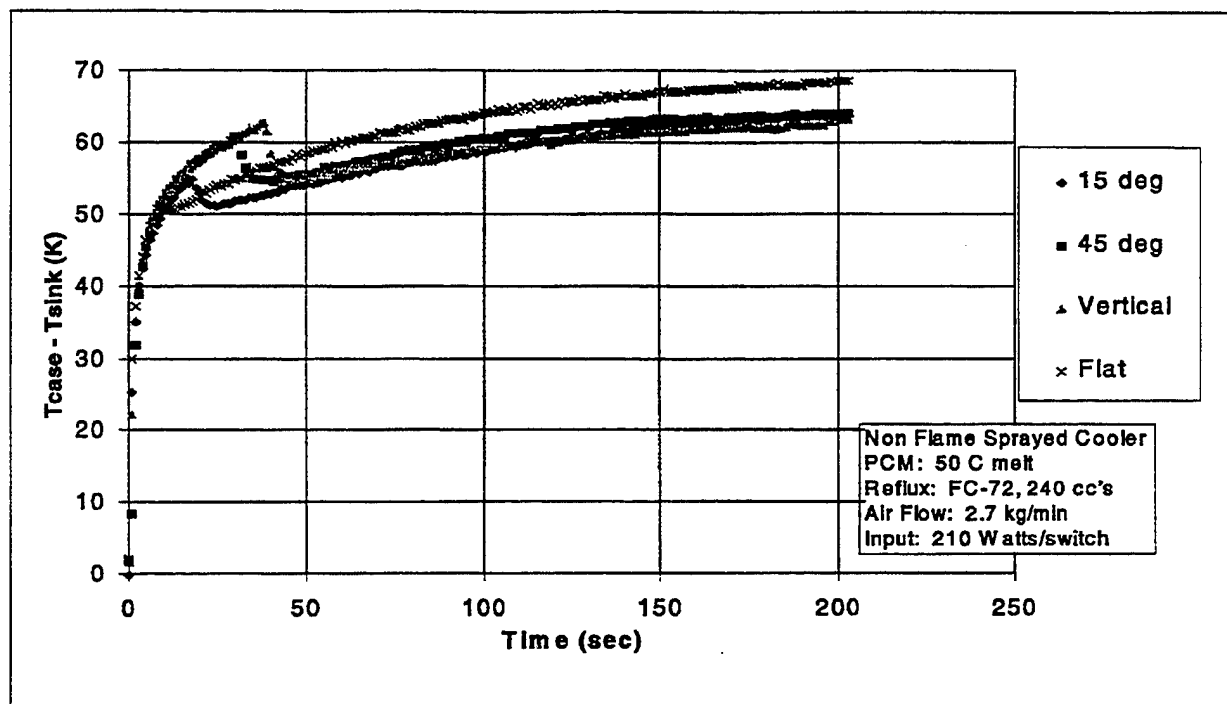


Figure 3.2.3-5 Case Temperature for Various Lateral Orientation

Parametric tests were done to determine the sensitivity of the switch position on the performance of the cooler. In the flat orientation—with all boiler surfaces in contact with the fluid—with two switches placed at the edge and two at the mid-span, and with all four switches powered to 200 W, the switches at the mid-span showed a five to ten percent decrease in case to sink resistance. This is due to increased thermal mass and spreading ability at the mid-span. Figure 3.2.3-6 shows the result.

In the vertical orientation, the switches can either be above or below the liquid level. Figure 3.2.3-7 shows that being below the liquid level is preferred. This confirms the result shown previously in Figure 3.2.3-3.

A hidden variable in the above plot is the effect of header size. When the cooler is flipped, differing sized headers are tested. In order to determine the effect of header size, Figure 3.2.3-8 must be used. In it, the same two curves shown previously in Figure 3.2.3-5 reappear, but a third curve appears as well. One can see the null consequence of header size for this particular design. It should be noted that the large header is 3 in.² and the small header is 1 in.². The slight performance improvement for the large header is really brought about because it is for switch # 1, which is at the center of the cooler. Again, switches at the center of the cooler perform better than those on an edge. So one can conclude that for the header sizes tested, there is little performance difference.

At low power levels, heat fluxes did not appear sufficient to sustain boiling, as shown in Figure 3.2.3-9, a plot of IGBT case to sink resistance as a function of time. Boiler surface heat fluxes for the low power test were on the order of 2 to 3 W/cm². As expected, the upper switch, switch #4, got hotter because it had to reject heat along the spreader to reach the liquid pool and other thermal masses. Also, switch #1, which was adjacent to the liquid pool, appeared to reject heat through convection during the low power test. However, when heat fluxes were 7 W/cm² or higher, boiling occurred and overall system resistance dropped significantly. System resistances for all of the higher power tests followed the same trend with resistances at the six minute point of approximately 0.32 K/W.

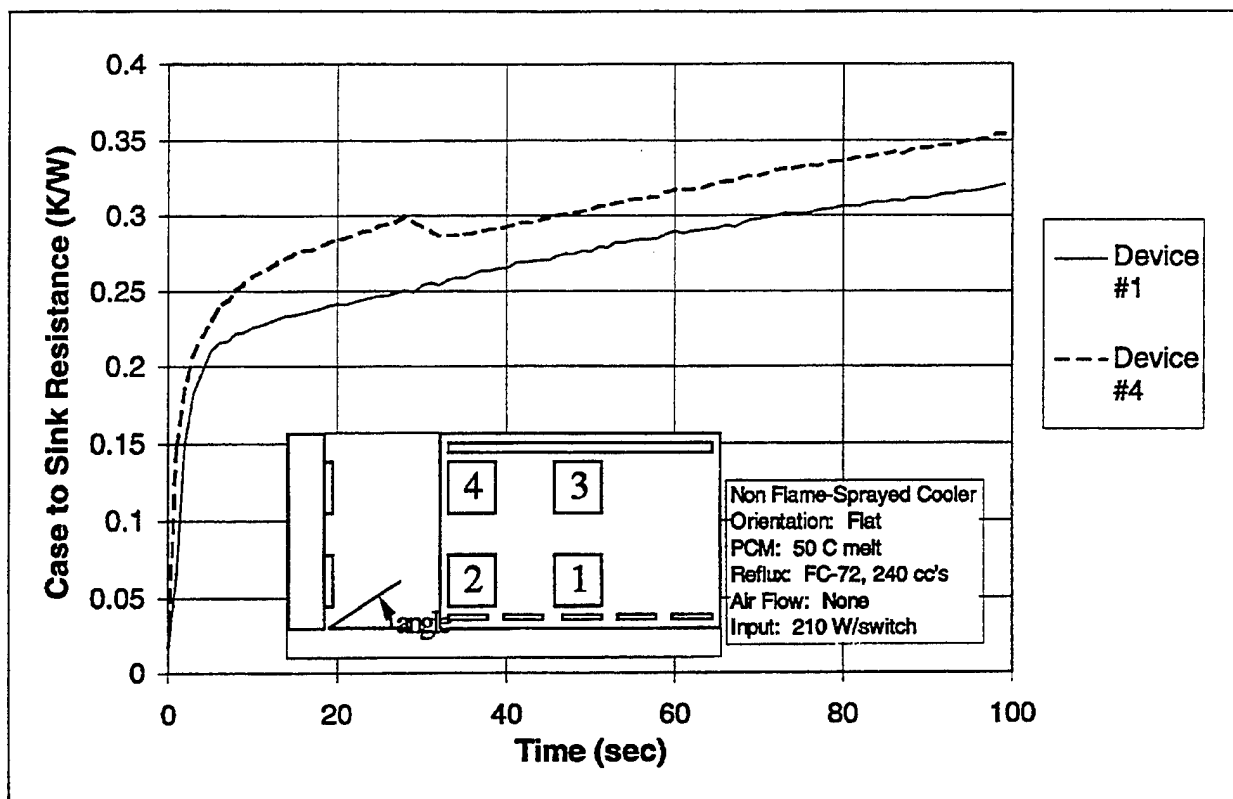


Figure 3.2.3-6 Effect of Switch Location

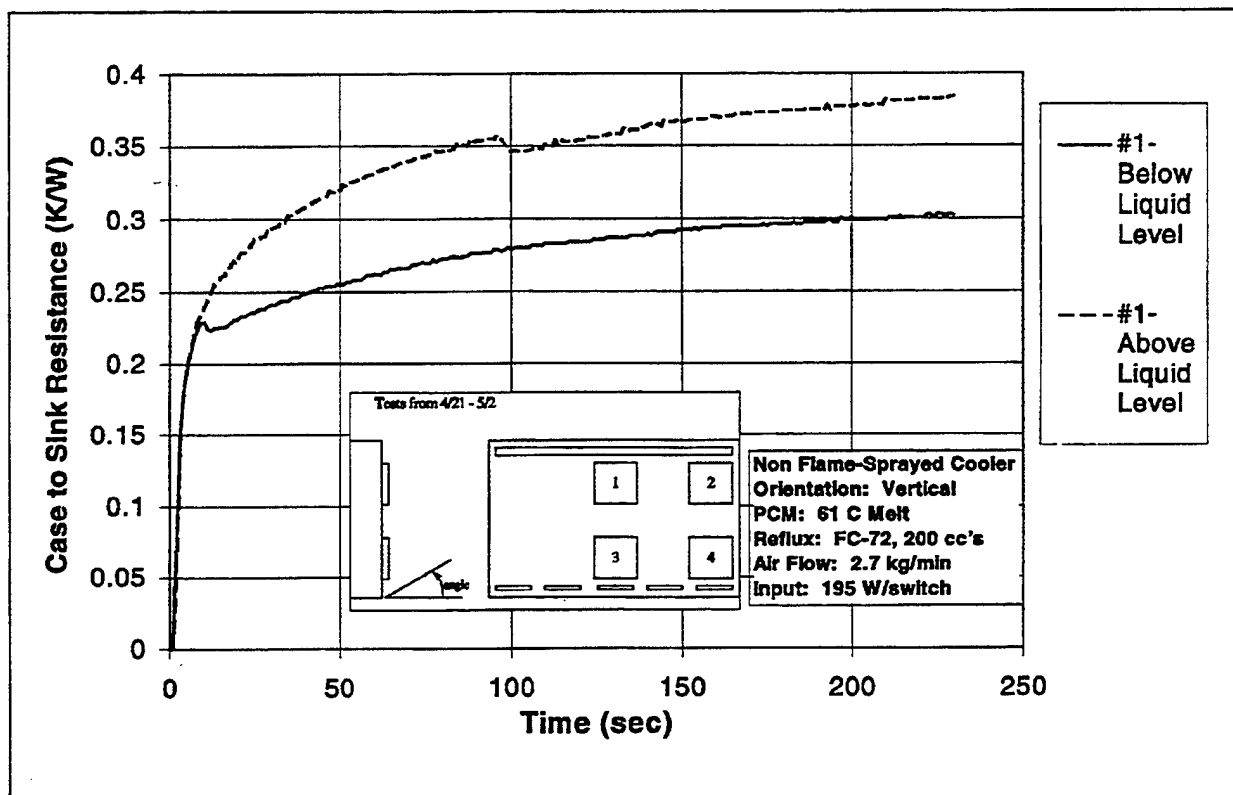


Figure 3.2.3-7 Effect on Being Above or Below the Liquid Level

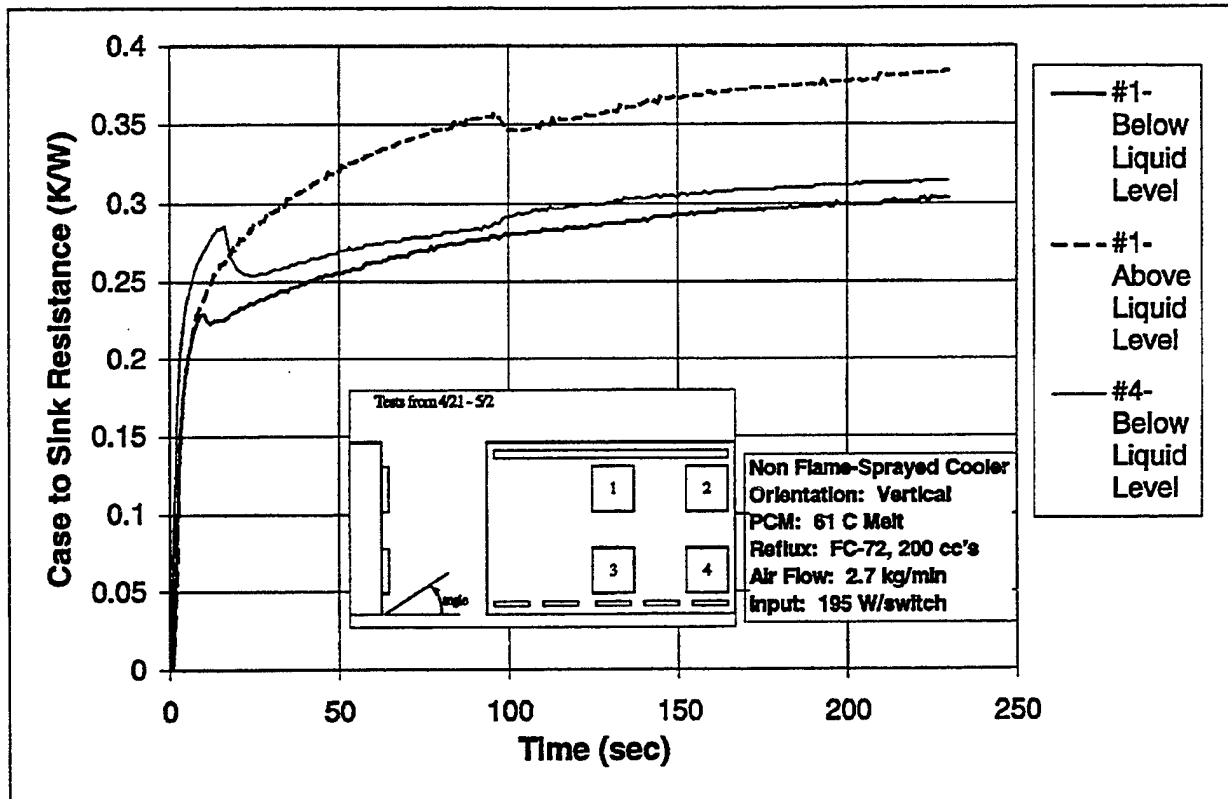


Figure 3.2.3-8 Negligible Effect of Header Size

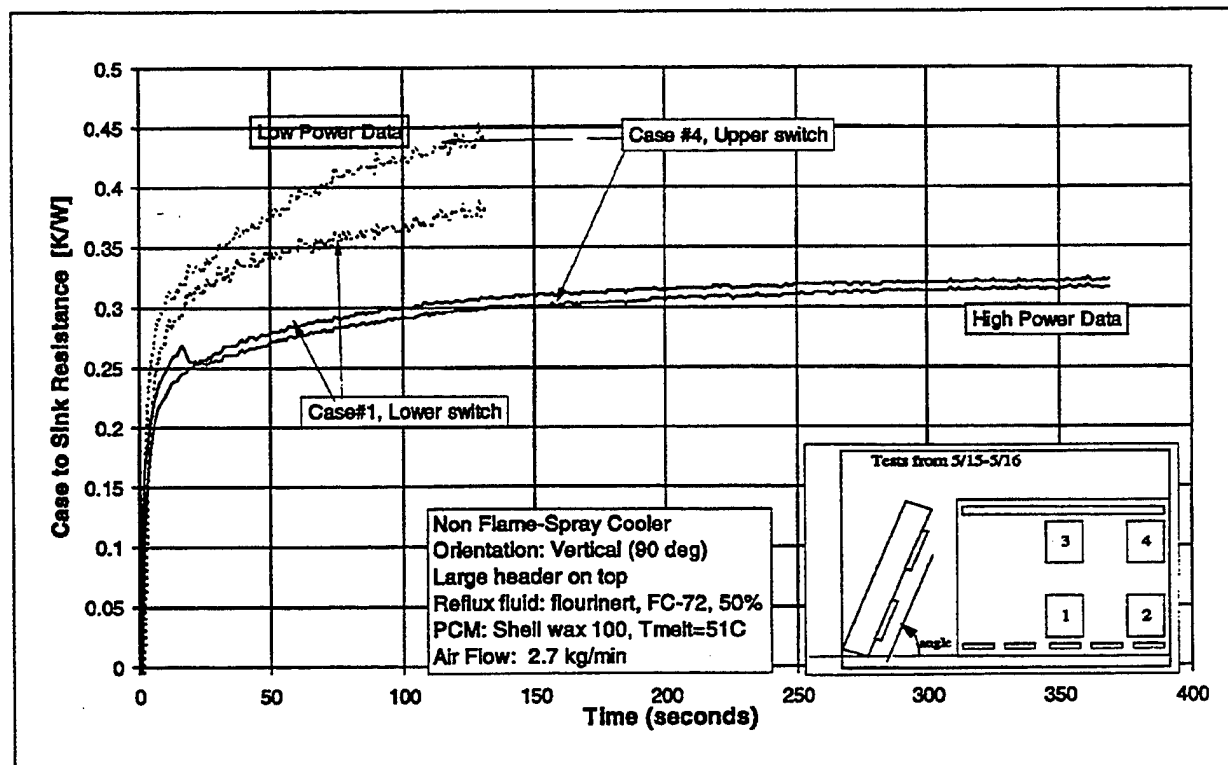


Figure 3.2.3-9 Power Level Effects on Cooler Response

As expected, the cooler resistance was affected by the air mass flow rate, as shown in Figure 3.2.3-10. The 2.7 kg/min flow rate corresponds to a flow velocity of 15 m/s. Cooler attitude did not have a significant effect on the air flow parametrics, indicating that natural convection in the air fins did not play a significant role.

Tests were performed with 51°C and 61°C melt temperature PCMs, as shown in Figure 3.2.3-11. During the tests with the 61°C PCM, the reflux fluid temperature did not exceed 55°C, thus prohibiting melting in the PCM. However, with the 51°C PCM, the reflux fluid would start melting the PCM about 100 seconds into the thermal cycle. From Figure 3.2.3-12 one can see that the 51°C PCM provided a 0.04 K/W system resistance reduction compared to the 61°C PCM, if one considers the resistance at the four minute point to be a quasi-steady value. Note that a plateau of the system temperatures near the melting point of the PCM is not pronounced in many tests, possibly because of the relatively small (15 percent) PCM thermal mass, and also because of the large and complex melting front of the PCM.

Wall flux and wall superheat data are given in Figure 3.2.3-13, which shows the effects of attitude. For reference, a typical nucleate boiling curve is plotted (Rohsenow, 1982). Interestingly, the wall superheat for a given heat flux was lower in the horizontal orientation. In this orientation, one would expect nucleate boiling to dominate at the boiler surface, while the vertical orientation should be aided by the flow boiling which occurs within a thermosiphon. However, it is important to note that the wall flux was measured beneath a switch which was adjacent to the vapor space at the top of the cooler, and thus could be impacted by superheating or simply an insufficient flow of carryover liquid to rewet nucleation sites. Further testing is required to determine which mechanisms caused this outcome. Also, note that the low flux data indicate that convection is the dominant means of heat transfer at the low power levels.

Comparison tests were performed on a cooler with a flame sprayed boiling surface. The purpose of this enhanced boiling surface was to lower the wall superheat and overall system resistance.

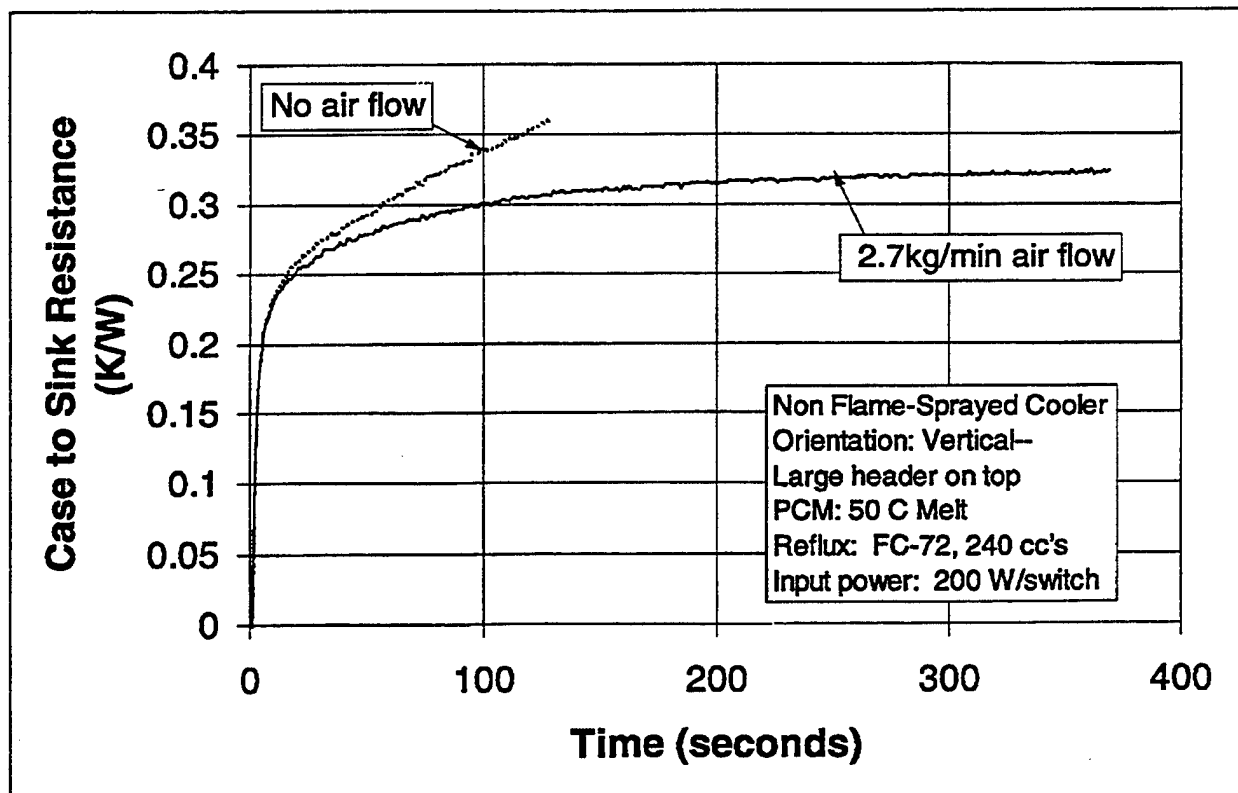


Figure 3.2.3-10 Air Flow Effects on Performance

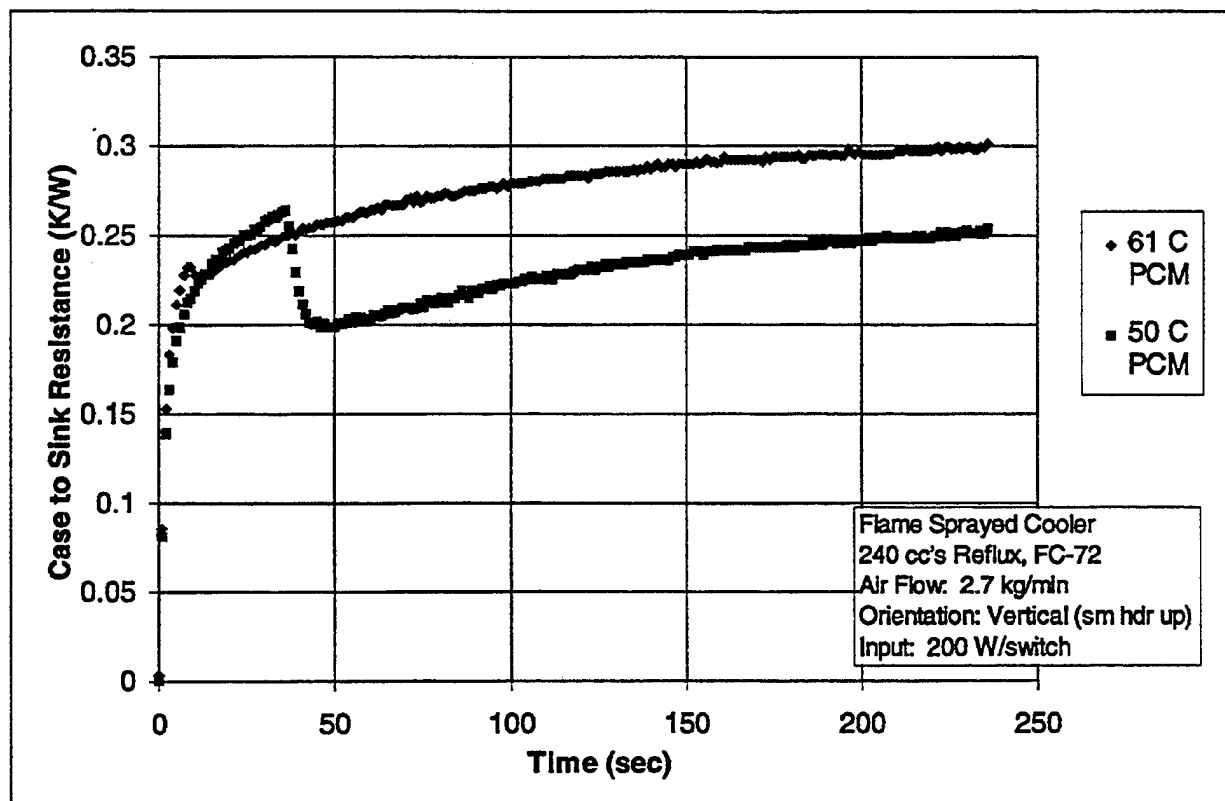


Figure 3.2.3-11 PCM Type Effect on Cooler Performance

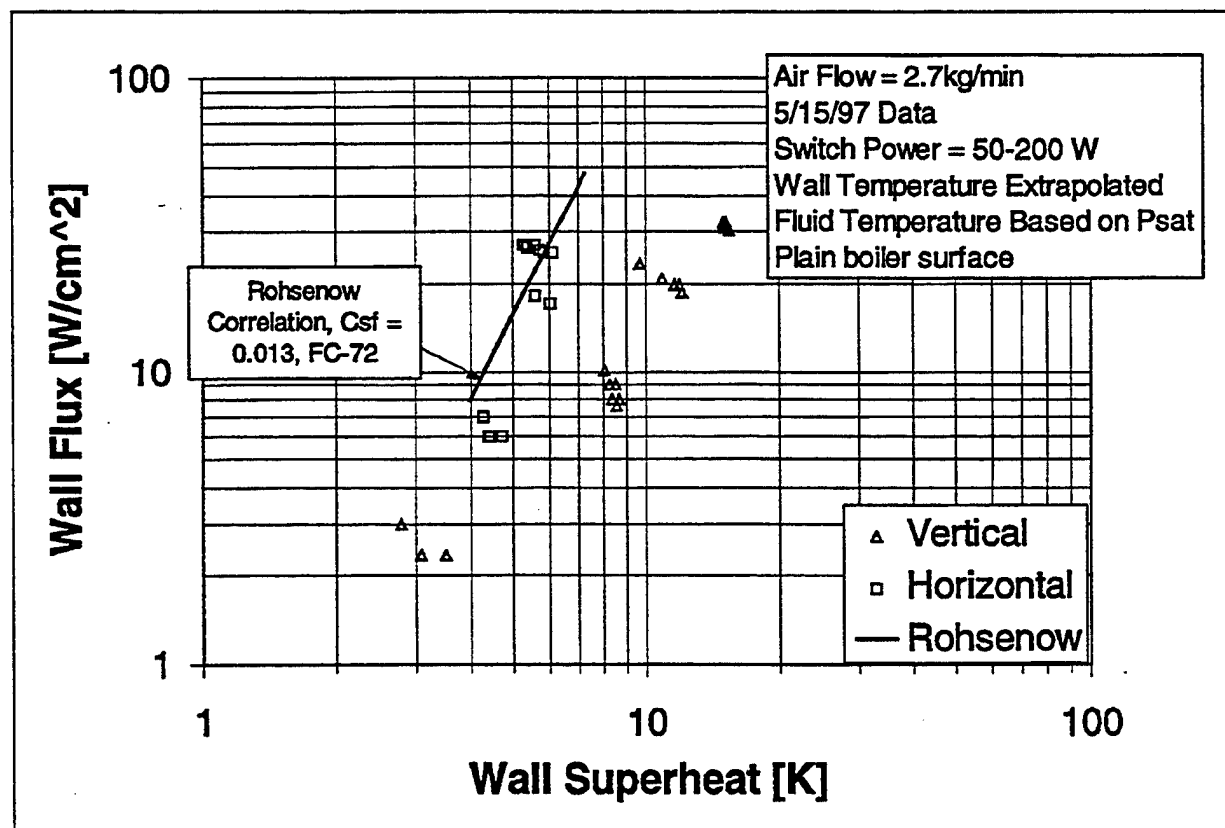


Figure 3.2.3-12 Boiler Performance

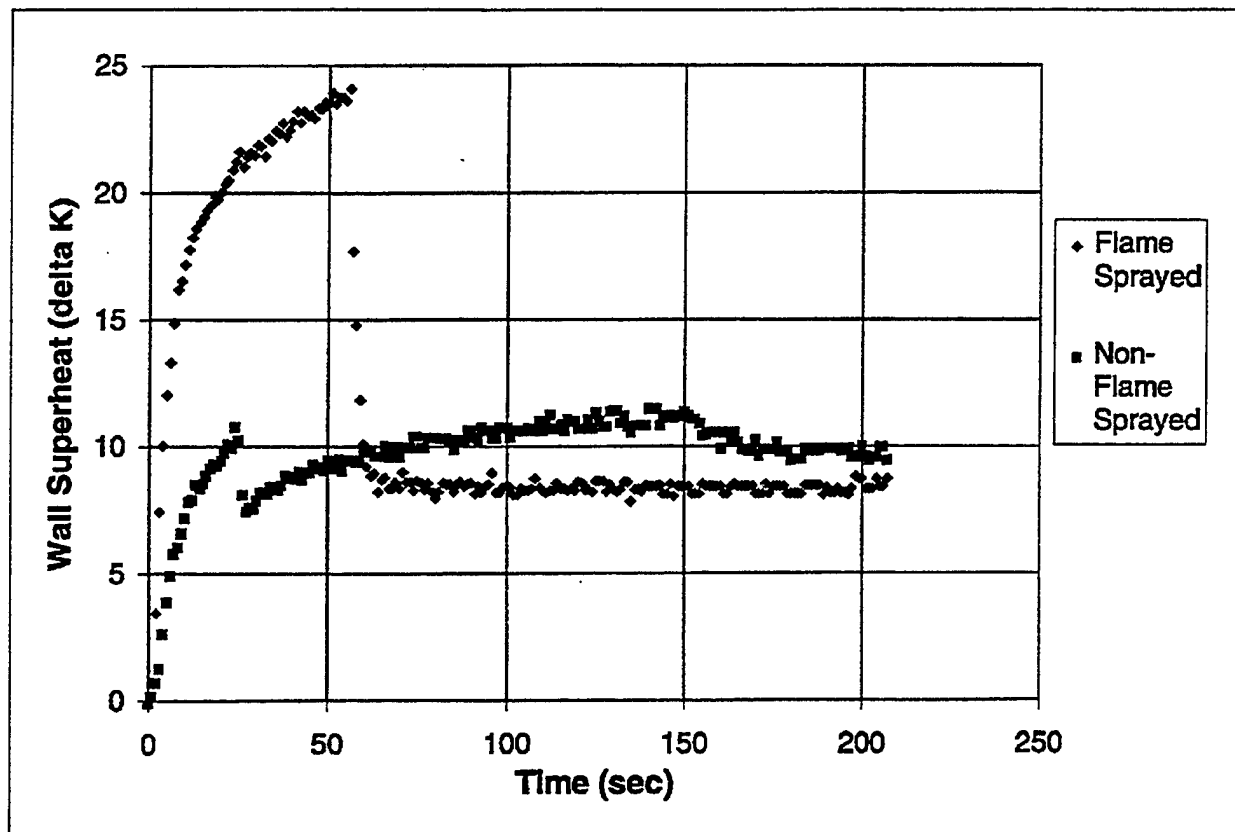


Figure 3.2.3-13 Wall Superheats for Flame Sprayed and Non-Flame Sprayed Coolers

Test data show a minimal reduction in wall superheat after incipience (2 to 3 K). However, a considerable increase in wall superheat is realized for a switch below the fluid level before the onset of boiling (10 to 12 K). Figure 3.2.3-14 illustrates this. The boiler to sink differential lowers by over ten percent for the flame sprayed cooler when the switch is below the fluid level after incipience, and is marginally higher before so. This is illustrated in Figure 3.2.3-15. Figure 3.2.3-16 shows what happens in the verticle orientation when the switch is above the fluid level. The poorer performance for the flame sprayed cooler could be due to the added fluid film friction caused by the flame spray.

Comparison tests were performed on an existing plate fin air-cooled heat exchanger which weighed 413 g. An optimized design would probably weigh approximately 300 g. Figure 3.2.3-17 shows the step response of both coolers to a high power input when they each have full air flow rate. The IGBT case to sink resistance is 38 percent higher for the air-only cooler. In fact, the performance of the air-only cooler has only marginal performance improvement as the air mass flow rate is increased beyond 0.057 kg/s.

Figure 3.2.3-18 shows the normalized results of a similar test in which the cooling air flow was set to zero. The air-only cooler has more than twice the system resistance than the reflux/PCM cooler. Therefore, with little or no air flow, the air-only cooler will not provide sufficient heat rejection for cases such as the spoiler EMA emergency descent.

Parametric testing on reflux fluid fill level has been performed, but was not of sufficient scope to make useful observations at this time.

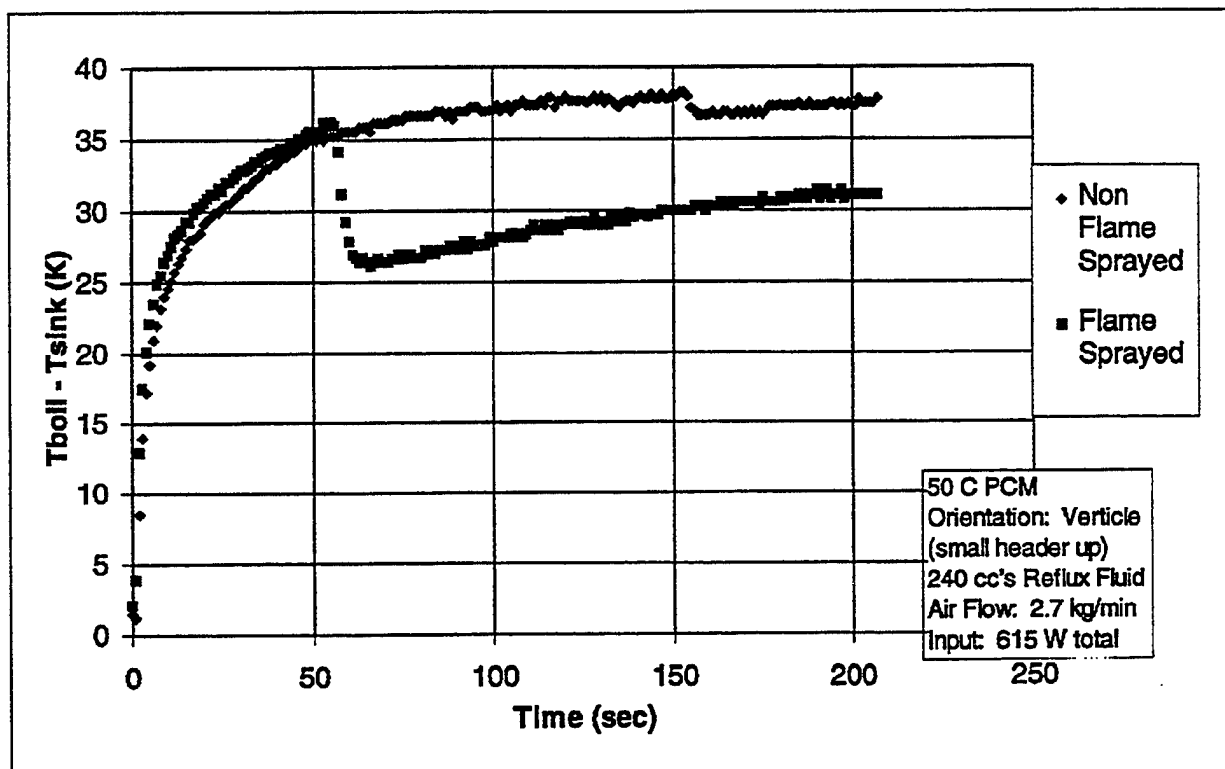


Figure 3.2.3-14 Boiler Temperature Rise for FS and nFS Coolers (SW Below Fluid Level)

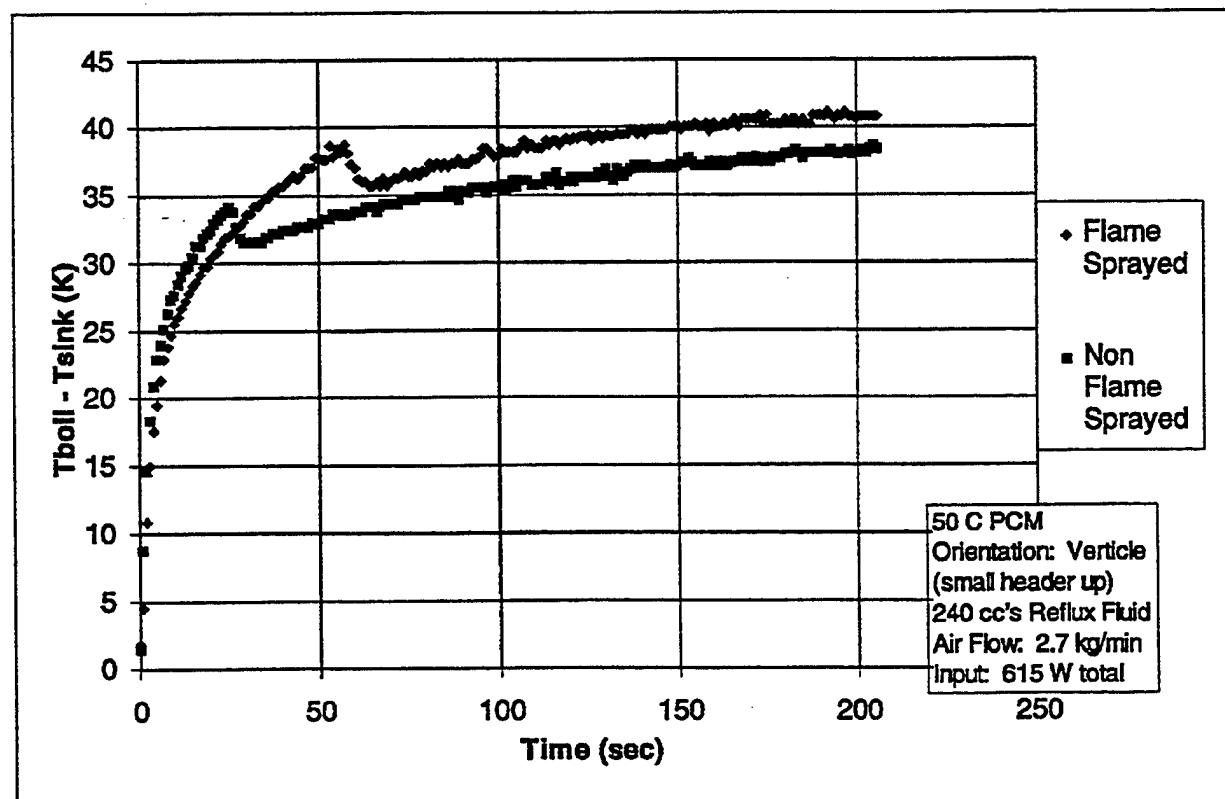


Figure 3.2.3-15 Boiler Temperature Rise for FS and nFS Coolers (SW Above Fluid Level)

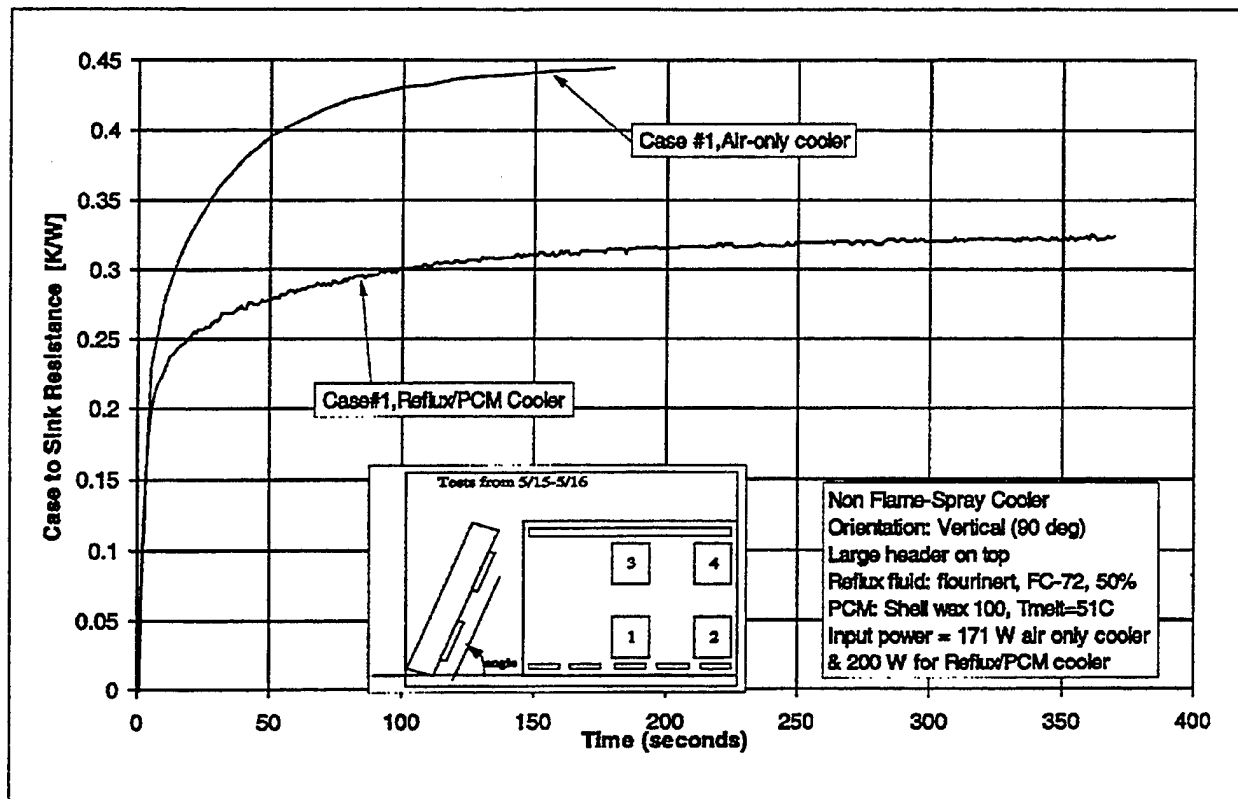


Figure 3.2.3-16 Comparison to Air-Cooler with Full Air Flow

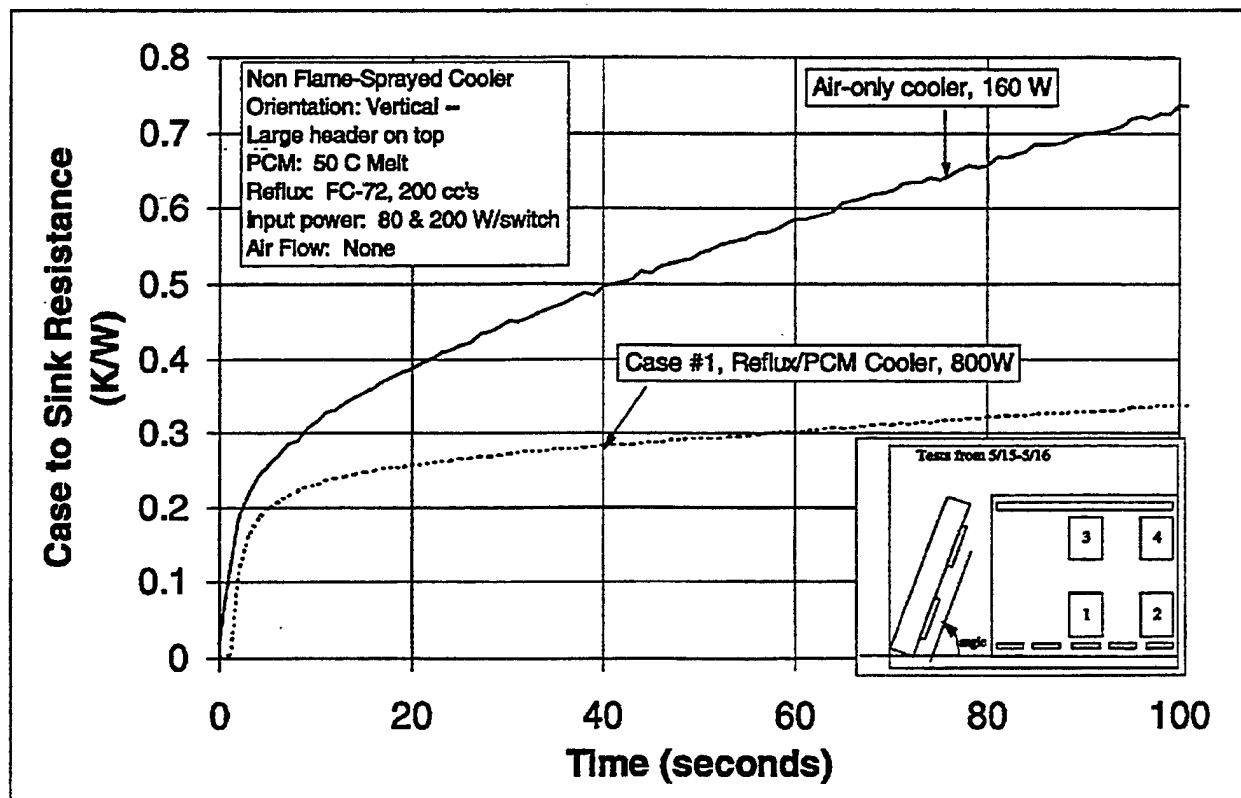


Figure 3.2.3-17 Comparison to Air-Cooler with No Air Flow

Cooler Weight Comparison Chart							
	Single Plate - 10 M-packs	Single Plate - 10 direct mounts	5 Plates - 2 M-packs each	5 Plates - 2 dies each	10 Plates - 1 M-pack each	Direct air cooled - 10 M-packs **	Direct air cooled - 10 direct mounts**
Cooler Volume * [In^3]	82.5	82.5	90.0	90.0	112.5	42.0	42.0
Cooler Weight w/o fluid (lbm)	2.20	2.20	2.88	2.88	3.60	1.78	1.78
PCM (lbm)	2.15	1.40	2.15	2.15	2.15	0.00	0.00
Reflux Fluid (lbm)	0.23	0.15	0.23	0.23	0.23	0.00	0.00
Electronics weight (lbm)	1.98	0.72	1.98	0.72	1.98	1.98	0.72
Total Weight	6.56	4.47	7.24	5.98	7.96	3.76	2.50
* Includes volume of air side fins and enclosed void spaces ** Air cooled versions reach 120C after 25 seconds @ full load, hot day.							

Figure 3.2.3-18 Cooler Weight Comparison Chart

Large Cooler Testing Conclusions

Tests on the large cooler to date have exceeded die and boiler surface fluxes of 80 and 20 W/cm², respectively, with a boiler wall superheat of 16K. Tests with an air-only cooler had higher IGBT case to sink resistance's of 37 and 100 percent for the high air flow and no air flow cases, respectively, for load durations of five to ten minutes. The maximum die heat flux for the no air flow case on the air-only cooler was 32 W/cm². Across a range of attitudes, power levels, and air flow rates, the large reflux/PCM cooler performed robustly. The 51°C PCM provided a 0.04 kW system resistance reduction compared to the 61°C PCM, if the resistance at the four minute point is considered to be a quasi-steady value. Future investigations should include additional parametric testing on reflux fluid fill level, thermosiphon riser section geometry, boiler coatings, and condenser enhancements.

3.2.4 Conclusions

Small and large reflux/PCM cooler testing has been done with air-only cooler testing used as a baseline.

Although small cooler testing revealed poorer than expected results, it revealed useful information which was used to enhance the performance of the large cooler design. This information included thickening the spreader to eliminate boiler burnout, increasing the PCM mass for added energy storage, and changing the condenser and air cooling fins to improve condenser performance. These changes yielded a cooler design that showed improved results over the baseline air-only design. Because of the testing performed, and additional testing in the area of enhanced PCM conduction performed by Sparta, Inc., the technology is moving toward being able to successfully cool the power electronics for EMAs without an active heat sink.

Finally, areas to work on in future programs should include additional work on preventing boiler burnout. If the heat fluxes at the boiler surface can be reduced, then the spreader thickness and overall case to boiler resistance can be reduced. Additionally, work on incorporating IGBTs directly to a cold plate would eliminate a contact resistance, which would also improve the overall performance.

4.0 Program Conclusions

4.0 Program Conclusions

From the motor cooler test program, the overall thermal resistance of the motor/cooler system was 31 K/kW for the reflux/PCM cooler vs. 52 K/kW for a natural convection cooled motor at a load cycle frequency of 0.005 Hz. Due to the inherent thermal mass of the motor, there was not a significant difference in thermal performance between the two cooling approaches for load cycle frequencies less than .02 Hz (50 second load period.)

After the motor cooling test program, a development was undertaken to apply reflux/PCM cooling technology to actuator motor drives. IGBT die and boiler surface fluxes exceeded 80 and 20 W/cm², respectively, during tests on the large cooler, with a boiler wall superheat of 16K. Across a range of attitudes, power levels, and air flow rates, the cooler performed robustly, with a system resistance of 0.32 K/W, on a per switch heat load basis, at the six minute point. Tests with an air-only cooler had higher IGBT case to sink resistance's of 37 and 100 percent for the high air flow and no air flow cases, respectively, for load durations of five to ten minutes. The maximum die heat flux for the no air flow case on the air-only cooler was 32 W/cm².

It is important to put these results into perspective to aid in choosing the correct cooler for a given application. One basis of comparison between coolers is the maximum heat flux at the IGBT die which they can effectively cool. For example, in the case where heat flux is low, a simple air-only cooler should be adequate, while higher fluxes might require a heat exchanger with PCM or reflux/PCM, while even higher fluxes might require heat sinks with active cooling such as a high performance pumped liquid cooler. Figure 4-1 compares the IGBT heat flux for three different coolers which are subjected to a step load, and all experience a 36K case to sink temperature rise after five minutes duration. A PCM only cooler, built by Sparta, Inc. is included

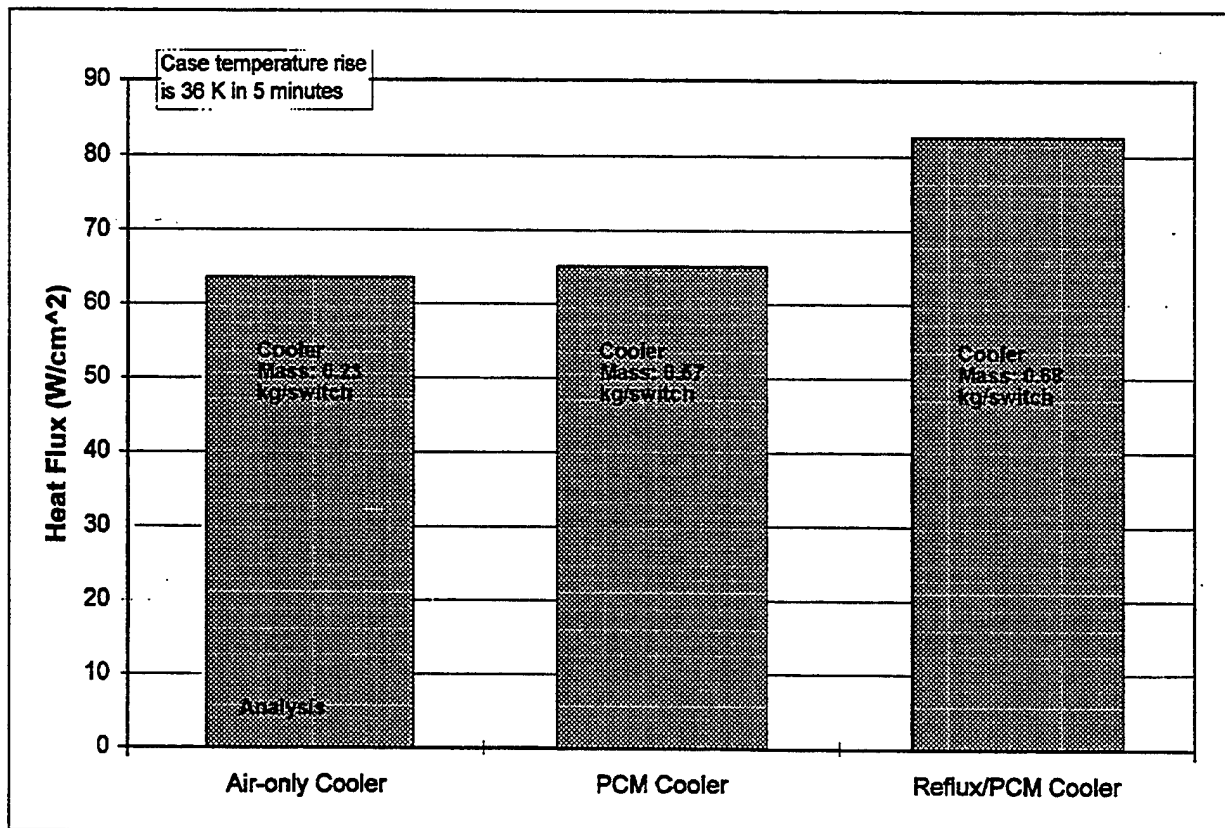


Figure 4-1 Flux Comparisons, Full Air Flow

in the chart to show how a cooler with no reflux fluid, but which does have thermal conductivity enhancement in the PCM section, performs in comparison (Vrable, 1998). Note that with full air flow, the coolers have similar performance, making the lighter air-only cooler the preferred choice at 0.23 kg of heat sink per switch. Figure 4-2 shows the same three coolers subjected to a step load, but in which there is no air flow to reject the heat from the coolers. In this case a cooler with additional thermal mass, such as the PCM cooler or the reflux/PCM cooler, may be preferred because of the larger heat flux they can support.

Another basis of comparison amongst the cooler types is the time it takes for the electronic device case to reach 100°C after a step load is imposed upon it. Figure 4-3 shows the response of the three coolers to a step load of 150 W per IGBT. The air-only cooler had only two switches, and the case temperature reached 100°C after only 51 seconds, even with full air flow. The PCM and reflux/PCM coolers took 145 and 245 seconds, respectively, to reach the same temperature at the device case, even with no air flow. With no air flow, the air-only cooler would reach the 100°C point sooner, although the response is not linear with load or flow due to the non-linearity of heat spreading in the device and cooler in the presence of low air-side heat transfer coefficients. While Figure 4-3 may not quantitatively separate the performance differences between the coolers, it does highlight the qualitative differences.

Finally, a figure of merit forwarded by Vrable and Whatley of Sparta, Inc., is a specific energy stored and transferred by a given cooler, in kJ/kg. To determine the value of this metric for a given cooler, the input power is integrated over the time it takes the device case to reach 100°C, giving the input energy. That input energy is then divided by the mass of the cooler to find the energy per unit mass. For instance, the reflux/PCM cooler was subjected to 823 W of input power for 159 seconds before the case temperatures reached 100°C, yielding an input energy of 131 kJ. Dividing by the 2.907 kg mass of the cooler gives a specific energy of the cooler of 45

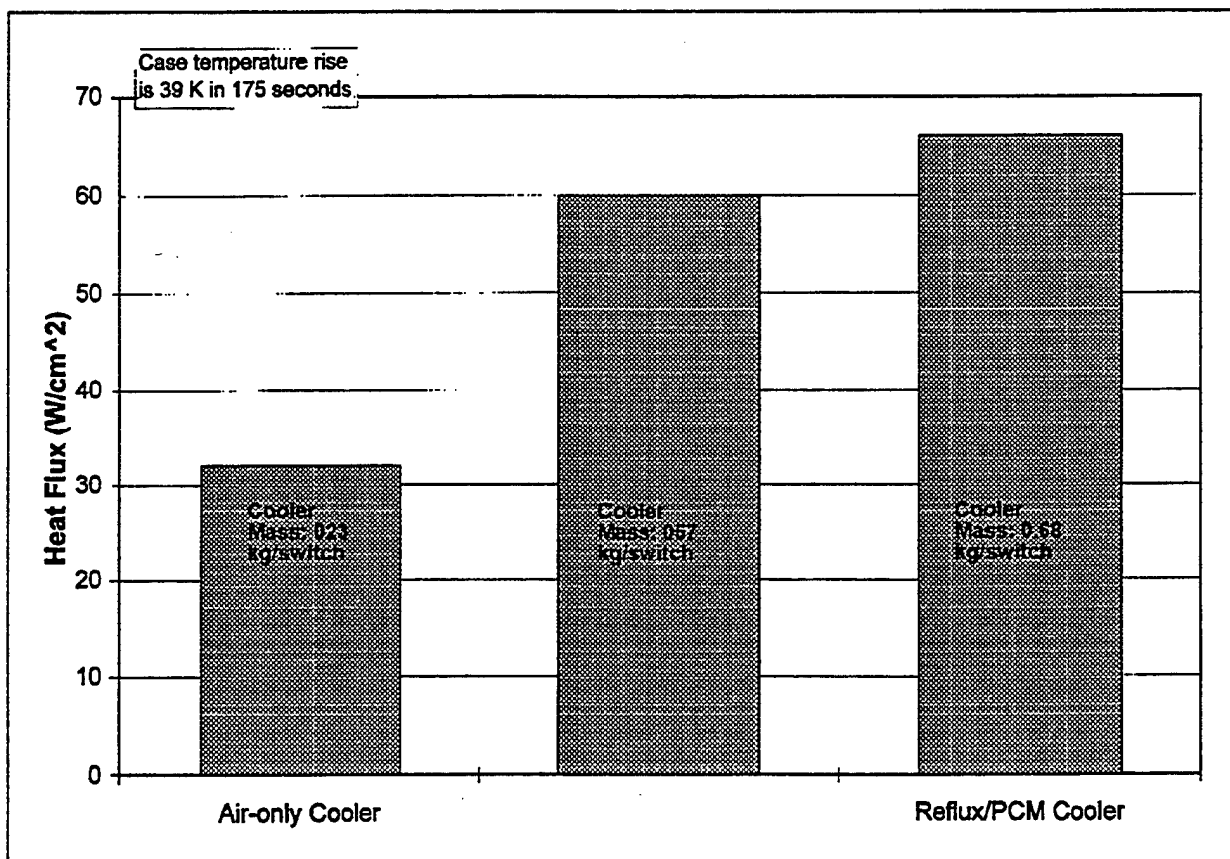


Figure 4-2 Flux Comparisons, No Air Flow

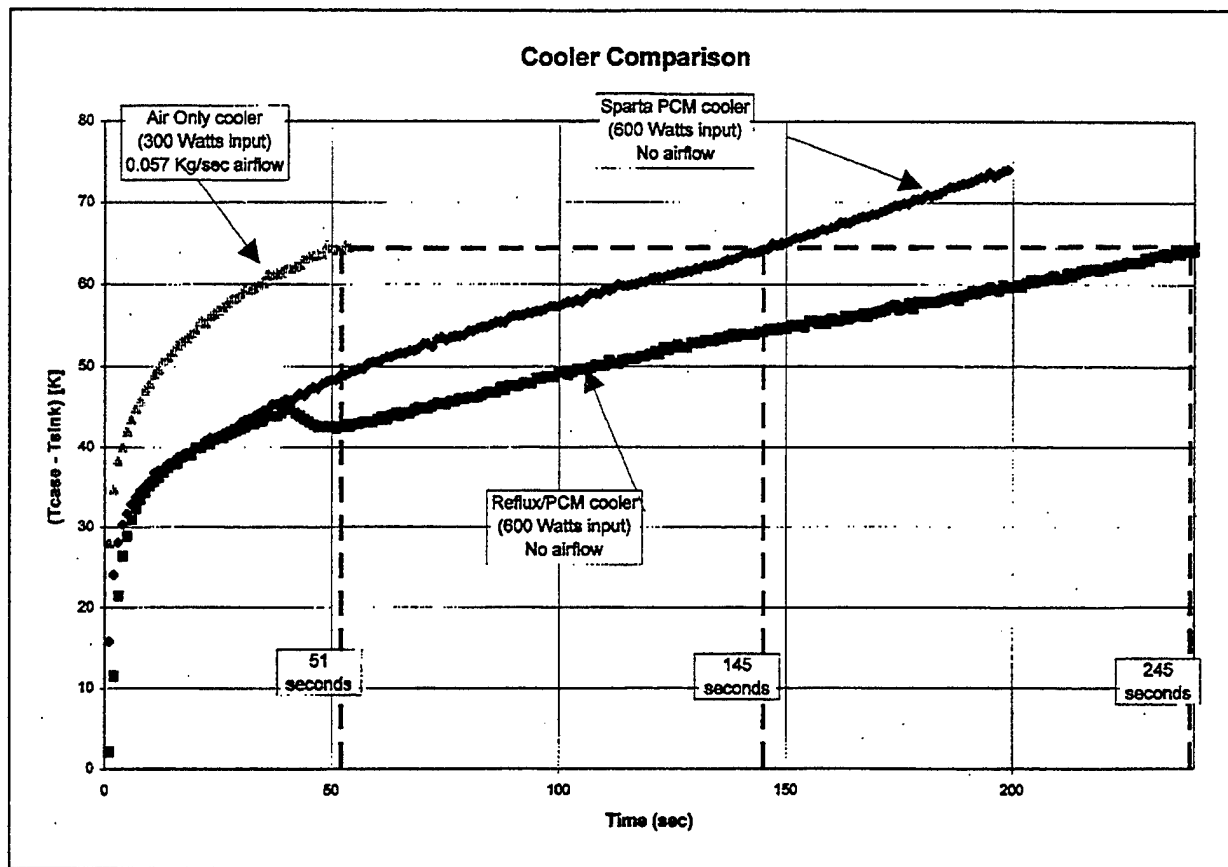


Figure 4-3 Comparison of Time to Reach 100°C

kJ/kg. Further, if one assumes that the entire mass of the cooler was not used because of the fact that only four of the ten switches were powered, the specific cooling energy, on a per switch basis, is 113 kJ/kg. However, the reflux fluid should promote spreading of input heat over the entire cooler thermal mass, making the per switch basis (113 kJ/kg) optimistic. Therefore, a realistic basis of comparison used the entire cooler mass. One test point with the Sparta Ten switch cooler had 820 W for 120 seconds, yielding a cooler specific energy of 41 kJ/kg, and a per switch specific energy of 102 kJ/kg. Vrabie reports several test points in which the cooler specific energy, on a per switch basis, for the ten switch cooler were in the 140-180 kJ/kg/switch range, or 56-72 kJ/kg for the entire cooler. Finally, the air-only cooler had a specific energy of 33 kJ/kg. Therefore, on an entire cooler mass basis, the specific energies for the air-only, PCM-only, and reflux/PCM coolers are 33, 41-72, and 45 kJ/kg, respectively, with a significant range in test data about each of these values.

Acknowledgments and Bibliography

Acknowledgments and Bibliography

Acknowledgments

The authors wish to acknowledge the guidance of Dr. J. Beam and Dr. K. Yerkes of Wright-Patterson Air Force Base; Mr. R. Scott Downing of Sundstrand Corporation; and laboratory support provided by Mr. Nacer Thomas and Mr. John Horowy. This work was performed under Air Force Contract No. F33615-91-C-2139. The authors also wish to express their appreciation to Dr. Daniel L. Vrable and Dr. Walter J. Whatley, of Sparta, Inc., for sharing data on the performance of their PCM-only cooler.

Bibliography

- Bland, T.J. and Funke, K.D., "Advanced Cooling for High Power Electric Actuators", SAE Paper 921022, April 7-10, 1992.
- Rohsenow, W.M., "Pool Boiling", *Handbook of Multiphase Systems*, Editor, Hestroni, G., McGraw-Hill-Hemisphere, New York, 1982.
- Hale, D.V., Hoover, M.J., and O'Neill, M.J., *Phase Change Materials Handbook*, Lockheed Missiles and Space Company, NASA Contractor Report CR-61363, September, 1971.
- Fluorinert Electronic Liquids - Product Manual*, 3M Co., 1990.
- Chen, W., Wong, I., Shah, N., and Garrigan, N., "An Assessment of Power Requirements for Electric Flight Control Actuators," SAE Paper 941189, April 18-22, 1994.
- Schneider, M.G., and Bland, T.J., "Preliminary Test Results of Reflux-Cooled Electromechanical Actuator," AIAA Paper 94-2014, June 20, 1994.
- Schneider, M.G., and Bland, T.J., "Advanced Passive Cooling For High Power Electromechanical Actuators," SAE Paper 931397, April 20-23, 1993.
- Schrage, D.S., "On the Use of a Small-Scale Two-Phase Thermosiphon to Cool High Power Electronics," ASME/AIAA Heat Transfer and Thermophysics Conference, Seattle, WA, June, 1990. HTD Vol. 135, pp1-10.
- Holman, J.P., *Heat Transfer*, 2nd Ed., McGraw-Hill Book Company, 1981.
- Culimore, B.A., et al, *SINDA User's Manual - Version 2.2*, Martin Marietta Corporation, November, 1987.
- Schneider, M.G., Bland, T.J., and Yerkes, K.L., "Reflux Cooling and Phase Change Thermal Storage," 24th National Heat Transfer Conference, Portland, OR, August, 1995, ASME.
- Humphries, W.R. and Griggs, E.I., *Design Handbook for Phase Change Thermal Control and Energy Storage Devices*, NASA Technical Paper 1074, November 1977.
- Vrable, Daniel L, and Yerkes, Kirk L., "A Thermal Management Concept for More Electric Aircraft Power System Applications," SAE Paper 981289, SAE Power Systems Conference, April, 1998.